8th Human Amyloid Imaging

January 15-17, 2014
Miami, Florida

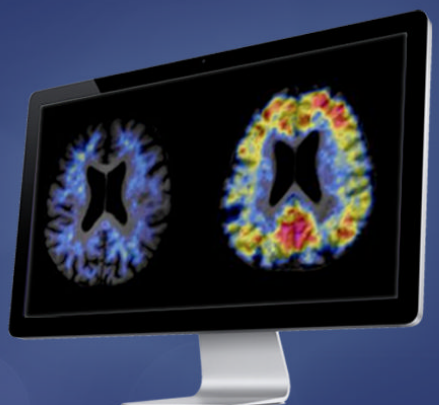

Co-Organizers:
Keith A. Johnson, MD • William J. Jagust, MD • William E. Klunk, MD, PhD • Chester Mathis, PhD

Program and Abstract Book

www.worldeventsforum.com/hai

To locate a poster by presenter's last name, view Table of Contents at page 4.

To locate a poster by number, view Program at page 11.

To view program, posters and abstracts on your mobile or tablet, please scan the QR code below or visit http://my.yapp.us/HAI2014

TABLE OF CONTENTS

PROGRAM *(all sessions will be held at the Miami Beach Resort)* **9**

ORAL PRESENTATIONS **19**

SESSION 1: Tau PET I **19**

PET imaging of tau deposits in Alzheimer's disease patients using ^{18}F-THK5105 and ^{18}F-THK5117 19

Presented by: Okamura, Nobuyuki *19*

Tau deposition estimated by [^{11}C]PBB3 PET in Alzheimer's disease, MCI with and without amyloid deposition, and cognitive healthy subjects 20

Presented by: Shimada, Hitoshi *20*

Tau PET: Initial experience with F18 T807 21

Presented by: Johnson, Keith *21*

SESSION 2: Tau PET II **22**

Detection of PHF-Tau pathology with T557, T726 and [18F]-T807 in brain sections from Alzheimer's and non-Alzheimer's tauopathy patients 22

Presented by: Skovronsky, Daniel M. *22*

Imaging tau pathology in vivo in FTLD: initial experience with [18F] T807 PET 23

Presented by: Dickerson, Brad *23*

PET Tau imaging with [F-18]-T807 (AV-1451) in normal subjects and patients with cognitive impairment due to Alzheimer's disease: Review of initial analyses 24

Presented by: Mintun, Mark A. *24*

SESSION 3: Keynote Lecture **25**

Tau protein - from native unfolding to pathological folding: structural aspects of Tau, Tau aggregates, and Tau interacting compounds 25

Presented by: Eckhard Mandelkow *25*

SESSION 4: Abeta PET: Assessment of Cognition and Disease Progression **26**

Amyloid change early in disease is related to increased glucose metabolism and episodic memory decline 26

Presented by: Landau, Susan *26*

Amyloid-β deposition in mild cognitive impairment is associated with hippocampal hyperactivation, atrophy and clinical progression 27

Presented by: Huijbers, Willem *27*

Gene-Environment interactions over the lifecourse: Cognitive activity, apolipoprotein E genotype, and brain beta-amyloid 28

Presented by: Wirth, Miranka *28*

Preclinical effects of Aβ deposition on episodic memory and disease progression 29

Presented by: Villemagne, Victor L *29*

SESSION 5: Abeta PET: Relation to Co-morbid Conditions **30**

Vascular and amyloid pathologies are independent predictors of cognitive decline in cognitively normal elderly 30

Presented by: Vemuri, Prashanthi *30*

Multiple brain markers contribute to age-related variation in cognition 31
Presented by: Hedden, Trey *31*
Cerebral amyloid related alterations in neuronal metabolism and the contribution of multimodal measures of vascular function 32
Presented by: McDade, Eric *32*
Binding of Pittsburgh Compound B to both normal and abnormal white matter in elderly cognitively normal controls. 33
Presented by: Cohen, Ann *33*
SESSION 6: Invited Lecture **34**
The Centiloid method for quantifying Amyloid PET studies: Great illuminator or master or illusion 34
Presented by: Koeppe, Robert *34*
SESSION 7: Technical Emphasis **35**
Modeling the influence of white matter contamination on detectability of brain amyloid changes in longitudinal studies of Alzheimer's progression: Segmentation analyses using the PET β-Amyloid tracer 18F NAV4694 ... 35
Presented by: Seibyl, John *35*
Amyloid PET screening results by APOE ε4 status from a Phase 1b Clinical Study (221AD103) in patients with prodromal to mild Alzheimer's disease 36
Presented by: Chiao, Ping *36*
Liberal thresholds for PIB-positivity optimally capture high-burden postmortem amyloid pathology 37
Presented by: Cohn-Sheehy, Brendan I. *37*
Existing thresholds for PIB positivity are too high 38
Presented by: Villeneuve, Sylvia *38*
SESSION 8: Neuropathologic Correlations **39**
PiB PET and FDG PET quantitative analysis methods with autopsy correlation 39
Presented by: Lowe, Val *39*
Evaluation of cotton wool plaques using amyloid binding compounds and Aβ immunohistochemistry: implications for PiB PET imaging 40
Presented by: Ikonomovic, Milos *40*
[^{18}F]Flutemetamol amyloid PET detection of Aβ plaque phases 4 and 5 and significant diffuse plaque burden 41
Presented by: Buckley, Chris *41*
Diagnostic accuracy of amyloid and FDG PET in pathologically-confirmed dementia 42
Presented by: Rabinovici, Gil D. *42*
Senile plaques: Classification, distribution, clinical correlation and Amyloid imaging 43
Presented by: Beach, Thomas G. *43*
SESSION 10: Memory Complaints/JADNI **44**
Subjective memory complaints are related to default network disruption in clinically normal older adults with high amyloid burden 44
Presented by: Vannini, Patrizia *44*

Amyloid burden and neurodegeneration independently contribute to greater subjective cognitive concerns in clinically normal older individuals 45
Presented by: Amariglio, Rebecca *45*
Longitudinal amyloid deposition with ^{11}C-PiB in Japanese ADNI study 46
Presented by: Ishii, Kenji *46*
Higher Aβ burden in subjective memory complainers: A flutemetamol sub-study in AIBL 47
Presented by: Rowe, Christopher C *47*

Poster Presentations *(Alphabetized by presenting author)* 48
POSTER SESSION 48
Early functional changes in the language network in response to increased amyloid beta deposition in healthy older adults 48
Presented by: Adamczuk, Katarzyna *48*
**To locate a poster by number, view Program at page 10.* *48*
Patterns of Av-45 uptake using VOIs based multivariate analysis in elderly peoples 49
Presented by: Adel, Djilali *49*
Prevalence of amyloid burden in elderly subjects in a PET-AV45 multicenter study 50
Presented by: Adel, Djilali *50*
Imaging amyloid in adults with Down's syndrome using PiB-PET 51
Presented by: Annus, Tiina *51*
Exploring the best methods to detect longitudinal change in amyloid imaging 52
Presented by: Baker, Suzanne *52*
Comparison of reference regions for [18F]Florbetapir PET SUVR computation 53
Presented by: Bedell, Barry *53*
Statistically-driven, automated subject classification based on amyloid PET scans 54
Presented by: Bedell, Barry *54*
Body mass index is associated with verbal episodic memory in cognitively normal older individuals with low fibrillar amyloid-beta measured by [^{11}C]-PiB 55
Presented by: Bilgel, Murat *55*
[^{18}F]Flutemetamol blinded image interpretation: assessment of the electronic training program for Japanese readers 56
Presented by: Buckley, Chris *56*
Disclosure of amyloid imaging results in cognitively normal individuals 57
Presented by: Burns, Jeffrey *57*
Differential temporal patterns of Amyloid-β and functional imaging markers across mutation types in autosomal dominant Alzheimer's disease: Findings from the DIAN Study 58
Presented by: Chhatwal, Jasmeer *58*
Comparison of PIB-PET data to Florbetapir-PET data acquired from different patient cohorts and the role of age in the discriminative power of amyloid imaging 59
Presented by: Chiotis, Konstantinos *59*

The value of early F18-Florbetapir scan information as an estimate of regional cerebral blood flow and comparison to F18-FDG measures of cerebral metabolism 60
Presented by: Devous, Michael *60*
Amyloid imaging changes diagnosis and treatment in patients with progressive cognitive impairment: Multicenter evaluation of 3-month post-scan outcomes 61
Presented by: Doraiswamy, P. Murali *61*
Practice effects relate to flutemetamol uptake, but not FDG or hippocampal volume: Moving cognition earlier in Jack's curves 62
Presented by: Duff, Kevin *62*
Alpha-synuclein imaging: Identifying small molecules that bind to aggregated Alpha-synuclein 63
Presented by: Eberling, Jamie *63*
Evaluation of F-18 radiolabeled cromolyn as a potential Aβ polymerization inhibitor and PET tracer 64
Presented by: Elmaleh, David R. *64*
Effects of age and amyloid on the encoding of visual scene detail 65
Presented by: Elman, Jeremy *65*
Clinical presentation and imaging findings in complex ALS with AD-like cognitive impairment 66
Presented by: FARID, Karim *66*
Striatal 11C-PiB retention in AD, MCI and HC: the pathotololgical significance of high PIB retention in the putamen 67
Presented by: FARID, Karim *67*
Advanced education mediates the impact of amyloid burden on reasoning in healthy older adult 68
Presented by: Farrell, Michelle E. *68*
Early-frame PiB PET perfusion and FDG PET glucose metabolism comparison in cognitively normal persons at three levels of genetic risk for Alzheimer's disease 69
Presented by: Fleisher, Adam *69*
Florbetapir-PET has greater clinical impact than FDG-PET in the differential diagnosis of AD and FTD 70
Presented by: Ghosh, Pia M. *70*
Source of cognitive complaint and amyloid binding in mild cognitive impairment 71
Presented by: Gifford, Katherine *71*
Striatal and extrastriatal dopamine transporter levels relate to cognition in Lewy body diseases 72
Presented by: Gomperts, Stephen *72*
Is there a binary relationship of mean brain Amyloid concentrations to cognitive, functional, metabolic and volumetric MRI variables in the ADNI cohort 73
Presented by: Goryawala, Mohammed *73*
Relationship of regional cerebral volumes to mean brain Amyloid concentration, APOE genotype and disease stage in the ADNI 2 cohort 74
Presented by: Goryawala, Mohammed *74*
Genetic resilience to Tau- and Amyloid-related neurodegeneration 75
Presented by: Hohman, Timothy *75*

Specificity of [^{3}H]T808, [^{3}H]THK-5105 and [^{3}H]AV-45 (florbetapir) binding to aggregated tau and amyloid plaques in human AD tissue *in vitro* ... 76

Presented by: Honer, Michael ... *76*

Arterial stiffness is associated with amyloid accumulation over two years in very elderly adults ... 77

Presented by: Hughes, Timothy ... *77*

Estimation of the number of physicians specializing in treating adult dementia patients in the US: Applying appropriate use criteria to medicare claims data ... 78

Presented by: Hunter, Craig A. ... *78*

Modeling intra-brain Amyloid-ß propagation via an epidemic spreading framework ... 79

Presented by: Iturria Medina, Yasser ... *79*

The potential of florbetapir F 18 and an early scan PET protocol (0-20 minutes after injection) to evaluate for the presence of amyloid ... 80

Presented by: Joshi, Abhinay D. ... *80*

Comparing concordance of different SUVR calculation methods with florbetapir visual reads ... 81

Presented by: Klein, Gregory ... *81*

Early age of onset is associated with greater neuroinflammation in Alzheimer's disease ... 82

Presented by: Kreisl, William Charles ... *82*

The association between glucose metabolism in Alzheimer's disease-vulnerable regions and cognitive reserve is modified by amyloid status within clinically normal individuals ... 83

Presented by: LaPoint, Molly ... *83*

Quantification and accuracy of clinical [11C]-PiB PET/MRI: The effect of MR-based attenuation correction ... 84

Presented by: Law, Ian ... *84*

Relationship between Amyloid burden and clinical course across AD pathophysiologic stages ... 85

Presented by: Margolin, Richard ... *85*

Aβ accumulation is associated with hippocampal hypometabolism in cognitively normal older adults regardless of Aβ level ... 86

Presented by: Marks, Shawn ... *86*

Is there an asymmetric distribution of in vivo Amyloid in primary progressive aphasia? ... 87

Presented by: Martersteck, Adam ... *87*

CogState computerized testing and neurodegenerative and amyloid imaging: Implications for secondary preventive trials ... 88

Presented by: Mielke, Michelle ... *88*

Longitudinal Amyloid measurement for clinical trials: A new approach to overcome variability ... 89

Presented by: Matthews, Dawn ... *90*

Prediction of Amyloid-beta hepatic clearance using sandwich cultured primary rat hepatocytes ... 91

Presented by: Mohamed, Loqman ... *91*

Identifying cost-effective predictive rules of Amyloid-β level by integrating neuropsychological tests and plasma-based marker ... 92

Presented by: Morgan, Dave ... *92*

Associations between beta-amyloid, markers of neurodegeneration, and cognition in clinically normal individuals from the Harvard Aging Brain Study 93
Presented by: Mormino, Elizabeth *93*
Beta-amyloid has a greater impact on memory in females than males across the clinical spectrum 94
Presented by: Mormino, Elizabeth *94*
PiB-PET significantly differs across neuropathologic classification of Alzheimer-type pathology and tangle predominant dementia 95
Presented by: Murray, Melissa E. *95*
Brain Amyloid deposition influences the Cognition-Mobility Interface (COMBINE) in cognitively normal older adults 96
Presented by: Nadkarni, Neelesh *96*
Astrocytosis, amyloid deposition and gray matter density in parahippocampus of MCI patients 97
Presented by: Nordberg, Agneta *97*
Regional brain activity and functional connectivity during memory encoding are differentially affected by age and β-amyloid deposition in cognitively normal older adults 98
Presented by: Oh, Hwamee *98*
Prevalence of Amyloid in cognitively normal, MCI and demented subjects – A meta-analysis of Amyloid PET studies 99
Presented by: Ossenkoppele, Rik *99*
Longitudinal quantification of brain amyloidosis in a rat model of Alzheimer's disease using [18F]NAV4694 100
Presented by: Parent, Maxime J. *100*
Potential value of an interpretation method that incorporates quantitative estimate of cortical to cerebellar SUVr as an adjunct to visual interpretation of florbetapir PET scans 101
Presented by: Pontecorvo, Michael *101*
The Alzheimer's structural connectome: Patterns of cortical reorganization with increasing neuritic amyloid plaque burden 102
Presented by: Prescott, Jeff *102*
Mathematical modeling of amyloid-β disposition by brain endothelial cells 103
Presented by: Qosa, Hisham *103*
Amyloid burden influences the relationship between hippocampal volume and default mode network connectivity in cognitively normal elderly 104
Presented by: Schultz, Aaron *104*
Update on the multicenter phase 3 histopathology study for ß-amyloid brain PET imaging 105
Presented by: Seibyl, John *105*
TAU Tracer F^{18}-T807 inversely relates with brain functional hubs of elderly normals 106
Presented by: Sepulcre, Jorge *106*
Amyloid PET screening for enrollment into Alzheimer's disease clinical trials: Initial experience in a Phase 1b clinical trial 107
Presented by: Sevigny, Jeff *107*

Antidepressant decreases CSF Aβ production in healthy individuals and in transgenic mice 108
Presented by: Sheline, Yvette *108*
Impact of regional flow/perfusion heterogeneity and metabolism on the quantification of amyloid tracers: a preclinical exploration 109
Presented by: Staelens, Steven *109*
In Vivo assessment of two isomers of [^{18}F]-THK5105 and [^{18}F]-THK511 110
Presented by: Tamagnan, Gilles *110*
Evaluation of different target-to-reference region definitions for quantitative categorization of [^{18}F]flutemetamol images into either normal or abnormal amyloid levels 111
Presented by: Thurfjell, Lennart *111*
En attendant Centiloid 112
Presented by: Villemagne, Victor L *112*
Investigating the involvement of the striatum in Down's syndrome and Alzheimer's disease with 11C-Pittsburgh Compound B-positron emission tomography (PiB-PET) 113
Presented by: Wilson, Liam Reese *113*
Utility of regional [18F]-Florbetapir PET imaging SUVRs in discriminating Alzheimer's disease and its prodromal stages 114
Presented by: Zhou, Qi *114*
Diagnostic value of Amyloid imaging in early onset dementia 115
Presented by: Zwan, Marissa *115*

8th Annual Human Amyloid Imaging

Miami, Florida, January 15 - 17, 2014

PROGRAM *(all sessions will be held at the Miami Beach Resort)*

Wednesday, 15 January

05:00 pm - 06:30

CHECK-IN and POSTER INSTALLATION (Starlight Room/Top Level)

06:30pm - 08:30

WELCOME RECEPTION (Oceanview Room/Lower Level)

Thursday, 16 January

07:00 am - 8:00

CHECK-IN and BREAKFAST (Regency Ballroom/Ground Floor)

08:00 - 08:15

WELCOME REMARKS (Grande Promenade/Ground Floor)

08:00 **Introductions and Welcome Remarks**

08:15 - 9:30

SESSION 1: Tau PET I

CHAIRS: William Jagust (University of California, Berkeley) and Keith Johnson (Massachusetts General Hospital)

08:15 SESSION 1-T1-O-01

PET imaging of tau deposits in Alzheimer's disease patients using ^{18}F-THK5105 and ^{18}F-THK5117

Nobuyuki Okamura (Tohoku University School of Medicine), Shozo Furumoto, Ryuichi Harada, Katsutoshi Furukawa, Aiko Ishiki, Michelle Fodero-Tavoletti, Rachel Mulligan, Ren Iwata, Manabu Tashiro, Kazuhiko Yanai, Colin Masters, Hiroyuki Arai, Christopher Rowe, Victor Villemagne, Yukitsuka Kudo

08:30 SESSION 1-T1-O-02

Tau deposition estimated by [^{11}C]PBB3 PET in Alzheimer's disease, MCI with and without amyloid deposition, and cognitive healthy subjects

Hitoshi Shimada (National Institute of Radiological Sciences, Chiba-Shi), Makoto Higuchi, Hitoshi Shinotoh, Shigeki Hirano, Shogo Furukawa, Yoko Eguchi, Keisuke Takahata, Fumitoshi Kodaka, Yasuyuki Kimura, Makiko Yamada, Masahiro Maruyama, Harumasa Takano, Ming-Rong Zhang, Hiroshi Ito, Tetsuya Suhara, et al.

08:45 SESSION 1-T1-O-03

Tau PET: Initial experience with F18 T807

Keith Johnson (Massachusetts General Hospital), John A. Becker, Jorge Sepulcre, Dorene Rentz, Aaron Schultz, Leslie Pepin, Marlie Philiossaint, Jonathan Alverio, Kelly Judge, Neil Vasdev, Tom Brady, Brad Hyman, Reisa Sperling

9:00	DISCUSSION SESSION 1
9:30	BREAK (Regency Ballroom/Ground Floor)

9:50 - 11:05

SESSION 2: Tau PET II

CHAIRS: Victor Villemagne (Austin Health) and Mark A. Mintun (Avid Radiopharmaceuticals, Inc.)

9:50 SESSION 2-T2-O-01

PET Tau imaging with [F-18]-T807 (AV-1451) in normal subjects and patients with cognitive impairment due to Alzheimer's disease: Review of initial analyses

Mark A. Mintun (Avid Radiopharmaceuticals, Inc.), Abhinay Joshi, Sergey Shcherbinin, Adam J. Schwarz, Ming Lu, Michael Pontecorvo, Michael Devous Sr., Daniel M. Skovronsky, Hartmuth Kolb

10:05 SESSION 2-T2-O-02

Detection of PHF-Tau pathology with T557, T726 and [18F]-T807 in brain sections from Alzheimer's and non-Alzheimer's Tauopathy patients

Hartmuth C. Kolb, Giorgio Attardo, Kelly Conway, Felipe Gomez, Qianwa Liang, Yin-Guo Lin, Andrew Siderowf, Daniel M. Skovronsky (Avid Radiopharmaceuticals, Inc.), Mark A. Mintun

10:20 SESSION 2-T2-O-03

Imaging tau pathology in vivo in FTLD: initial experience with [18F] T807 PET

Brad Dickerson (Massachusetts General Hospital/Harvard Medical School), Kimiko Domoto-Reilly, Daisy Sapolsky, Michael Brickhouse, Michael Stepanovic, Keith Johnson

10:35	DISCUSSION SESSION 2

11:05 - 11:50

SESSION 3: KEYNOTE LECTURE

11:05 **KEYNOTE LECTURE: Tau protein - from native unfolding to pathological folding: structural aspects of Tau, Tau aggregates, and Tau interacting compounds**

Eckhard Mandelkow (Max Planck Research unit for Structural Molecular Biology at DESY)

11:35	DISCUSSION SESSION 3
11:50	LUNCH (Starlight Room/Top Level)

1:20 - 2:50

SESSION 4: Abeta PET: Assessment of Cognition and Disease Progression

CHAIRS: Susan Landau (University of California, Berkeley) and Prashanthi Vemuri (Mayo Clinic Rochester)

1:20 SESSION 4-T4-O-01

Amyloid-β deposition in mild cognitive impairment is associated with hippocampal hyperactivation, atrophy and clinical progression

Willem Huijbers (Brigham and Women's Hospital/Harvard Medical School, Massachusetts General Hospital), Elizabeth Mormino, Aaron Schultz, Jasmeer Chhatwal, Brendon Boot, Rebecca Amariglio, Gad Marshall, Dorenne Rentz, Keith Johnson, Reisa Sperling

1:35 SESSION 4-T4-O-02

Amyloid change early in disease is related to increased glucose metabolism and episodic memory decline

Susan Landau (University of California, Berkeley), Allison Fero, Suzanne Baker, William Jagust

1:50 SESSION 4-T4-O-03

Preclinical effects of Aβ deposition on episodic memory and disease progression

Victor L Villemagne (Austin Health), Samantha Burnham, Pierrick Bourgeat, Belinda Brown, Kathryn Ellis, Olivier Salvado, Ralph Martins, Lance Macaulay, David Ames, Colin L Masters, Christopher C Rowe

2:05 SESSION 4-T4-O-04

Gene-environment interactions over the lifecourse: Cognitive activity, apolipoprotein E genotype, and brain beta-amyloid

Miranka Wirth (University of California, Berkeley), Sylvia Villeneuve, Renaud La Joie, Shawn Marks, William Jagust

2:20	DISCUSSION SESSION 4
2:50	BREAK (Regency Ballroom/Ground Floor)

3:10 - 4:40

SESSION 5: Abeta PET: Relation to Co-morbid Conditions

CHAIRS: Clifford Jack (Mayo Clinic Rochester) and Ann Cohen (University of Pittsburgh School of Medicine)

3:10 SESSION 5-T5-O-01

Multiple brain markers contribute to age-related variation in cognition

Trey Hedden (Massachusetts General Hospital, Harvard Medical School), Aaron Schultz, Anna Rieckmann, Elizabeth C. Mormino, Keith A. Johnson, Reisa A. Sperling, Randy L. Buckner

3:25 SESSION 5-T5-O-02

Cerebral Amyloid related alterations in neuronal metabolism and the contribution of multimodal measures of vascular function

Eric McDade (University of Pittsburgh), Albert Kim, Tim Hughes, Beth Snitz, Anne Cohen, Julie Price, Chester Mathis, James Becker, William Klunk, Oscar Lopez

3:40 SESSION 5-T5-O-03

Vascular and Amyloid pathologies are independent predictors of cognitive decline in cognitively normal elderly

Prashanthi Vemuri (Mayo Clinic Rochester), Timothy Lesnick, Scott Przybelski, David Knopman, Gregory Preboske, Kejal Kantarci, Mary Machulda, Michelle Mielke, Val Lowe, Matthew Senjem, Jeffrey Gunter, Ronald Petersen, Clifford Jack

3:55 SESSION 5-T5-O-04

Binding of Pittsburgh Compound B to both normal and abnormal white matter in elderly cognitively normal controls.

Anna Goodheart, Erica Tamburo, Davneet Minhas, Howard Aizenstein, Eric McDade, Lisa Weissfeld, Beth Snitz, Julie Price, Chester Mathis, Oscar Lopez, William Klunk, Ann Cohen (University of Pittsburgh School of Medicine)

4:10 DISCUSSION SESSION 5

Thursday, 16 January – Starlight Room (Top Level)

POSTER PRESENTATIONS - 4:40 - 19:30

(Posters listed by assigned number)

POSTER-P-01

Evaluation of F-18 radiolabeled cromolyn as a potential Aβ polymerization inhibitor and PET tracer

David R. Elmaleh (Massachusetts General Hospital), Timothy M. Shoup, Alan J. Fischman, Kazue Takahashi, Mykol Larvie, Erik Vogan

POSTER-P-02

Is there a binary relationship of mean brain amyloid concentrations to cognitive, functional, metabolic and volumetric MRI variables in the ADNI cohort?

Mohammed Goryawala (Florida International University), Malek Adjouadi, David Loewenstein, Warren Barker, Ranjan Duara

POSTER-P-03

Amyloid PET screening for enrollment into Alzheimer's disease clinical trials: Initial experience in a Phase 1b clinical trial

Sevigny Jeff (Biogen Idec), Suhy Joyce, Chiao Ping, Klein Gregory, Oh Joonmi, Purcell Derk, Verma Ajay, Sampat Mehul, Barakos Jerome

POSTER-P-04

Amyloid imaging changes diagnosis and treatment in patients with progressive cognitive impairment: Multicenter evaluation of 3-month post-scan outcomes

P. Murali Doraiswamy (Duke UniversityAvid Radiopharmaceuticals, Inc.), Andrew Siderowf (Duke UniversityAvid Radiopharmaceuticals, Inc.), Michael Pontecorvo, Stephen P. Salloway, Adam S. Fleisher, Carl H. Sadowsky, Anil K. Nair, Ming Lu, Anupa K. Arora, Daniel M. Skovronsky, Mark A. Mintun, Michael Grundman, AV45-A17 Study Group

POSTER-P-05

Diagnostic value of Amyloid imaging in early onset dementia

Marissa Zwan (VU University Medical Center), Femke Bouwman, Wiesje van der Flier, Adriaan Lammertsma, Bart van Berckel, Philip Scheltens

POSTER-P-06

In Vivo assessment of two isomers of [^{18}F]-THK5105 and [^{18}F]-THK511

Olivier Barret, David Alagille, Danna Jennings, Nobuyuki Okamura, Shozo Furumoto, Yukitsuka Kudo, Kenneth Marek, John Seibyl, Gilles Tamagnan (Molecular Neuroimaging)

POSTER-P-07

Patterns of Av-45 uptake using VOIs based multivariate analysis in elderly peoples

Djilali Adel (Inserm, UMR 825, Toulouse University Hospital, Paul Sabatier University, Toulouse University), Anne-Sophie Salabert, Florent Aubry, Julien Delrieu, Thierry Voisin, Sophie Gillette, Anne Hitzel, Bruno Vellas, Pierre Payoux

POSTER-P-08

Utility of Regional [18F]-Florbetapir PET imaging SUVRs in discriminating Alzheimer's disease and its prodromal stages

Qi Zhou (Florida International University), Mohammed Goryawala, David Loewenstein, Warren Barker, Ranjan Duara, Malek Adjouadi

POSTER-P-09

Arterial stiffness is associated with amyloid accumulation over two years in very elderly adults

Timothy Hughes (Wake Forest School of Medicine, Wake Forest University.), Lewis Kuller, Emma Barinas-Mitchell, Eric McDade, William Klunk, Ann Cohen, Chester Mathis, Steven DeKosky, Julie Price, Oscar Lopez

POSTER-P-10

Brain Amyloid deposition influences the Cognition-Mobility Interface (COMBINE) in cognitively normal older adults

Neelesh Nadkarni (University of Pittsburgh School of Medicine), Beth Snitz, Annie Cohen, Stephanie Studenski, Subashan Perera, Oscar Lopez, Robert Nebes, William Klunk

POSTER-P-11

Striatal and extrastriatal dopamine transporter levels relate to cognition in Lewy body diseases

Marta Marquie, Joseph Locascio, Dorene Rentz, Alex Becker, Trey Hedden, Keith Johnson, John Growdon, Stephen Gomperts (Massachusetts General Hospital)

POSTER-P-12

Aβ accumulation is associated with hippocampal hypometabolism in cognitively normal older adults regardless of Aβ level

Shawn Marks (University of California, Berkeley), Jacob Vogel, Cindee Madison, William Jagust

POSTER-P-13

Relationship between Amyloid burden and clinical course across AD pathophysiologic stages

Richard Margolin (CereSpir, Inc.ADM Diagnostics LLC), Jianing Di, Randolph Andrews (CereSpir, Inc.ADM Diagnostics LLC), Steven Salloway, Reisa Sperling, Leslie Shaw, HR Brashear, Enchi Liu, Mark Schmidt, Dawn Matthews

POSTER-P-14

Associations between beta-amyloid, markers of neurodegeneration, and cognition in clinically normal individuals from the Harvard Aging Brain Study

Elizabeth Mormino (Massachusetts General Hospital, Harvard Medical School), Rebecca Betensky, Trey Hedden, Aaron Schultz, Rebecca Amariglio, Dorene Rentz, Keith Johnson, Reisa Sperling

POSTER-P-15

Comparison of PIB-PET data to Florbetapir-PET data acquired from different patient cohorts and the role of age in the discriminative power of amyloid imaging

Konstantinos Chiotis (Karolinska Institutet), Stephen F. Carter, Agneta Nordberg

POSTER-P-16

Prediction of Amyloid-beta hepatic clearance using sandwich cultured primary rat hepatocytes

Loqman Mohamed (University of Louisiana at Monroe), Amal Kaddoumi

POSTER-P-17

Comparison of reference regions for [18F]Florbetapir PET SUVR computation

Arnaud Charil, Felix Carbonell, Alex Zijdenbos, Alan Evans, Robert Koeppe, Jeff Sevigny, Ping Chiao, Barry Bedell (Biospective Inc. & Montreal Neurological Institute, McGill University)

POSTER-P-18

Is there an asymmetric distribution of in vivo amyloid in primary progressive aphasia?

Adam Martersteck (Northwestern University (NU) Feinberg School of Medicine), Christopher Murphy, Christina Wieneke, Kewei Chen, Ji Luo, Pradeep Thiyyagura, M.-Marsel Mesulam, Emily Rogalski

POSTER-P-19

Longitudinal quantification of brain amyloidosis in a rat model of Alzheimer's disease using [18F]NAV4694

Maxime J. Parent (McGill Centre for Studies in Aging), MinSu P. Kang, Sonia Do Carmo, Antonio Aliaga, Cornelia Reininger, Jean-Paul Soucy, Serge G. Gauthier, A. Claudio Cuello, Pedro Rosa-Neto

POSTER-P-20

Antidepressant decreases CSF Aβ production in healthy individuals and in transgenic mice

Yvette Sheline (University of Pennsylvania Perelman School of Medicine), Tim West, Kevin Yarasheski, Robert Swarm, Mateusz Jasielec, Jonathan Fisher, Ping Yan, Chengjie Xiong, Christine Frederiksen, Robert Chott, Randall Bateman, John Morris, Mark Mintun, Jin-Moo Lee, John Cirrito

POSTER-P-21

Specificity of [^{3}H]T808, [^{3}H]THK-5105 and [^{3}H]AV-45 (florbetapir) binding to aggregated tau and amyloid plaques in human AD tissue *in vitro*

Michael Honer (F. Hoffmann-La Roche Ltd), Henner Knust, Luca Gobbi, Dieter Muri, Edilio Borroni

POSTER-P-22

Astrocytosis, amyloid deposition and gray matter density in parahippocampus of MCI patients

Il Han Choo, Stephen F Carter, Michael Schöll, Agneta Nordberg (Karolinska Institutet)

POSTER-P-23

Genetic resilience to Tau- and Amyloid- related neurodegeneration

Timothy Hohman (Vanderbilt University Medical Center), Mary Ellen Koran, Tricia Thornton-Wells

POSTER-P-24

TAU Tracer F^{18}-T807 inversely relates with brain functional hubs of elderly normals

Jorge Sepulcre (Massachusetts General Hospital and Harvard Medical School), Sperling Sperling, Keith Johnson

POSTER-P-25

Early-frame PiB PET perfusion and FDG PET glucose metabolism comparison in cognitively normal persons at three levels of genetic risk for Alzheimer's disease

Hillary Protas, Kewei Chen, Ji Luo, John Thompson Rausch, Robert Bauer III, Sandra Goodwin, Nicole Richter, Daniel Bandy, Richard Caselli, Adam Fleisher (Banner Alzheimer's Institute;Arizona Alzheimer's Consortium), Eric Reiman

POSTER-P-26

Evaluation of different target-to-reference region definitions for quantitative categorization of [^{18}F]flutemetamol images into either normal or abnormal amyloid levels

Lennart Thurfjell (GE Healthcare), Roger Lundqvist, Johan Lilja, Chris Buckley, Adrian Smith, Paul Sherwin

POSTER-P-27

Statistically-driven, automated subject classification based on Amyloid PET scans

Felix Carbonell, Arnaud Charil, Alex Zijdenbos, Alan Evans, Jeff Sevigny, Ping Chiao, Barry Bedell (Biospective Inc. & Montreal Neurological Institute, McGill University)

POSTER-P-28

PiB-PET significantly differs across neuropathologic classification of Alzheimer-type pathology and tangle predominant dementia

Melissa E. Murray (Mayo Clinic Jacksonville), Dennis W. Dickson, Emily S. Lundt, Stephen D. Weigand, Scott A. Przybelski, Lennon G. Jordan, Joseph E. Parisi, David S. KNopman, Bradley F. Boeve, Kejal Kantarci, Ronald C. petersen, Clifford R. Jack, Jr., Val J. Lowe

POSTER-P-29

Advanced education mediates the impact of amyloid burden on reasoning in healthy older adult

Michelle E. Farrell (University of Texas at Dallas), Gérard N. Bischof, Karen M. Rodrigue, Kristen M. Kennedy, Denise C. Park

POSTER-P-30

Potential value of an interpretation method that incorporates quantitative estimate of cortical to cerebellar SUVr as an adjunct to visual interpretation of florbetapir PET scans

Michael Pontecorvo (Avid Radiopharmaceuticals, Inc.), Michael Devous Sr., Anupa K. Arora, Marybeth Devine, Ming Lu, Andrew Siderowf, Stephen P. Truocchio, Catherine Devadanam, Abhinay D. Joshi, Christopher Breault, Stephen L. Heun, Daniel M. Skovronsky, Mark A. Mintun

POSTER-P-31

The association between glucose metabolism in Alzheimer's disease-vulnerable regions and cognitive reserve is modified by amyloid status within clinically normal individuals

Molly LaPoint (Massachusetts General Hospital, Harvard Medical School), Elizabeth Mormino, Rebecca Amariglio, Aaron Schultz, Trey Hedden, J. Alex Becker, Keith Johnson, Reisa Sperling, Dorene Rentz

POSTER-P-32

Clinical presentation and Imaging findings in complex ALS with AD-like cognitive impairment

Karim Farid (Karolinska Institutet), Stephen Carter, Elena Rodriguez-Vieitez, Ove Almkvist, Pia Andersen, Anders Wall, Peter Andersen, Agneta Nordberg

POSTER-P-33

Investigating the involvement of the striatum in Down's syndrome and Alzheimer's disease with 11C-Pittsburgh Compound B-positron emission tomography (PiB-PET)

Liam Reese Wilson (Cambridge Intellectual and Developmental Disabilities Research Group, University of Cambridge), Tiina Annus, Shahid Zaman, Young Hong, Tim Fryer, Robert Smith, Franklin Aigbirhio, Anthony Holland

POSTER-P-34

Differential temporal patterns of Amyloid-β and functional imaging markers across mutation types in autosomal dominant Alzheimer's disease: Findings from the DIAN study

Jasmeer Chhatwal (Massachusetts General Hospital, Harvard Medical School), Aaron Schultz, Keith Johnson, Tammie Benzinger, Clifford Jack, Beau Ances, Caroline Sullivan, Stephen Salloway, John Ringman, Robert Koeppe, Daniel Marcus, Paul Thompson, Andrew Saykin, John Morris, Reisa Sperling, et al.

POSTER-P-35

Practice effects relate to flutemetamol uptake, but not FDG or hippocampal volume: Moving cognition earlier in Jack's curves

Kevin Duff (University of Utah), Norman Foster, Richard King, John Hoffman

POSTER-P-36

Striatal ^{11}C-PiB retention in AD, MCI and HC: the pathotololgical significance of high PIB retention in the putamen

Karim FARID (Karolinska Institutet), Ove ALMKVIST, Katharina BRUEGGEN, Stephen CARTER, Anders WALL, Karl HERHOLZ, Agneta NORDBERG

POSTER-P-37

Exploring the best methods to detect longitudinal change in amyloid imaging

Suzanne Baker (Lawrence Berkeley National Lab), Shawn Marks, Susan Landau, William Jagust

POSTER-P-38

***En attendant* Centiloid**

Victor L Villemagne (Austin Health), Paul Yates, Kevin Ong, Belinda Brown, Svetlana Pejoska, Robert Williams, Robyn Veljanoski, Stephanie Rainey-Smith, Kevin Taddei, Ralph Martins, Colin L Masters, Christopher C Rowe

POSTER-P-39

Mathematical modeling of amyloid-β disposition by brain endothelial cells

Hisham Qosa (University of Louisiana at Monroe), Bilal Abuasal, Jeffrey Keller, Amal Kaddoumi

POSTER-P-40

Update on the multicenter phase 3 histopathology study for ß-amyloid brain PET imaging

Osama Sabri, Andrew Stephens, Ana Catafau, Henryk Barthel, John Seibyl (Institute for Neurodegenerative Disorders)

POSTER-P-41

Early functional changes in the language network in response to increased amyloid beta deposition in healthy older adults

Katarzyna Adamczuk (KU Leuven), An-Sofie De Weer, Natalie Nelissen, Patrick Dupont, Koen Van Laere, Rik Vandenberghe

POSTER-P-42

Imaging amyloid in adults with Down's syndrome using PiB-PET

Tiina Annus (University of Cambridge), Liam R. Wilson, Shahid Zaman, Young T. Hong, Tim Fryer, Franklin Aigbirhio, Rob Smith, Anthony J. Holland

POSTER-P-43

Amyloid burden influences the relationship between hippocampal volume and default mode network connectivity in cognitively normal elderly.

Aaron Schultz (Massachusetts General Hospital, Harvard Medical School), Elizabeth Mormino, Willem Huijbers, Jasmeer Chhatwal, Andrew Ward, Sarah Wigman, Molly LaPoint, Trey Hedden, Keith Johnson, Reisa Sperling

POSTER-P-44

Source of cognitive complaint and amyloid binding in mild cognitive impairment

Katherine Gifford (Vanderbilt University), Stephen Damon, Angela Jefferson

POSTER-P-45

Disclosure of Amyloid imaging results in cognitively normal individuals

David Johnson, Vidoni Eric, Magdalena Leszko, Rebecca Bothwell, Jeffrey Burns (University of Kansas Medical Center)

POSTER-P-46

Modeling intra-brain Amyloid-ß propagation via an epidemic spreading framework

Yasser Iturria Medina (Montreal Neurological Institute, and Biospective Inc), Roberto C. Sotero, Alan C. Evans (Montreal Neurological Institute and Biospective Inc.)

POSTER-P-47

Longitudinal Amyloid measurement for clinical trials: a new approach to overcome variability

Dawn Matthews (ADM Diagnostics LLC), Boris Marendic, Randolph Andrews, Ana Lukic, Steven Einstein, Enchi Liu, Richard Margolin, Mark Schmidt, for the Alzheimer's Disease Neuroimaging Initiative

POSTER-P-48

Quantification and accuracy of clinical [11C]-PiB PET/MRI: The effect of MR-based attenuation correction

Ian Law (Rigshospitalet), Flemming L. Andersen, Adam E. Hansen, Steen G. Hasselbalch, Claes Ladefoged, Sune H Keller, Søren Holm, Lotte Højgaard

POSTER-P-49

Florbetapir-PET has greater clinical impact than FDG-PET in the differential diagnosis of AD and FTD

Pia M. Ghosh (University of California San Francisco, University of California Berkeley, Lawrence Berkeley National Laboratory), Cindee Madison, Miguel Santos, Kristin Norton, Suzanne Baker, Adam L. Boxer, Howard J. Rosen, Zachary A. Miller, Marilu Gorno-Tempini, Bruce L. Miller, William J. Jagust, Gil D. Rabinovici

POSTER-P-50

Impact of regional flow/perfusion heterogeneity and metabolism on the quantification of amyloid tracers: a preclinical exploration

Ann-Marie Waldron, Leonie Wyffels, Stefanie Dedeurwaerdere, Jill Richardson, Mark Schmidt, Xavier Langlois, Sigrid Stroobants, Steven Staelens (Antwerp University)

POSTER-P-51

[^{18}F]Flutemetamol blinded image interpretation: Assessment of the electronic training program for Japanese readers

Chris Buckley (GE Healthcare), Brian J McParland, Jan Wolber, Paul Sherwin, Michelle Zanette, Gill Farrar

POSTER-P-52

CogState computerized testing and neurodegenerative and amyloid imaging: Implications for Secondary Preventive Trials

Michelle Mielke (Mayo Clinic, Rochester), Heather Wiste, Stephen Weigand, Prashanthi Vemuri, Val Lowe, Mary Machulda, Rosebud Roberts, Kejal Kantarci, David Knopman, Bradly Boeve, Clifford Jack, Petersen Ronald

POSTER-P-53

Prevalence of amyloid burden in elderly subjects in a PET-AV45 multicenter study

Djilali Adel (Inserm, UMR 825, Toulouse University Hospital, Paul Sabatier University, Toulouse University), Anne Hitzel, Julien Delrieu, Thierry Voisin, Sophie Gillette-Guyonnet, Bruno Vellas, Pierre Payoux, et al.

POSTER-P-54

Alpha-synuclein imaging: Identifying small molecules that bind to aggregated Alpha-synuclein

Dale Mitchell, Kevin Nash, David Hardick, David Cronk, Paul Kotzbauer, Zhude Tu, Jinbin Xu, Robert Mach, Jamie Eberling (Michael J. Fox Foundation), N. Scott Mason, William Klunk, Chester Mathis

POSTER-P-55

Beta-amyloid has a greater impact on memory in females than males across the clinical spectrum

Elizabeth Mormino (Massachusetts General Hospital, Harvard Medical School), Reisa Sperling

POSTER-P-56

Body mass index is associated with verbal episodic memory in cognitively normal older individuals with low fibrillar amyloid-beta measured by [^{11}C]-PiB

Murat Bilgel (National Institute on Aging, NIH; Johns Hopkins University School of Medicine), Yi-Fang Chuang, Yang An, Jerry Prince, Dean Wong, Madhav Thambisetty, Susan Resnick

POSTER-P-57

The Alzheimer's Structural Connectome: Patterns of cortical reorganization with increasing neuritic Amyloid plaque burden

Jeff Prescott (Duke University Medical Center), Arnaud Guidon, P. Murali Doraiswamy, Kingshuk Choudhury, Chunlei Liu, Jeffrey Petrella

POSTER-P-58

Comparing concordance of different SUVR calculation methods with Florbetapir visual reads

Gregory Klein (Synarc, Inc.), Ping Chiao, Jerome Barakos, Derk Purcell, Mehul Sampat, Joonmi Oh, Jeff Sevigny, Joyce Suhy

POSTER-P-59

The value of early F18-Florbetapir scan information as an estimate of regional cerebral blood flow and comparison to F18-FDG measures of cerebral metabolism

Michael Devous (Avid Radiopharmaceuticals, Inc.), Abhinay Joshi, Michael Navitsky, Michael Pontecorvo, Daniel Skovronsky, Mark Mintun

POSTER-P-60

Relationship of regional cerebral volumes to mean brain Amyloid concentration, APOE genotype and disease stage in the ADNI 2 cohort

Mohammed Goryawala (Florida International University), David Loewenstein, Warren Barker, Ranjan Duara, Malek Adjouadi

POSTER-P-61

Estimation of the number of physicians specializing in treating adult dementia patients in the US: Applying appropriate use criteria to medicare claims data

Noam Y. Kirson, Urvi Desai, Alice Kate G. Cummings, Howard G. Birnbaum, Craig A. Hunter (Eli Lilly and Company)

POSTER-P-62

Effects of age and amyloid on the encoding of visual scene detail

Jeremy Elman (Lawrence Berkeley Natl Laboratory), Hwamee Oh, Cindee Madison, Suzanne Baker, Jacob Vogel, Sam Crowley, William Jagust

POSTER-P-63

The potential of florbetapir F 18 and an early scan PET protocol (0-20 minutes after injection) to evaluate for the presence of amyloid

Abhinay D. Joshi (Avid Radiopharmaceuticals Inc.), Michael D. Devous Sr., Michael J. Pontecorvo, Michael Navitsky, Ian Kennedy, Mark A. Mintun, Daniel M. Skovronsky, and Alzheimer's Disease NeuroImaging Intiative

POSTER-P-64

Identifying cost-effective predictive rules of Amyloid-β Level by integrating neuropsychological tests and plasma-based marker

Shuai Huang, Amanda Smith, Mona Haghighi, Brent Small, Dave Morgan (Byrd Alzheimer's Institute, University of South Florida)

POSTER-P-65

Regional brain activity and functional connectivity during memory encoding are differentially affected by age and β-amyloid deposition in cognitively normal older adults

Hwamee Oh (University of California, Berkeley), Jeremy Elman, Suzanne Baker, Cindee Madison, Jacob Vogel, Sam Crowley, William Jagust

POSTER-P-66

Prevalence of Amyloid in cognitively normal, MCI and demented subjects – A meta-analysis of Amyloid PET studies

Rik Ossenkoppele (VU University Medical Center), Willemijn Jansen, Bart van Berckel, Pieter Jelle Visser

POSTER-P-67

Early age of onset is associated with greater neuroinflammation in Alzheimer's disease

William Charles Kreisl (National Institute of Mental Health), Chul Hyoung Lyoo, Meghan McGwier, Joseph Snow, Kimberly Jenko, Winston Corona, Cheryl Morse, Sami Zoghbi, Victor Pike, Francis McMahon, R. Scott Turner, Robert Innis

Friday, 17 January

08:30 - 9:15

SESSION 6: Invited Lecture

08:30 SESSION 6-T6-O-01

The Centiloid method for quantifying Amyloid PET studies: Great illuminator or master or illusion

Robert Koeppe (University of Michigan)

9:00 DISCUSSION SESSION 6

09:15 - 10:45

SESSION 7: Technical Emphasis

CHAIRS: Chester Mathis (University of Pittsburgh) and John Seibyl (Institute for Neurodegenerative Disorders)

09:15 SESSION 7-T7-O-01

Existing thresholds for PIB positivity are too high

Sylvia Villeneuve (University of California, Berkeley), Cindee Madison, Nagehan Ayakta, Renaud La Joie, Brendan I. Cohn-Sheehy, Jacob Vogel, Shawn Marks, Samia K. Arthur-Bentil, Bruce Reed, Charles DeCarli, Gil Rabinovici, William Jagust

09:30 SESSION 7-T7-O-02

Liberal thresholds for PIB-Positivity optimally capture high-burden postmortem Amyloid pathology

Brendan I. Cohn-Sheehy (University of California, San Francisco; Unversity of California, Berkeley; Lawrence Berkeley National Laboratory), Pia M. Ghosh, Sylvia Villeneuve, Gautam Tammewar, Cindee M. Madison, Manja Lehmann, Bruce L. Miller, Lea T. Grinberg, William W. Seeley, Howard J. Rosen, William J. Jagust, Gil D. Rabinovici

09:45 SESSION 7-T7-O-03

Modeling the influence of white matter contamination on detectability of brain Amyloid changes in longitudinal studies of Alzheimer progression: Segmentation analyses using the PET β-Amyloid tracer 18F NAV4694

John Seibyl (Institute for Neurodegenerative Disorders), Osama Sabri, Henryk Barthel, Olivier Barret, Kenneth Marek, Cornelia Reininger

10:00 SESSION 7-T7-O-04

Amyloid PET screening results by APOE ε4 status from a Phase 1b clinical study (221AD103) in patients with prodromal to mild Alzheimer's disease

Chiao Ping (Biogen Idec), Suhy Joyce, Barakos Jerome, Burke Meredith, Klein Gregory, Verma Ajay, Sevigny Jeff

10:15 DISCUSSION SESSION 7

10:45 Break (Regency Ballroom/Ground Floor)

11:05 - 12:35

SESSION 8: Neuropathologic Correlations

CHAIRS: William Klunk (University of Pittsburgh) and Gil Rabinovici (University of California San Francisco)

11:05 SESSION 8-T8-O-01

Diagnostic accuracy of Amyloid and FDG PET in pathologically-confirmed dementia

Gil D. Rabinovici (University of California San Francisco, University of California Berkeley Lawrence Berkeley National Laboratory), Manja Lehmann, Howard J. Rosen, Pia M Ghosh, Brendan I Cohn-Sheehy, John Q. Trojanowski, Mario F. Mendez, Harry V. Vinters, Dennis W. Dickson, Marilu Gorno-Tempini, Adam L. Boxer, Bruce L. Miller, Lea T. Grinberg, William W. Seeley, William J. Jagust

11:20 SESSION 8-T8-O-02

[^{18}F]flutemetamol amyloid PET detection of Aβ plaque phases 4 and 5 and significant diffuse plaque burden

Thomas Beach, Dietmar Thal, Michelle Zanette, Kirsten Heurling, Chris Buckley (GE Healthcare), Adrian Smith

11:35 SESSION 8-T8-O-03

PiB PET and FDG PET quantitative analysis methods with autopsy correlation

Val Lowe (Mayo Clinic, Rochester), Melissa Murray, Emily Lundt, Stephen Weigand, Scott Przybelski, Lenon Jordan, Dennis Dickson, Joseph Parisi, David Knopman, Kejal Kantarci, Clifford Jack, Ronald Petersen

11:50 SESSION 8-T8-O-04

Evaluation of cotton wool plaques using amyloid binding compounds and Aβ immunohistochemistry: implications for PiB PET imaging

Milos Ikonomovic (University of Pittsburgh), Eric Abrahamson, Julie Price, Chester Mathis, William Klunk

12:05	DISCUSSION SESSION 8
12:35	AWARDS
12:45	LUNCH (Starlight Room/Top Floor)

2:15 - 2:45

SESSION 9: KEYNOTE LECTURE

2:15 SESSION 9-T09-O-01

KEYNOTE LECTURE: Senile plaques: Classification, distribution, clinical correlation and Amyloid imaging

Thomas G. Beach (Banner Sun Health Research Institute)

2:45	DISCUSSION SESSION 9

3:00 - 3:45

SESSION 10: Memory Complaints/JADNI

CHAIRS: Reisa Sperling (Massachusetts General Hospital/Harvard Medical School) and Christopher Rowe (Austin Health)

3:00 SESSION 10-T10-O-01

Subjective memory complaints are related to default network disruption in clinically normal older adults with high Amyloid burden

Patrizia Vannini (Brigham and Women's Hospital, Harvard Medical School), Rebecca Amariglio, Andrew Ward, Sarah Wigman, Willem Huijbers, Koene Van Dijk, Aaron Schultz, Tamy-Fee Meneide, Trey Hedden, Dorene Rentz, Keith Johnson, Reisa Sperling

3:15 SESSION 10-T10-O-02

Amyloid burden and neurodegeneration independently contribute to greater subjective cognitive concerns in clinically normal older individuals

Rebecca Amariglio (Brigham and Women's Hospital), Elizabeth Mormino, Patrizia Vannini, Gad Marshall, Keith Johnson, Reisa Sperling, Dorene Rentz

3:30	DISCUSSION
3:45	Break (Regency Ballroom/Ground Floor)

4:05 SESSION 10-T10-O-03

Longitudinal Amyloid deposition with ^{11}C-PiB in Japanese ADNI study

Kenji Ishii (Tokyo Metropolitan Institute of Gerontology), Muneyuki Sakata, Keiichi Oda, Jun Toyohara, Kiichi Ishiwata, Michio Senda, Kengo Ito, Ryozo Kuwano, Takeshi Iwatsubo, Study Group for Japanese Alzheimer's Disease Neuroimaging Initiative

4:20 SESSION 10-T10-O-04

Higher Aβ burden in subjective memory complainers: A flutemetamol sub-study in AIBL

Christopher C Rowe (Austin Health), Vincent Doré, Pierrick Bourgeat, Rachel Buckley, Robyn Veljanoski, Olivier Salvado, Robert Williams, Kevin Ong, Alan Rembach, Lance Macaulay, David Ames, Colin L Masters, Victor L Villemagne

4:35	DISCUSSION

4:50 CLOSING/DISCUSSION

ORAL PRESENTATIONS

SESSION 1: Tau PET I

Chairs: William Jagust (University of California, Berkeley) and Keith Johnson (Massachusetts General Hospital)

PET imaging of tau deposits in Alzheimer's disease patients using ^{18}F-THK5105 and ^{18}F-THK5117

Noboyuki Okamura [1], Shozo Furumoto [2], Ryuichi Harada [1], Katsutoshi Furukawa [3], Aiko Ishiki [3], Michelle Fodero-Tavoletti [4], Rachel Mulligan [5], Ren Iwata [2], Manabu Tashiro [2], Kazuhiko Yanai [1], Colin Masters [4], Hiroyuki Arai [3], Christopher Rowe [5], Victor Villemagne [5], Yukitsuka Kudo [6]

[1] *Department of Pharmacology, Tohoku University School of Medicine, Sendai, Japan*
[2] *Cyclotron and Radioisotope Center, Tohoku University, Sendai, Japan*
[3] *Department of Geriatrics and Gerontology, Institute of Development, Aging and Cancer, Tohoku University, Sendai, Japan*
[4] *The Florey Institute of Neuroscience and Mental Health, The University of Melbourne, VIC, Australia*
[5] *Centre for PET, Austin Health, Melbourne, Australia*
[6] *Clinical Research, Innovation and Education Center, Tohoku University Hospital, Sendai, Japan*

Background: Non-invasive imaging of tau protein deposits would be useful for early and differential diagnosis of dementia, tracking disease progression and evaluating treatment efficacy in Alzheimer's disease (AD). We have developed two PET tracers, ^{18}F-THK5105 and ^{18}F-THK5117, that label tau protein deposits with high affinity and high selectivity. In this study, we evaluated the clinical usefulness of ^{18}F-THK5105 and ^{18}F-THK5117 as tau-imaging radiotracers in AD patients.

Methods: Sixteen subjects (8 AD patients and 8 age-matched healthy control (HC) subjects) underwent ^{18}F-THK5105 PET scans at Austin Health. Fifteen subjects (8 AD patients and 7 HC subjects) underwent ^{18}F-THK5117 PET scans at Tohoku University. In both clinical studies, standard uptake value ratios (SUVR) were calculated using the cerebellar cortex as the reference region. Regional distribution of ^{18}F-THK5105 or ^{18}F-THK5117 in the brain was compared to that of PiB.

Results: No toxic event was observed during the clinical studies. Most AD patients showed ^{18}F-THK5105 and ^{18}F-THK5117 retention in the lateral and medial temporal cortices, areas known to contain high concentrations of tau deposits in AD. Regional distribution of ^{18}F-THK5105 and ^{18}F-THK5117 differed considerably from that of ^{11}C-PiB in AD patients. ^{18}F-THK5117 showed faster kinetics and higher signal-to-background ratio than ^{18}F-THK5105. ^{18}F-THK5105 and ^{18}F-THK5117 retention in the neocortex was associated with the severity of dementia. In HC subjects, ^{18}F-THK5105 and ^{18}F-THK5117 retention was significantly higher in the hippocampus than in the neocortex.

Conclusion: Both ^{18}F-THK5105 and ^{18}F-THK5117 selectively binds to tau in AD patients, providing regional quantitative information on tau deposits in living subjects.

Presented by: Okamura, Nobuyuki

Tau deposition estimated by [^{11}C]PBB3 PET in Alzheimer's disease, MCI with and without amyloid deposition, and cognitive healthy subjects

Hitoshi Shimada [1], Makoto Higuchi [1], Hitoshi Shinotoh [2], Shigeki Hirano [3], Shogo Furukawa [3], Yoko Eguchi [1], Keisuke Takahata [1], Fumitoshi Kodaka [1], Yasuyuki Kimura [1], Makiko Yamada [1], Masahiro Maruyama [1], Harumasa Takano [1], Ming-Rong Zhang [1], Hiroshi Ito [1], Tetsuya Suhara [1], et al.

[1] Molecular Imaging Center, National Institute of Radiological Sciences, Chiba-shi, Chiba, Japan
[2] Molecular Imaging Center, National Institute of Radiological Sciences, Chiba-shi, Chiba, Japan; Neurology Chiba, Chiba-shi, Chiba, Japan
[3] Molecular Imaging Center, National Institute of Radiological Sciences, Chiba-shi, Chiba, Japan; Department of Neurology, Graduate School of Medicine, Chiba University, Chiba-shi, Chiba, Japan

Background and aims: [^{11}C]PBB3 is a novel tau imaging PET ligand, showing high affinity and selectivity for tau deposits. Our preliminary clinical data suggested [^{11}C]PBB3 binding could reflect the dementia severity in AD patients. The aim of the present study was to investigate characteristics of [^{11}C]PBB3 binding and its relation with clinical aspects in cognitively healthy subjects and patients with cognitive impairments.

Methods: Participants were 14 AD patients, 13 mild cognitive impairments (MCI) patients and 22 healthy controls (HCs). We performed [^{11}C]PBB3 PET as well as [^{11}C]PIB PET. Standardized uptake value ratio (SUVR) was calculated for each PET image using the cerebellar cortex as reference region. Three-dimensional T1-weighted MRI was also acquired, and brain atrophy was also assessed using voxel-based morphometry technique.

Results: All HCs were PIB-negative, and all AD patients and 7 of 13 MCI patients were PIB-positive. [^{11}C]PBB3 was highly accumulated in the medial temporal cortex of all AD and PIB-positive MCI patients, in which binding of [^{11}C]PIB was minimal. Distribution of [^{11}C]PBB3 accumulation observed in AD and PIB-positive MCI patients extended to the entire limbic system and subsequently to the neocortex as a function of the disease severity. Mean cortical [^{11}C]PBB3 binding showed significantly positive correlation with dementia severity assessed with clinical dementia rating scale (CDR) sum of boxes among AD and PIB-positive MCI patients ($r = 0.67$, $p = 0.02$; adjusted by age and educational background). Some PIB-negative MCI patients and HCs showed noticeable accumulation of [^{11}C] PBB3. Interestingly, one PIB-negative MCI patients showed asymmetrical cortical atrophy around ambient gyrus resembling argyrophilic grain dementia (AGD), a sporadic 4-repeat tauopathy, accompanying high uptake of [^{11}C]PBB3.

Conclusions: The present study supported the spread of [^{11}C]PBB3 binding reflect the dementia severity in AD and MCI due to AD patients. Furthermore, [^{11}C]PBB3 PET could enable the antemortem diagnosis of AGD.

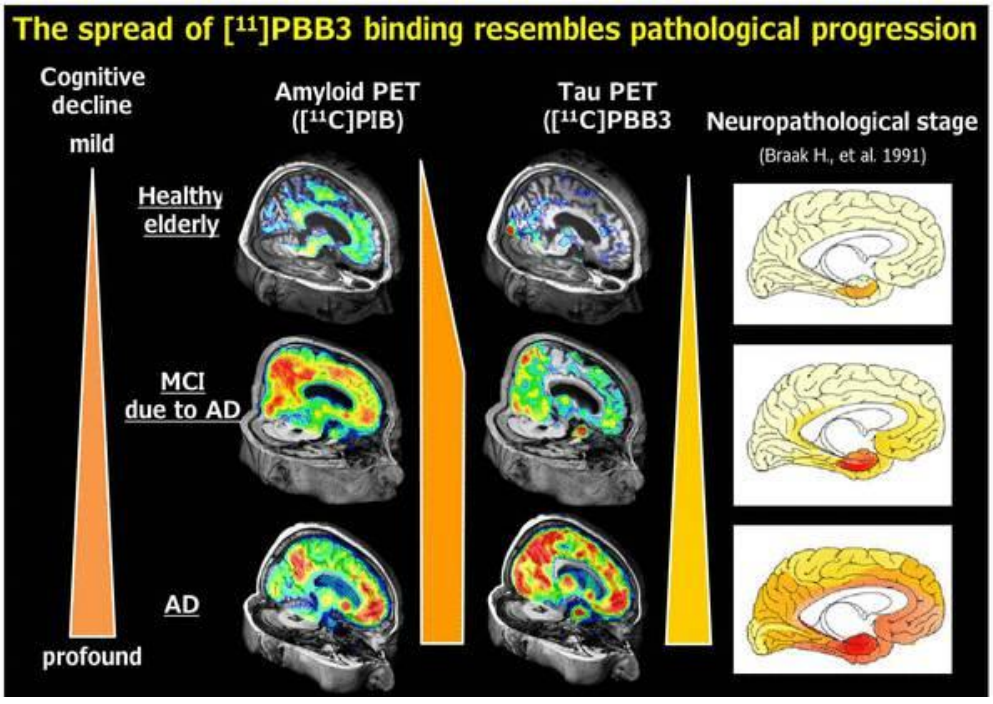

Keywords: *Tau imaging, [11C]PBB3, Alzheimer's disease, mild cognitive impairment, argyrophilic grain dementia*

Presented by: Shimada, Hitoshi

Tau PET: Initial experience with F18 T807

Keith Johnson , John A. Becker , Jorge Sepulcre , Dorene Rentz , Aaron Schultz , Leslie Pepin , Marlie Philiossaint , Jonathan Alverio , Kelly Judge , Neil Vasdev , Tom Brady , Brad Hyman , Reisa Sperling

Massachusetts General Hospital

Recent development of [F18] T807, a PET tracer that selectively binds paired helical filament tau aggregates, has enabled imaging of tangle pathology *in vivo*. Here we report our initial experience with T807 tau PET in Alzheimer disease (AD) dementia, mild cognitive impairment (MCI), and in clinically normal (CN) subjects, investigating the relationship between tau PET, amyloid-β PET, and cognitive performance. Five AD, 5 MCI, and 30 older CN individuals (mean age, SD = 74.1, 6.8) underwent tau PET imaging with [18F] T807, amyloid PET imaging with [11C] PiB, and cognitive testing. PET measures of T807 (20 min. acquisition from 80 – 100 min.; SUVRcerebellum) and PiB (0 - 60 min. acquisition; DVRcerebellum) were evaluated in cortical regions. When the impaired subject group (AD and MCI) was compared to the CN group (SPM, threshold $p<0.005$) elevated T807 binding was seen in neocortical regions, more prominently temporal and occipital. More severely impaired subjects' binding extended to parietal and frontal areas. Among CNs, T807 binding was 1) most intense in hippocampus and its posterior extension into the fornix; 2) highly variable in temporal allocortex; and 3) at low levels in neocortex. In the full sample, worse memory performance on delayed recall (Logical Memory-IIa) was associated with greater T807 binding in entorhinal cortex (FS ROI; r-sq = 0.46; $p<0.0001$), and with greater global cortical PiB retention (r-sq = 0.14; $p<0.04$). These preliminary findings suggest that T807 PET is a promising new biomarker that relates to both clinical and cognitive status.

Keywords: *Tau PET, Amyloid PET*

Presented by: Johnson, Keith

SESSION 2: Tau PET II

Chairs: Victor Villemagne (Austin Health) and Mark A. Mintun (Avid Radiopharmaceuticals, Inc.)

Detection of PHF-Tau pathology with T557, T726 and [18F]-T807 in brain sections from Alzheimer's and non-Alzheimer's tauopathy patients

Hartmuth C. Kolb , Giorgio Attardo , Kelly Conway , Felipe Gomez , Qianwa Liang , Yin-Guo Lin , Andrew Siderowf, Daniel M. Skovronsky , Mark A. Mintun

Avid Radiopharmaceuticals, Inc.

Background: The fluorescent probes T557 and T726, and the radiolabeled analog [18F]-T807 were shown to bind to PHF-Tau in brain sections from Alzheimer's Disease (AD) patients, raising the question, whether they would also adhere to PHF-Tau in non-AD tauopathies, such as Chronic Traumatic Encephalopathy (CTE), Frontotemporal Dementia (FTD), Pick's Disease and Progressive Supranuclear Palsy (PSP).

Objective: To compare the Tau ligand staining of AD and non-AD brain sections with immunohistochemistry staining, in order to evaluate whether these ligands bind to non-AD Tau.

Methods: Brain sections from AD, CTE, FTD, PSP and Pick's Disease patients were stained with various Tau antibodies, specifically the phospho-Tau antibodies, AT8 and AT100, 3R-Tau and 4R-Tau antibodies, the conformational Tau antibody, MC-1, the total Tau antibody, DA9, and the nitrated Tau antibody, nY29. Pair-wise staining (i.e. immunohistochemistry – T557 or T726 double staining) was performed to investigate whether the small molecule ligands are capable of marking the same Tau pathology as the antibodies. Additionally, autoradiography staining with [18F]-T807 in the absence and the presence of "cold" T807 was conducted to investigate the radioligand's ability to label Tau pathology in the brain samples.

Results: Generally, a good agreement between the immunohistochemistry and fluorescence staining patterns was observed for the AD and non-AD samples. Autoradiography staining with [18F]-T807 is blocked by addition of "cold" T807, suggesting specific binding.

Conclusions: The match between immunohistochemistry and T557/T726 fluorescence staining suggests that these agents are able to label Tau pathology in the AD and non-AD samples studied. Autoradiography experiments with the labeled analogue, [18F]-T807, suggest that radioligand binding is specific in nature.

Keywords: *Tau imaging,Alzheimer's Disease,Non AD Tauopathy,Pathology*

Presented by: Skovronsky, Daniel M.

Imaging tau pathology in vivo in FTLD: initial experience with [18F] T807 PET

Brad Dickerson , Kimiko Domoto-Reilly , Daisy Sapolsky , Michael Brickhouse , Michael Stepanovic , Keith Johnson

Massachusetts General Hospital/Harvard Medical School

Objective: To image tau pathology in vivo using PET in patients with Frontotemporal Lobar Degeneration (FTLD)

Background: A critical unmet need for FTLD research, especially therapeutic trials, is the development of biomarkers to distinguish FTLD-tau from FTLD-TDP and other non-tau FTLD pathologies.

Methods: We are using [18F] T807, a novel PET ligand, to scan a series of patients with FTLD, to date including one MAPT P301L mutation carrier with moderate severity FTD dementia, an asymptomatic carrier of the same mutation, and a patient with sporadic mild progressive agrammatic aphasia. We analyzed SUVR (cerebellum reference) data to localize and quantify [18F] T807 signal. We also co-registered analyzed [18F] T807 images to MRI images for visualization and calculation of % atrophy relative to controls.

Results: [18F] T807 signal was elevated in frontal, insular, and anterior temporal cortex in symptomatic patients, and colocalized with atrophy. In the aphasic patient, [18F] T807 signal was highest in inferior frontal and middle temporal gyri and temporal pole with marked asymmetry, most prominent in the dominant hemisphere, and localized remarkably well with atrophy. The asymptomatic carrier had mildly elevated signal in frontal, insular, and anterior temporal cortex as well as white matter.

Conclusions: T807 is a promising new PET ligand for imaging tau pathology in vivo in patients with FTLD.

Funding: R21NS084156, R21NS077059, P50-AG005134

Keywords: *tau, frontotemporal dementia, progressive aphasia*

Presented by: Dickerson, Brad

PET Tau imaging with [F-18]-T807 (AV-1451) in normal subjects and patients with cognitive impairment due to Alzheimer's disease: Review of initial analyses

Mark A. Mintun [1], Abhinay Joshi [1], Sergey Shcherbinin [2], Adam J. Schwarz [2], Ming Lu [1], Michael Pontecorvo [1], Michael Devous Sr. [1], Daniel M. Skovronsky [1], Hartmuth Kolb [1]

[1] *Avid Radiopharmaceuticals, Inc.*
[2] *Eli Lilly and Company*

Background: [F-18]-T807 (also known as [F-18]-AV-1451) was reported (Xia et al., 2013) as having high affinity and selectivity to the aggregated fibrillar form of tau pathology. Chien et al. (2012) described the first PET imaging results in 6 human subjects. Additional subjects have now been studied with [F-18]-T807 and the combined data are under analysis.

Methods: To date, 33 [F-18]-T807 PET scans have been completed. Whole Body PET: 9 participants (age 56.3 ± 4.4 S.D. years) underwent a biodistribution study in which multiple whole body PET scans were obtained over 6 hours after iv injection of T807. Brain PET: 24 subjects received brain imaging comprising of dynamic (0-60 min) and static (80-100 min) scans after injection of approximately 10 mCi of T807: 3 young healthy subjects (27.0 ± 1.7 years), 7 old healthy subjects (64.0 ± 3.8 years), 5 diagnosed with mild cognitive impairment (MCI) likely due to AD (76.2 ± 4.8 years), and 9 clinically diagnosed with AD (70.8 ± 8.5 years). Images were viewed with co-registered T1-weighted MRI scans. Quantitative processing comprises intra-subject scan registration, spatial normalization to MNI space and application of AAL regions with cerebellum as a reference region.

Results: Biodistribution demonstrated predominantly hepatobiliary clearance with some urinary excretion. Dosimetry estimates will be presented. Brain images visually demonstrated increased T807 retention, with some areas showing intense uptake, in patterns similar to Braak tau staging for aging, MCI and AD patients. Quantitative analysis with both kinetic and static data will be presented, but preliminary results appear to confirm the visual impression in that increasing age and impairment are associated with higher T807 retention. For example, current 80-100 min scan analysis, show the SUVR values in multiple regions significantly ($p<0.05$) correlate with Mini-Mental State Exam scores.

Conclusions: Further investigation of [F-18]-T807 PET to image tau deposits is warranted.

Keywords: *Alzheimer's Disease,Tau,biodistribution,disease progression*

Presented by: Mintun, Mark A.

SESSION 3: KEYNOTE LECTURE

Tau protein - from native unfolding to pathological folding: structural aspects of Tau, Tau aggregates, and Tau interacting compounds

Eckhard Mandelkow, Eva-Maria Mandelkow

DZNE, German Center for Neurodegenerative Diseases, CAESAR Research Center/Max-Planck Soc.

This presentationtation will summarize structural features of Tau that are relevant to understanding its interactions with cell components, drug-like compounds, and its assembly into pathological fibers.

- Tau is a major microtubule-associated protein in the brain, located mainly in neurons. Its primary role is the stabilization of microtubules, but in addition it interacts with numerous other cell components (cytoskeletal proteins, signalling proteins, chaperones, RNA etc.). Tau is normally restricted to axons, due to axon-directed sorting mechanisms and a retrograde barrier at the axon initial segment, but in pathological conditions Tau becomes missorted into the somatodendritic compartment (which represents an early marker of neurodegeneration).
- Tau occurs in 6 main isoforms in the CNS generated by alternative splicing of the gene on chromosome 17. The isoforms differ by two near-N-terminal inserts (29-mers, N1, N2, encoded by exons 2, 3) and the second of four quasi-repeated 31-mers (R2, encoded by exon 10). The largest human isoform contains 441 residues, the smallest 352.
- The sequence of Tau is dominated by hydrophilic/charged residues which prevent folding into a compact structure. Tau is therefore the prototype of a "natively unfolded" and highly soluble protein, which makes it accessible to multiple interactions and modifications (e.g. phosphorylation, proteolysis).
- Because of its unfolded nature, Tau is largely devoid of secondary structure and is flexible and dynamic along the entire chain. However, there are some short-lived elements of secondary structure (alpha helix, poly-proline II helix, beta strand). Some transient short beta strands (hexapeptide motifs 275-VQIINK-280 at the beginning of R2 and 306-VQIVYK-311 in R3) can become stabilized by inter-chain interactions and can thus form the beta-sheet nucleus of self-assembly into filaments. Thus, from a protein folding perspective, "pathological misfolding" of Tau corresponds to a gain of folded structure, rather than a loss of proper folding.
- In spite of predominant disorder, Tau tends to assume a global conformation whereby the N- and C-terminal domains approach each other and the repeat domain ("paperclip" conformation). This arrangement of domains tends to protect the repeat domain from self-assembly; conversely this explains why opening-up of the repeat domain (e.g. by proteolysis of adjacent domains) unprotects it and promotes self-assembly.
- Self-assembly can be promoted by compensating the overall positive charge of Tau by negatively charged molecules, e.g. by heparin, RNA, acidic peptides etc. Some of this interaction may mimick the interaction of Tau with the acidic C-terminal domain of tubulin.
- Self-assembly is also promoted by modifying the beta-propensity around the hexapeptide motifs, which can be enhanced (leading to "pro-aggregant" forms of Tau, examples are the mutations DeltaK280 and P301L that occur in familial frontotemporal dementias) or suppressed (e.g. by inserting beta-breaking prolines into the hexapeptide motifs, leading to "anti-aggregant" Tau). Since assemblies of Tau (fibers and oligomers) tend to be toxic to neurons, such mutations can be used to generate cell or animal models with accelerated Tau pathology, or control models where fiber assembly is prevented.
- The core of Tau filaments is formed by the repeat domain (in particular repeats R2, R3) which becomes immobilized and acquires enhanced beta structure (comprising <25% of the Tau sequence). This is thought to explain the increased interaction with fluorescent dyes such as thioflavin S or T which are used to stain Tau fibers and neurofibrillary tangles in vitro and in situ. The domains flanking the repeats (>75%) cover the surface of Tau filaments in a highly flexible and disordered fashion, resembling a "polymer brush" (also called "fuzzy coat"). This surface coat has a low contrast by standard imaging methods (e.g. electron microscopy, atomic force microscopy) so that fibers made of full-length Tau tend to resemble fibers made of the repeat domain only.
- The interaction of Tau with its major cellular partner, microtubules, is also based on the repeat domain (largely determined by the complementary charges of Tau and the tubulin C-terminal tail), but strong Tau-MT binding requires in addition the domains flanking the repeat domain of Tau ("jaws"-model). Tau lacking the repeat domain binds to MT in a non-productive manner, i.e. it lacks the ability to induce MT-assembly. The binding of Tau to MT is biphasic and does not lead to a defined saturation, i.e. Tau can be "overloaded" on the MT surface.
- The repeat domain of Tau also accounts for interactions with other molecules (e.g. chaperones, RNA, drugs such as methylene blue). By contrast, interactions with important signalling molecules containing SH3-domains (e.g. tyrosine kinases fyn, src, scaffold proteins PSD-95) are determined by the "proline-rich" domain preceding the repeats which contains several PXXP motifs.
- The interaction of Tau with microtubules, as well as the interactions leading to Tau self-assembly, are strongly modulated by posttranslational modifications of Tau, notably by phosphorylation. Tau contains numerous Ser/Thr residues, almost all of which can be phosphorylated by various Ser/Thr kinases, due to Tau's disordered state. Dephosphorylation can be achieved by several phosphatases, notably by PP-2a. The physiological role of many phosphorylation sites is still poorly understood. Phosphorylation in the repeat domain (notably at the KXGS motifs) decreases the affinity for microtubules and therefore detaches Tau from MT.
- In pathological conditions (Alzheimer disease and other tauopathies), Tau occurs in a state of enhanced phosphorylation ("hyperphosphorylation"). This is likely due to an altered balance between kinases and phosphatases, and/or to the inability of phosphatases to clear phosphates from assembled forms of Tau. Hyperphosphorylation can be detected by various phosphorylation site-specific antibodies which are therefore important tools for diagnosing pathological conditions. This holds in particular for the numerous Ser-Pro motifs which can be phosphorylated by proline-directed kinases.
- In Alzheimer disease, assembled forms of Tau appear to spread in a well-defined pattern along anatomically connected pathways, starting from the entorhinal region and hippocampus towards the cortex. There is a close correspondence between the distribution of aggregated Tau and the clinical stages of dementia (Braak stages). Several mechanisms have been proposed to contribute to the spreading of Tau pathology, including (transsynaptic) signalling events, the transfer of Tau molecules between cells, the "prion-like" imprinting of pathological Tau conformations to endogenous Tau, etc.
- Several Tau-based treatment approaches to neurodegeneration have been proposed. They include the reduction of Tau phosphorylation (by kinase inhibitors), upregulation of Tau dephosphorylation (by activation of phosphatases), downregulation of pathological intracellular Tau (e.g. via pathways based on proteasomes, autophagy, chaperones), scavenging of extracellular Tau (by antibodies), stabilization of microtubules (to compensate for loss of Tau binding), and inhibition of Tau assembly (by assembly-blocking small molecules, for example methylene blue). These approaches are still in different stages of exploration.

Review: *Mandelkow EM, Mandelkow E (2012). Biochemistry and cell biology of tau protein in neurofibrillary degeneration.* Cold Spring Harb. Perspect. Med. 2:a006247.

SESSION 4: Abeta PET: Assessment of Cognition and Disease Progression

CHAIRS: Susan Landau (University of California, Berkeley) and Prashanthi Vemuri (Mayo Clinic Rochester)

Amyloid change early in disease is related to increased glucose metabolism and episodic memory decline

Susan Landau [1], Allison Fero [2], Suzanne Baker [2], William Jagust [3]

[1] *UC Berkeley*
[2] *Lawrence Berkeley National Lab*
[3] *UC Berkeley, Lawrence Berkeley National Lab*

We examined longitudinal cortical florbetapir retention, glucose metabolism in a set of pre-defined ROIs (metaROIs), and episodic memory measurements over a two year interval in ADNI Normal (N=68), Early MCI (N=84), Late MCI (N=28), and AD participants (N=15; 195 participants total). We addressed several methodological challenges related to the measurement of florbetapir change. For example, in order to reduce the influence of intra-individual changes in nonspecific white matter retention over time, we used a combination of reference regions that included subcortical white matter, brainstem, and cerebellum.

Average annual absolute florbetapir change was reasonably consistent across diagnostic groups (1.3 – 1.6% change) but was highly variable across individuals (SD=1.0-1.2%). Glucose metabolism declined on average, with greater declines observed with increasing diagnostic severity (range: -0.7 to -4.6% annual decline), and these measurements were also variable (SD=2.9 – 4.1%).

Florbetapir and glucose metabolism metaROI change were related such that normal and EMCI individuals who were amyloid-positive at baseline (but not those who are amyloid-negative, and not other diagnostic groups) had increasing glucose metabolism that correlated with increasing florbetapir uptake (N=75, $R = 0.31$, $p = 0.007$) controlling for age, sex, education, and ApoE4 status. This relationship remained significant after eliminating several individuals who had decreasing glucose metabolism and decreasing florbetapir, which could reflect partial volume effects.

We also observed an association between florbetapir and memory change, but only in normal individuals. In normal, increasing florbetapir was associated with worsening episodic memory (N=44, R=-0.33, p=0.03), controlling for age, sex, education, and ApoE4 status.

Our findings indicate that amyloid-positive but cognitively normal and EMCI individuals experience a period of glucose hypermetabolism that parallels further increases in amyloid deposition. Furthermore, increasing amyloid in amyloid-negative and amyloid-positive normals has subtle but significant consequences for episodic memory performance.

Keywords: *episodic memory, FDG-PET*

Presented by: Landau, Susan

Amyloid-β deposition in mild cognitive impairment is associated with hippocampal hyperactivation, atrophy and clinical progression

Willem Huijbers [1], Elizabeth Mormino [2], Aaron Schultz [2], Jasmeer Chhatwal [2], Brendon Boot [1], Rebecca Amariglio[1], Gad Marshall [1], Dorenne Rentz [1], Keith Johnson [2], Reisa Sperling [1]

[1] Center for Alzheimer Research and Treatment, Department of Neurology, Brigham and Women's Hospital, Harvard Medical School, Boston. Athinoula A. Martinos Center for Biomedical Imaging, Department of Neurology, Massachusetts General Hospital.
[2] Athinoula A. Martinos Center for Biomedical Imaging, Department of Neurology, Massachusetts General Hospital, Harvard Medical School, Charlestown, Department of Radiology, Massachusetts General Hospital, Harvard Medical School, Boston

Rationale: Hyperactive neurons may facilitate the deposition of amyloid-β and promote excitotoxic neuronal loss. Older adults with mild cognitive impairment (MCI) often demonstrate hippocampal hyperactivity, as measured by task-based functional magnetic resonance imaging (fMRI) and this has been linked to clinical progression of Alzheimer's disease (AD). Recent studies have demonstrated that MCI patients with elevated cortical amyloid-β (Aβ+ MCI) are also more likely to progress to AD dementia compared to MCI patients with low cortical amyloid-β (Aβ- MCI). However, it remains unclear if hippocampal hyperactivation in the presence of amyloid-β is associated with clinical progression.

Methods: We followed 33 MCI's longitudinally for up to 36 months and examined baseline amyloid deposition in relation to longitudinal measures of hippocampal fMRI activity, hippocampal volume (HV) and clinical progression. Amyloid-β deposition was assessed using PiB-PET imaging and predefined cortical regions of interest. FMRI activity in the hippocampus was assessed using a face-name memory test (contrasting novel faces versus passive rest). HV was quantified using structural MRI. Finally, clinical progression was assessed using the Clinical Dementia Rating sum of boxes (CDR-SB).

Results: We found that at baseline, Aβ+ MCI's showed hippocampal hyperactivation, smaller HV, and worse CDR-SB scores compared to Aβ- MCI's. Over time, Aβ+ MCI's were also more likely to progress clinically and show hippocampal atrophy. Finally, a linear mixed effects model indicated that baseline HV was the strongest predictor of clinical decline followed by longitudinal fMRI activity and baseline levels of amyloid-β.

Conclusion: These finding demonstrate that MCI patients with elevated cortical amyloid-β are more likely to show hippocampal hyperactivation, hippocampal atrophy, and clinical progression over time. Together, these results suggest that amyloid deposition promotes excitotoxic loss of neurons in the hippocampus of MCI's who are likely to develop AD dementia.

Keywords: *hyperactivation, longitudinal fMRI, MCI, amyloid-β, cognitive decline*

Presented by: Huijbers, Willem

Gene-Environment interactions over the lifecourse: Cognitive activity, apolipoprotein E genotype, and brain beta-amyloid

Miranka Wirth , Sylvia Villeneuve , Renaud La Joie , Shawn Marks , William Jagust

Helen Wills Neuroscience Institute, University of California, Berkeley, CA 94720, USA

Objective: Some data has suggested that cognitive activity reduces AD risk by mitigating the deposition of the β-amyloid (Aβ) protein, thought to be an instigator of AD development. We examined the relationships between cognitive activity over different periods of life and brain Aβ burden in carriers of the APOE ε4 allele, the major genetic risk factor of AD.

Methods: We obtained measures of lifetime cognitive activity in 92 cognitively normal older individuals (mean age: 75.26 [SD = 5.57] years) using a validated questionnaire that included measures during early, middle, and current life epochs. Regression models were conducted to examine effects of APOE ε4 carrier status, cognitive activity and the interaction of the two factors with cortical Aβ deposition, quantified using [11C] Pittsburgh-compound-B (PIB)-PET.

Results: As expected, the APOE ε4 carriers exhibited higher PIB retention compared to non-carriers. There was, however, a significant interaction between lifetime, in particular early and middle life, cognitive activity and APOE genotype (Figure 1, A-C). That is, PIB retention was diminished in cognitively active ε4 carriers to a level seen in cognitively active non-carriers. Less cognitively active ε4 carriers exhibited increased PIB retention throughout heteromodal cortical areas (Figure 2).

Conclusion: The findings suggest that higher lifetime cognitive activity may forestall AD pathology in APOE ε4 carriers. The pronounced effect in earlier life could indicate that training effects promote increased neural efficiency that retards the lifelong neurally-mediated deposition of brain Aβ.

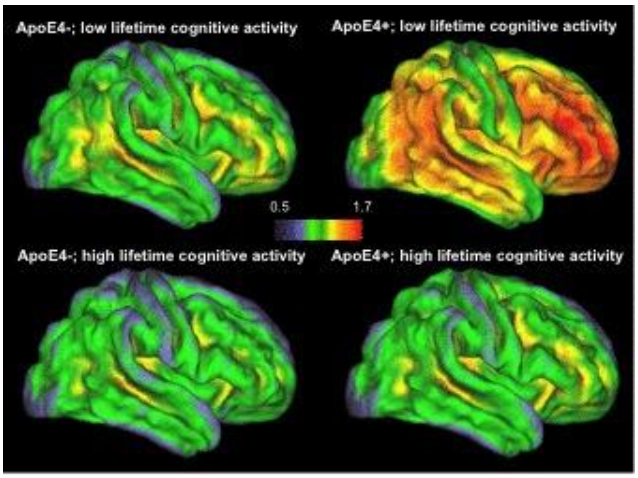

Figure 2: Estimated cortical PIB retention for APOE ε4 carrier status (ApoE4+, ApoeE4-) and lifetime cognitive activity (low, high). APOE ε4 carrier with low lifetime cognitive activity exhibit increased PIB retention.

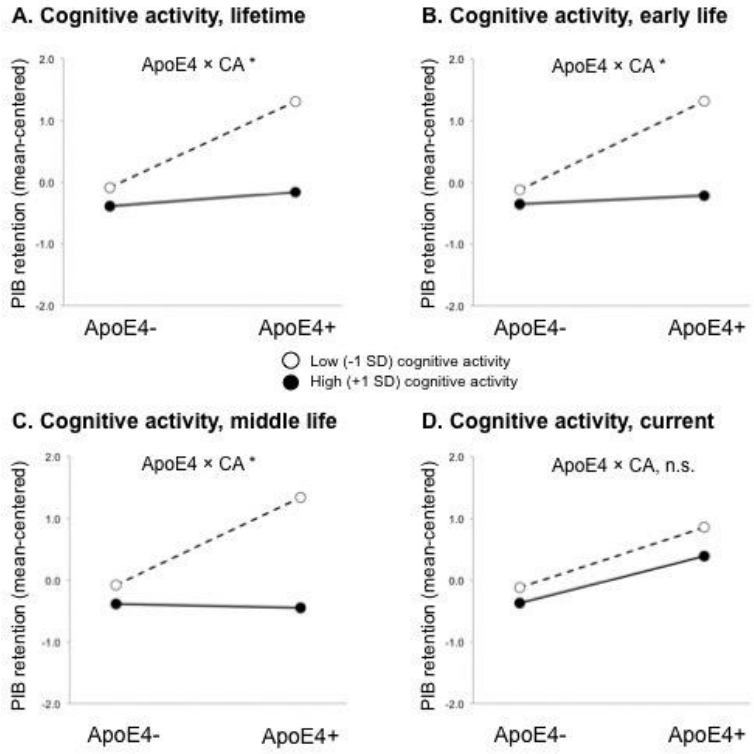

Figure 1: Interaction between APOE ε4 carrier status (ApoE4+, ApoeE4-) and cognitive activity (CA, early, middle and current life). Asterisks indicate significant interaction.

Keywords: *Alzheimer's disease, Aging, Lifestyle Activity, APOE, Beta-aymloid*

Presented by: Wirth, Miranka

Preclinical effects of Aβ deposition on episodic memory and disease progression

Victor L Villemagne [1], Samantha Burnham [2], Pierrick Bourgeat [3], Belinda Brown [4], Kathryn Ellis [5], Olivier Salvado [3], Ralph Martins [4], Lance Macaulay [6], David Ames [7], Colin L Masters [8], Christopher C Rowe [1]

[1] *Department of Nuclear Medicine & Centre for PET, Austin Health, Melbourne, VIC, Australia*
[2] *CSIRO Preventative Health Flagship: Mathematics, Informatics and Statistics, Floreat, WA, Australia*
[3] *CSIRO Preventative Health Flagship: The Australian e-Health Research Centre, Brisbane, QLD, Australia*
[4] *Edith Cowan Univerity, Perth, WA, Australia*
[5] *Dept of Psychiatry, The University of Melbourne, VIC, Australia*
[6] *CSIRO Preventative Health Flagship: Materials Science and Engineering, Melbourne, VIC, Australia*
[7] *National Ageing Research Institute, Melbourne, VIC, Australia*
[8] *The Florey Institute of Neuroscience and Mental Health, The University of Melbourne, VIC, Australia*

Background: Predicting the rate of evolution of preclinical changes and the onset of clinical phase of AD might prove essential for the design and timing of disease-modifying therapeutic interventions.

Methods: 207 participants (152 HC; 36 MCI; 19 AD) underwent periodic neuropsychological examination, MRI and PiB-PET scans for a mean follow up of 4.2 (CI 3.4-4.8) years. A $SUVR_{cb}$ of 1.5 was used to discriminate high (Aβ+) from low (Aβ-) Aβ burdens. Analyses were adjusted for age, gender, years of education, and ApoE status.

Results: 170 (82%) of 207 participants (79% HC, 89% MCI, 100% AD), were deemed Aβ accumulators. In HC and MCI, Aβ deposition and memory decline were significantly faster in Aβ+ than in Aβ-. Aβ deposition was significantly faster in participants who transitioned to either MCI or AD, although baseline Aβ burden was a better predictor of progression. Significant associations between rates of Aβ deposition and rates of episodic memory (EM) decline were found in HC (R^2=0.13; p=0.004). There were no associations between Aβ deposition and EM decline in MCI or AD. When Aβ+HC and Aβ-HC were considered separately, a significant association between rates of Aβ deposition and EM decline was found only in Aβ+HC (R^2=0.22; p=0.022), association that persisted after adjusting for baseline Aβ burden. There was no association between rates of Aβ deposition and EM decline in Aβ-HC, not even when those with positive rates of Aβ accumulation were examined separately.

Conclusions: Aβ seems to have a threshold/trigger effect on EM at the early stages of Aβ deposition. While this support the theory that Aβ plays a fundamental role in the development of AD, it suggests that other factors have a more direct effect on symptom progression at later stages of the disease. These results also suggest that in order to prevent memory decline, anti-Aβ therapy should target these early stages of Aβ deposition.

Keywords: *Aβ deposition, memory decline, disease progression*

Presented by: Villemagne, Victor L

SESSION 5: Abeta PET: Relation to Co-morbid Conditions

CHAIRS: Clifford Jack (Mayo Clinic Rochester) and Ann Cohen (University of Pittsburgh School of Medicine)

Vascular and amyloid pathologies are independent predictors of cognitive decline in cognitively normal elderly

Prashanthi Vemuri , Timothy Lesnick , Scott Przybelski , David Knopman , Gregory Preboske , Kejal Kantarci , Mary Machulda , Michelle Mielke , Val Lowe , Matthew Senjem , Jeffrey Gunter , Ronald Petersen , Clifford Jack

Mayo Clinic Rochester

Objective: To investigate the effect of vascular and amyloid pathologies on rate of cognitive decline in cognitively normal elderly between 70-90 years of age.

Methods: We studied 393 cognitively normal (CN) elderly participants in the population-based Mayo Clinic Study of Aging who had a baseline 3T FLAIR-MRI assessment, PiB-PET scan, baseline cognitive assessment, lifestyle measures and at least one additional clinical follow-up. We computed Aβ load from PiB-PET images and white matter hyperintensity load (WMH) from FLAIR-MRI images using automated pipelines. Brain infarcts [Cortical (≥1 cm) and subcortical infarcts] were ascertained by a trained analyst and confirmed by a radiologist. We classified subjects as being in the amyloid pathophysiological pathway if they had an Aβ SUVR≥1.5 and in a vascular pathway if they had a brain infarct and/or WMH load ≥ 1.11% of total intracranial volume (TIV) [which corresponds to top 25% of WMHs in an independent non-demented sample from the MCSA]. We used a multi-domain global cognitive Z-score as a measure of cognition. We used linear mixed-effects models to investigate the associations of demographics, lifestyle measures, and presence or absence of vascular and amyloid pathologies with global cognitive Z-score trajectories.

Results: In this population-based sample of CN elderly, 21% of subjects had only amyloid pathology, 23% had only vascular pathology and 11% had both vascular and amyloid pathologies. Baseline cognitive performance was lower in older individuals, males, those with lower education/occupation, and those on the amyloid or vascular pathway ($p<0.001$ for all). Higher rates of cognitive decline were associated with increasing age ($p<0.001$) and with amyloid ($p=0.0003$) or vascular ($p=0.0037$) pathologies. In subjects with both vascular and amyloid pathologies, the effect of pathologies on cognition was additive and not multiplicative.

Interpretation: Amyloid and vascular pathologies appear to be independent processes that both affect baseline cognition and cognitive decline adversely.

Keywords: *PIB, White matter hyperintensities, brain infarcts, vascular pathologies, longitudinal cognitive decline*

Presented by: Vemuri, Prashanthi

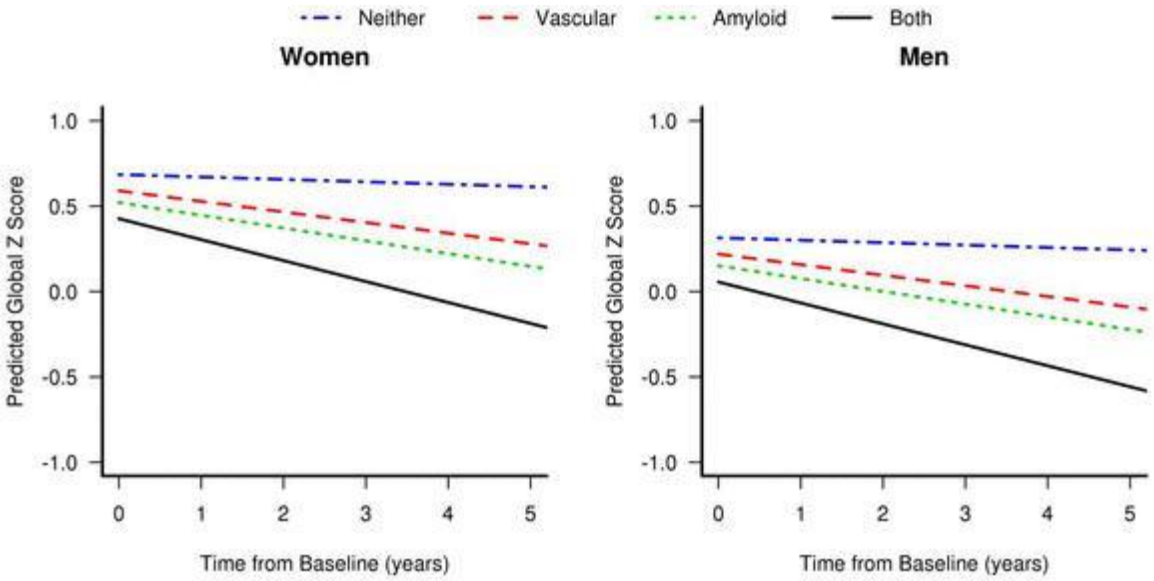

Multiple brain markers contribute to age-related variation in cognition

Trey Hedden [1], Aaron Schultz [1], Anna Rieckmann [1], Elizabeth C. Mormino [2], Keith A. Johnson [3], Reisa A. Sperling [4], Randy L. Buckner [5]

[1] Athinoula A. Martinos Center for Biomedical Imaging, Department of Radiology, Massachusetts General Hospital, Harvard Medical School
[2] Department of Neurology, Massachusetts General Hospital, Harvard Medical School
[3] Athinoula A. Martinos Center for Biomedical Imaging, Departments of Radiology and Neurology, Massachusetts General Hospital, Harvard Medical School;
[4] Athinoula A. Martinos Center for Biomedical Imaging, Departments of Radiology and Neurology, Massachusetts General Hospital, Harvard Medical School; Center for Alzheimer Research and Treatment, Department of Neurology, Brigham and Women's Hospital
[5] Athinoula A. Martinos Center for Biomedical Imaging, Department of Radiology, Massachusetts General Hospital, Harvard Medical School; Department of Psychology and Center for Brain Science, Harvard University

Rationale: Although aging is accompanied by evident changes in brain morphometry, function, and disease-related biomarkers, direct links between neural markers and cognition have been elusive. Most studies have compared a small number of brain markers or exhibit relatively small effect sizes (Hedden et al., 2013; Salthouse, 2011). Here, we examined shared and selective contributions of multiple brain markers to age-related variation in cognition.

Methods: 144 cognitively normal older adults aged 65-90 from the Harvard Aging Brain Study were characterized on MRI markers of cortical gray matter thickness and volume, white matter lesions (WML) and fractional anisotropy (FA), resting state functional connectivity, functional activity during task-switching, and PET markers of glucose metabolism and amyloid burden. Episodic memory, executive function, and processing speed were separately assessed. Brain markers were primarily global in nature and were selected a priori without regard to relationships to age or cognition in the current dataset. Hierarchical regression analyses examined the age-related variance in cognition shared with each brain marker individually, and the unique age-related variance contributed by each marker when controlling for all other markers.

Results: The largest individual and unique relationships to all cognitive factors involved FA and WML, with an additional contribution of hippocampal volume to episodic memory. Individually, amyloid burden contributed ~9% of age-related variance in memory, but only ~1% was unique to amyloid. Approximately 60% of the age-related variance in cognition could be accounted for when all brain markers were combined (but only ~20% of total variance), and most of this age-related variance was shared among two or more brain markers.

Conclusion: These results suggest that the majority of age-related variation in cognition is shared among multiple brain markers, but point to limited specificity of associations between brain markers and cognitive domains, motivating additional study of markers of neural health in advanced aging.

Keywords: *biomarkers, FDG, PiB, fMRI, fcMRI*

Presented by: Hedden, Trey

Cerebral amyloid related alterations in neuronal metabolism and the contribution of multimodal measures of vascular function

Eric McDade [1], Albert Kim [2], Tim Hughes [3], Beth Snitz [1], Anne Cohen [1], Julie Price [1], Chester Mathis [1], James Becker [1], William Klunk [1], Oscar Lopez [1]

[1] *University of Pittsburgh*
[2] *Medical College of Georgia*
[3] *Wake Forest University*

Objective: We explored how markers of vascular disease and cerebral blood flow (CBF) might impact the relationship between cerebral plaques and neuronal function.

Background: Given the epidemiologic and pathologic evidence linking cardio-cerebrovascular disease and Alzheimer's dementia, it is critical to identify mechanistic links between these two disorders. Recently we have identified a direct association between arterial stiffness and amyloid deposition implying vascular disease could contribute to some of the amyloid related impairments of neuronal and cognitive function.

Design/Methods: 71 cognitively normal or MCI elderly subjects (mean 85y/o) underwent 18F-FDG and amyloid PET scans, ultrasound measurement of central and peripheral arterial stiffness (PWV) and pulsed arterial spin labeled (pASL)-MRI measures of CBF. Anatomical SUVR values from the PET scans were used for the regression models. Spearman's correlations identified areas of association between regional amyloid load and regional FDG values. Areas of significant correlation were then added into separate linear regression models with FDG as the dependent variable, and regional amyloid, PWV, CBF, blood pressure, age and education as potential predictors together in a stepwise multivariate regression with a probability-of-F-to-enter less than .05 and Probability-of-F-to-remove greater than .100 for each model to determine the best fit.

Results: In the regression model greater amyloid deposition was a significant predictor of lower glucose utilization in frontal and posterior cortical regions, however reduced CBF and greater vascular stiffness and diastolic blood pressure were additionally found to improve the models predicting FDG metabolism mostly in areas of the frontal lobes vulnerable to AD whereas in the more posterior regions PWV and blood pressure were less important.

Conclusions: Given the recent strong association we have identified between peripheral vascular stiffness and cerebral amyloidosis our current work might indicate that part of the relationship between vascular disease and frontal lobe dysfunction could result from a priming of these regions by vascular disease to the pathological cascade associated with Alzheimer disease rather than direct vascular damage.

Keywords: *Arterial stiffness, Cerebrovascular, FDG-PET, PiB-PET.*

Presented by: McDade, Eric

Binding of Pittsburgh Compound B to both normal and abnormal white matter in elderly cognitively normal controls.

Anna Goodheart [1], Erica Tamburo [1], Davneet Minhas [2], Howard Aizenstein [1], Eric McDade [3], Lisa Weissfeld [4], Beth Snitz [3], Julie Price [2], Chester Mathis [2], Oscar Lopez [3], William Klunk [1], Ann Cohen [1]

[1] *University of Pittsburgh School of Medicine, Psychiatry*
[2] *University of Pittsburgh School of Medicine, Radiology*
[3] *University of Pittsburgh School of Medicine, Neurology*
[4] *University of Pittsburgh, Biostatistics*

The amyloid imaging agent, Pittsburgh Compound B (PiB), binds with high affinity to β-amyloid (Aβ) in the brain and it is well established that PiB also shows non-specific retention in white matter(WM). However, little is know about retention of PiB in areas of white matter hyperintensities (WMH), abnormalities commonly seen in older adults. Further, WMH are hypothesized to be related to both cognitive dysfunction and Aβ deposition. The goal of the present study was to explore PiB retention in both normal-appearing WM (NAWM) and WMH in a group of elderly, cognitively normal individuals.

Cognitively normal elderly (n=64; 86.5±2.6 years) who had a FLAIR-MRI, PiB-PET(SUVR 50-70, cerebellum reference) and visual WMH score were included in this analysis. Two ROI analyses were applied: (1) ROIs of standardized dimensions were placed over "typical" areas of periventricular WMH caps on all subjects, regardless of WMH burden or size. (2) Subject-specific maps of NAWM and WMH were created using C++ and ITK, these maps were then co-registered with the PiB-PET and mean SUVR values were calculated in these NAWM and WMH ROI. PiB retention was significantly reduced in the "typical-WMH" ROIs of subjects with high WMH compared to subjects with low WMH. Additionally, in subjects with high WMH, there was significantly lower PiB retention in subject-specific ROIs of WMH compared to NAWM, this was not observed in subjects with low WMH, likely because of the absence of WMH in this group.

These data suggest that white matter in areas of WMH may have different binding characteristics to PiB than does normal WM. Further exploration of this phenomenon may lead to insights about the molecular basis of this non-specific interaction.

Keywords: *Pittsburgh Compound B, White matter hyperintensities*

Presented by: Cohen, Ann

SESSION 6: INVITED LECTURE

The Centiloid method for quantifying Amyloid PET studies: Great illuminator or master or illusion

Robert A. Koeppe

University of Michigan, Ann Arbor, MI

This talk will focus on two technical aspects of human amyloid PET imaging. First will be a review of different metrics for defining amyloid load. The vast majority of amyloid research reported in the literature used SUVr, which is nothing more than simple ratios of radiotracer concentration in some target tissue to some reference tissue. While this has proved very useful in practice, it is important to keep in mind the potential limitations of SUVr measures compared to more quantitative measures of distribution volumes or distribution volume ratios obtained from compartmental modeling or reference tissue modeling, respectively. While the relationship between the measures has been looked at extensively for [^{11}C]PiB, there is considerably less information available concerning the correspondence between DVr and SUVr measures for the newer [^{18}F]labeled amyloid tracers. It will be important to examine this relationship for any new amyloid tracers being developed, as well as for the new tau tracers that are coming on-line.

Second will be a brief review of the methods of the centiloid project. This will be followed with a discussion of whether the centiloid approach will improve our ability to compare different radiotracers, different acquisition and analysis methods, and different methods of extraction of amyloid data from the PET scans or whether the approach will actually tend to cloud the differences by putting all radiotracers, and analysis approaches on to the same scale.

Presented by: Koeppe, Robert

SESSION 7: Technical Emphasis

CHAIRS: Chester Mathis (University of Pittsburgh) and John Seibyl (Institute for Neurodegenerative Disorders)

Modeling the influence of white matter contamination on detectability of brain amyloid changes in longitudinal studies of Alzheimer's progression: Segmentation analyses using the PET β-Amyloid tracer 18F NAV4694

John Seibyl [1], Osama Sabri [2], Henryk Barthel [2], Olivier Barret [1], Kenneth Marek [1], Cornelia Reininger [3]

[1] *Institute for Neurodegenerative Disorders*
[2] *University of Leipzig*
[3] *Navidea Biopharmaceuticals*

Objectives: Current generation 18F β-amyloid PET radiotracers demonstrate significant non-specific white matter uptake which influences quantitative assessment of cortical β-amyloid burden, e.g. for monitoring small within-subjects drug effects. 18F NAV4694 is a novel brain β-amyloid PET agent with purportedly less white matter binding. The purpose of the present investigation was to study the influence of the white matter uptake in NAV4694 PET images on the ability of the tracer to diagnose Alzheimer's disease (AD) and to monitor changes in brain β-amyloid load over time.

Methods: 20 subjects (10 AD, 10 age-matched HV) had 18F NAV4694 PET and MRI scans. Individual MRI-based gray matter segmentation of the PET data and a standardized VOI analysis were carried out determining SUVrs (reference region: cerebellar cortex). Further, a theoretical model was constructed for demonstrating the influence of the varying degrees of white matter contamination on resulting SUVr changes over time and effects on power to detect subtle changes in brain amyloid in longitudinal treatment trials.

Results: Composite SUVr for AD subjects were 2.60±0.6 and 2.53±0.6 for the segmentation analysis and the no-segmentation analysis, respectively (n.s.). HV had segmented composite SUVr of 1.56±0.5 and non-segmented SUVr of 1.55±0.5 (n.s.). In the theoretical model, increasing white matter signal in cortical VOIs reduces the measured percent change over time in cortical SUVrs in a direct fashion.

Conclusions: The theoretical model suggests an important white matter effect resulting in Type 2 errors in assessing longitudinal data using PET biomarkers of β-amyloid. NAV4694 may be advantageous evidenced by the fact that MRI segmentation to generate gray matter PET volumes does not impact cortical SUVrs. This is most likely due to lower white matter uptake of NAV4694 compared with other 18F amyloid radiotracers, hence white matter contribution to the SUVr is less, predicting better sensitivity and statistical power for detecting within subject changes.

Keywords: *PET, NAV4694, amyloid, biomarker*

Presented by: Seibyl, John

Amyloid PET screening results by APOE ε4 status from a Phase 1b Clinical Study (221AD103) in patients with prodromal to mild Alzheimer's disease

Ping Chiao [1], Suhy Joyce [2], Barakos Jerome [3], Burke Meredith [2], Klein Gregory [2], Verma Ajay [1], Sevigny Jeff [1]

[1] *Biogen Idec, Cambridge, MA, USA*
[2] *Synarc Inc, Newark, CA, USA*
[3] *Synarc Inc, Newark, CA, USA, California Pacific Medical Center, San Francisco, CA, USA*

Introduction: Requirement of a positive amyloid PET scan is being used as an enrichment technique in study 221AD103. Retrospective analyses of both bapineuzumab and solanezumab data have shown substantially higher percentages of negative amyloid PET findings in APOE ε4 non-carriers than in APOE ε4 carriers in patients with mild or moderate Alzheimer's disease (AD). We report our amyloid PET screening results by APOE ε4 status in patients with prodromal or mild AD.

Methods: During screening, patients fulfilling criteria for prodromal or mild AD underwent florbetapir PET scanning and APOE genotyping. Florbetapir PET scans were visually evaluated for amyloid plaque burden.

Results: Data from the first 250 patients (Tables 1 and 2) are shown. Previously reported data from bapineuzumab and solanezumab Phase 3 studies are also shown (Table 2).

Table 1. Patient demographics

	Mild AD	Prodromal	All
N	121	129	250
Mean age, years	74	72	73
Sex, % male	44	58	51

Table 2. Amyloid PET imaging results by APOE ε4 status

	APOE ε4 non-carrier	APOE ε4 carrier	All
BIIB037 study 221AD103			
Amyloid PET +	51	107	158
Amyloid PET -	68	24	92
% Amyloid PET -	57	18	37
Bapineuzumab study[a]			
% Amyloid PET -	36	7	16
Solanezumab study[a]			
% Amyloid PET -	38	9.5	22

[a]Phase III study results reported at HAI 2013

Conclusions: A substantially higher percentage of APOE ε4 non-carriers than APOE ε4 carriers had negative amyloid PET findings, similar to the bapineuzumab and solanezumab data. However, the overall incidence of negative amyloid scans observed in study 221AD103 is substantially higher than reported in the two Phase 3 studies, likely attributable to the earlier stage of AD patients being recruited in this study (prodromal/mild, mean MMSE ~ 25 versus mild/moderate, mean MMSE ~21 in the Phase 3 studies). This finding is also consistent with the solanezumab data which showed that the percentage of negative amyloid PET findings was higher in mild (27%) than in moderate (13%) AD groups.

These results suggest that (1) enrichment using amyloid PET imaging is effective and feasible, (2) enrichment by assessing amyloid plaque burden is critically important to clinical studies in early stages of AD because of a higher incidence of negative amyloid findings, and (3) APOE genotyping may potentially improve the economy of enrichment by amyloid PET by lowering the likelihood of negative amyloid findings.

Keywords: *Florbetapir, Alzheimer's disease, amyloid PET imaging, APOE4, clinical trial*

Presented by: Chiao, Ping

Liberal thresholds for PIB-positivity optimally capture high-burden postmortem amyloid pathology

Brendan I. Cohn-Sheehy[1], Pia M. Ghosh[1], Sylvia Villeneuve[2], Gautam Tammewar[2], Cindee M. Madison[2], Manja Lehmann[3], Bruce L. Miller[4], Lea T. Grinberg[4], William W. Seeley[4], Howard J. Rosen[4], William J. Jagust[1], Gil D. Rabinovici [1]

[1] Memory and Aging Center and Department of Neurology, University of California, San Francisco; Helen Wills Neuroscience Institute, University of California, Berkeley; Lawrence Berkeley National Laboratory
[2] Helen Wills Neuroscience Institute, University of California, Berkeley
[3] Memory and Aging Center and Department of Neurology, University of California, San Francisco; Helen Wills Neuroscience Institute, University of California, Berkeley
[4] Memory and Aging Center and Department of Neurology, University of California, San Francisco

Objective: To compare liberal and conservative quantitative thresholds for classifying PIB-positivity with postmortem amyloid pathology.
Methods: 32 patients diagnosed with various dementias underwent PIB-PET and autopsy (age at PET=66.8±8.0, $T_{autopsy}$-T_{PET}=2.9±1.8 years; see Rabinovici et al., submitted). Global amyloid was measured with a cortical PIB Index (grey cerebellum reference) via 0-90 minute DVR (N=28) and/or 50-70 min SUVR (N=30) and visually interpreted by two blinded raters. Amyloid at autopsy was classified using modified CERAD (unadjusted for age) and NIA-Reagan criteria (N=27, 5 cases unclassifiable). We compared conservative PIB-positivity thresholds in the literature ($SUVR_{high}$ =1.40, DVR_{high} =1.20) with more liberal thresholds derived from younger and older controls ($SUVR_{low}$ =1.21, DVR_{low} =1.08; see Villeneuve et al., submitted) versus CERAD frequent neuritic plaques and NIA-Reagan high-likelihood AD. Receiver operator characteristic (ROC) analyses were then performed to test overall classification accuracy and empirically derive optimal thresholds.
Results: Liberal thresholds were sensitive to CERAD frequent pathology ($SUVR_{low}$ 93%, DVR_{low} 91%, see FIGURE) and were 100% specific versus lower amyloid burden; conservative thresholds were less sensitive ($SUVR_{high}$ 64%, DVR_{high} 82%). Liberal thresholds performed similarly well for NIA-Reagan high-likelihood AD ($SUVR_{low}$ 91% sensitivity, 100% specificity; DVR_{low} 90% sensitivity, 100% specificity) while conservative thresholds were less sensitive ($SUVR_{high}$ 82%, DVR_{high} 80%). Interestingly, visual reads showed higher agreement with liberal than conservative thresholds (FIGURE).
ROC analyses yielded areas under the curve ranging from 0.927-0.978 (all above chance, p<0.001). The optimal thresholds derived from ROCs were nearly identical to our a priori, control-derived liberal thresholds (DVR=1.08 for CERAD frequent and NIA-Reagan high; SUVR=1.21-1.22 for CERAD frequent/NIA-Reagan high, respectively).

Conclusions: Liberal thresholds for PIB-positivity were sensitive to and specific for CERAD frequent neuritic plaques and NIA-Reagan high-likelihood AD as determined postmortem in a clinical population. More data are needed to test these thresholds in intermediate pathology cases and in independent cohorts.

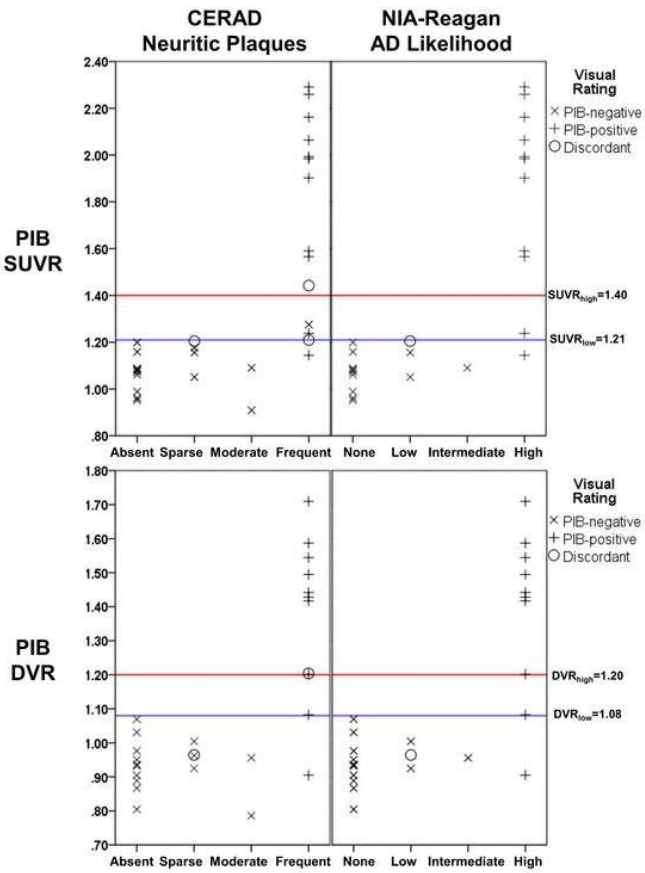

FIGURE: PIB-PET quantification versus postmortem pathology

Keywords: *PIB-PET, thresholds, pathology, autopsy, ROC*

Presented by: Cohn-Sheehy, Brendan I.

Existing thresholds for PIB positivity are too high

Sylvia Villeneuve [1], Cindee Madison [1], Nagehan Ayakta [1], Renaud La Joie [1], Brendan I. Cohn-Sheehy [2], Jacob Vogel [1], Shawn Marks [1], Samia K. Arthur-Bentil [1], Bruce Reed [3], Charles DeCarli [3], Gil Rabinovici [2], William Jagust [1]

[1] *University of California, Berkeley*
[2] *University of California, San Francisco*
[3] *University of California, Davis*

Background: There is no consensus about thresholds that define amyloid positivity, and there is little known about the earliest phases of amyloid accumulation in older adults.

Objective: To examine the pattern of amyloid accumulation and derive a cutoff that captures early accumulation using both DVR and SUVR data from the same subjects.

Methods: Amyloid accumulation was investigated in 152 cognitively normal older adults using: (1) a reference group of young adults, (2) Gaussian mixture modeling (GMM), (3) cluster analyses and (4) voxel-wise analyses. All analyses used DVR and SUVR data with a cerebellar gray reference ROI. For voxel-wise analyses, subjects were ranked based on their global DVR status. To track when and where amyloid starts accumulating we compared a group of 22 subjects with a mean DVR of 1 (control group) to the next 22 subjects (group of interest) and iteratively increased the mean DVR of the group of interest by dropping the subject with the lowest value and adding the subject with the next higher value. This procedure was repeated until the subject with the highest DVR was included in the group of interest.

Results: The threshold 2 SD above the young subjects was a DVR of 1.07 (SUVR = 1.19). Both the GMM and the cluster-derived thresholds were 1.09 (SUVR 1.22). The Figure shows that amyloid starts accumulating in the medial frontal cortex (mean DVR = 1.07, SUVR = 1.19), then spreads to the precuneus, the lateral frontal and parietal lobes, and finally the temporal lobe.

Conclusions: Amyloid starts to accumulate long before people reached the widely used SUVR cutoffs of 1.4 and 1.5. These results support an SUVR cutoff of 1.21 (DVR = 1.08) to capture early amyloid accumulation. This cutoff was confirmed by an autopsy study of 32 dementia cases (Cohn-Sheehy et al., submitted to HAI).

Keywords: *amyloid, pattern, threshold, SUVR, DVR*

Presented by: Villeneuve, Sylvia

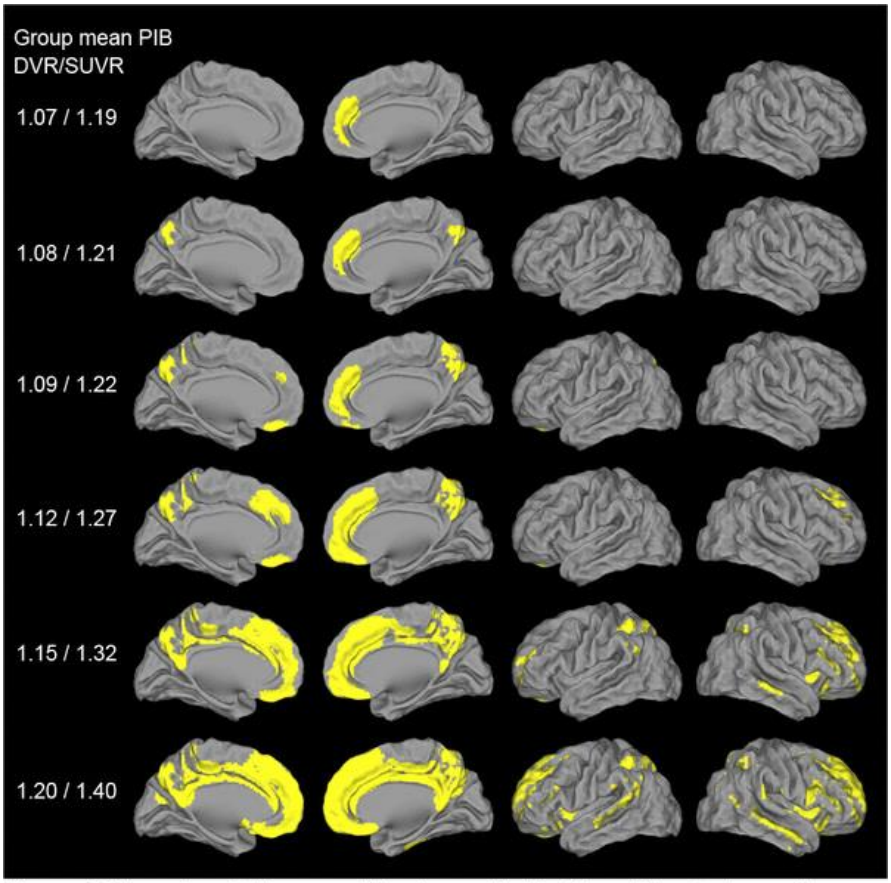

Figure. Pattern of amyloid accumulation in cognitively older adults. Each row of images reflects a voxel-wise contrast of 22 subjects with the mean value for global DVR/SUVR listed at left compared to a reference group (N=22) with a global DVR=1. Significant voxels first appeared when the group mean was DVR=1.07. Threshold at p <.05 after family-wise error correction, k >150.

SESSION 8: Neuropathologic Correlations

CHAIRS: William Klunk (University of Pittsburgh) and Gil Rabinovici (University of California San Francisco)

PiB PET and FDG PET quantitative analysis methods with autopsy correlation

Val Lowe [1], Melissa Murray [2], Emily Lundt [1], Stephen Weigand [1], Scott Przybelski [1], Lenon Jordan [1], Dennis Dickson [2], Joseph Parisi [1], David Knopman [1], Kejal Kantarci [1], Clifford Jack [1], Ronald Petersen [1]

[1] *Mayo Clinic, Rochester, MN*
[2] *Mayo Clinic, Jacksonville, Fl*

Background: Accurate biomarker evaluation methods are essential to discriminate changes in serial subjects and accurately characterize probable Alzheimer's disease. We evaluated different quantitative evaluation methods for PiB and FDG PET in subjects who had come to autopsy.

Methods: Autopsies from 40 subjects were available. Subjects with primary Alzheimer's disease pathology (n=14) and all without neurodegenerative disease (n=11) were selected for this comparison. Quantitiative analysis of PIB data was performed using grey matter segmentation vs grey+white matter, with partial volume correction (PVC), on or off, and cerebellar normalization using whole cerebellum (WCn) vs. peripheral cerebellum (crus) (CCn) normalization. FDG data was evaluated using an AD specific region method (Landau et al, 2010) vs. angular gyrus+posterior cingulate (AG+PC) regions with the above noted segmentation variations and PVC. Sensitivity, specificity, ROC and AUROC analysis were performed. Biomarker optimal cut-off values were determined and the influence of the quantitative methods on dynamic range was assessed.

Results: For PIB without PVC, all AD pathology subjects had more abnormal values than all control subjects. This complete separation was not observed after PVC. However, no AUROC difference was significant with any PiB method. Increased dynamic PiB range was observed when CCn was used. Optimal performance was seen with a PiB cutoff of 1.59-1.61 with non-PVC WCn and 1.70-1.72 with non-PVC CCn. For FDG, AG+PC AUROC ranged from 0.73-0.83 and Landau AUROC from 0.68-0.80 but differences were not significant. No different FDG AUROC values were seen with or without PVC. AUROC performance was better for any PiB method vs any FDG method ($p<0.05$).

Conclusions: There was no significant difference in disease detection accuracy between different PiB or FDG analysis methods tested. We observed suggestions of improved PiB accuracy when not using PVC and improved dynamic PiB range when using CCn. PiB disease characterization was superior to FDG.

Keywords: *Amyloid PET FDG PET Quantitative analysis Autopsy correlations*

Presented by: Lowe, Val

Evaluation of cotton wool plaques using amyloid binding compounds and Aβ immunohistochemistry: implications for PiB PET imaging

Milos Ikonomovic , Eric Abrahamson , Julie Price , Chester Mathis , William Klunk

University of Pittsburgh

Background: [C-11]PiB PET retention is believed to reflect amounts of cored/neuritic plaques consisting of fibrillar amyloid-β (Aβ) in Alzheimer's disease (AD). However, in familial AD (FAD) with presenilin-1 (PS-1) mutations, PiB retention is most prominent in the striatum which contains diffuse Aβ plaques, and moderate in neocortical regions containing both cored and diffuse Aβ plaques. The relationship between PiB binding and diffuse plaques is unclear.

Methods: We explored PiB labeling of striatal and neocortical plaques in FAD cases with PS-1 mutation (A426P) compared to sporadic AD. Sections of caudate, frontal and temporal cortices, and cerebellum were processed using highly fluorescent derivatives of PiB (6-CN-PiB) and Congo red (X-34), H&E, and Aβ immunohistochemistry (mab 4G8).

Results: In the neocortex of all cases, 6-CN-PiB and X-34 signals were strong in cored and weak in diffuse Aβ plaques. The only exception was cotton wool plaques (CWP) in FAD; in these Aβ-immunoreactive and H&E delineated deposits, positive X-34 labeling demonstrated their beta-sheet structure but 6-CN-PiB fluorescence was at background levels. Diffuse Aβ-immunoreactive, X-34-positive and 6-CN-PiB-negative plaques were also observed in the cerebellum of all cases. Striatal diffuse Aβ plaques were labeled moderately with 6-CN-PiB and X-34, similar in FAD and sporadic AD except for greater striatal plaque load in FAD.

Conclusions: This histological study provides a high resolution examination of the interaction between PiB and diffuse Aβ plaques, particularly of the CWP type. Besides cerebellar plaques, CWP are the second plaque type not detected using 6-CN-PiB histology. The possibility that the difference in CWP labeling between X-34 and 6-CN-PiB is due to differences in fluorescence intensities is unlikely as they showed comparable labeling in striatal and neocortical non-CWP plaques. The apparent beta-sheet structure of CWPs, demonstrated using X-34, suggests that a unique tertiary structure or modified Aβ forms may prevent their detection using PiB.

Keywords: *amyloid, cotton wool plaques, diffuse plaques, PET, PiB*

Presented by: Ikonomovic, Milos

[^{18}F]Flutemetamol amyloid PET detection of Aβ plaque phases 4 and 5 and significant diffuse plaque burden

Thomas Beach [1], Dietmar Thal [2], Michelle Zanette [3], Kirsten Heurling [4], Chris Buckley [5], Adrian Smith [5]

[1] *Civin Laboratory for Neuropathology, Banner Sun Health Research Institute, Sun City, AZ, USA.*
[2] *Institute of Pathology – Laboratory of Neuropathology, Center for biomedical Research, University of Ulm, Ulm, Germany.*
[3] *GE Healthcare, 101 Carnegie Center, Princeton ,NJ, USA*
[4] *GE Healthcare, Uppsala, Sweden.*
[5] *GE Healthcare The Grove Centre, White Lion Rd, Amersham, HP7 9LL U.K.*

Objectives: 1. To determine how amyloid PET imaging with [^{18}F]flutemetamol correlates with the hierarchical pattern of Aβ plaque deposition and which phases of Aβ pathology are detectable with PET amyloid imaging. 2. To ascertain the extent to which different types of amyloid plaques, namely neuritic and diffuse, contribute to amyloid PET images.

Methods: *Subjects:* 68 autopsy cases included in the efficacy analysis of the end of life study GE067-007.

Post-Hoc Amyloid phase analysis: Subsequent to the GE067-007 study, the phase of Aβ plaque pathology was determined by screening the Aβ-IHC stained sections for plaque distribution for each case. This was preformed blinded to clinical, imaging and other histopathological assessments.

Image assessment: The blinded assessment of [^{18}F]Flutemetamol PET images as normal or abnormal as recorded in the GE067-007 study was used for this post hoc analysis.

Results: *Abnormal image probability increases with amyloid phase:* The probability of a positive (abnormal) [^{18}F]flutemetamol image interpretation increases with increasing amyloid phase going from less than 0.0001 in Ab plaque phases 0 - 2, 0.111 in phase 3, 0.895 in phase 4 to 0.999 in phase 5.

[18F]Flutemetamol binding to diffuse plaques: The majority of deposits in the striatum were found in the form of diffuse plaques. In 8 cases, frequent diffuse plaques in the absence of any neuritic plaques were considered positive by PET visual assessment of the striatum (GE067-007 study), demonstrating that [^{18}F]flutemetamol can detect diffuse plaques when they are frequent.

Conclusion: [^{18}F]flutemetamol PET imaging is well suited to detect amyloid pathology in vivo. We found a high concordance of PET image abnormality with amyloid phase 4 to 5. This study also showed that [^{18}F]flutemetamol images could be positive in the striatal region in the absence of neuritic plaques if frequent diffuse plaques were present.

Keywords: *[18F]flutemetamol PET imaging, Aβ plaque pathology phasing, neuritic and diffuse amyloid plaques*

Presented by: Buckley, Chris

Diagnostic accuracy of amyloid and FDG PET in pathologically-confirmed dementia

Gil D. Rabinovici [1], Manja Lehmann [2], Howard J. Rosen [3], Pia M Ghosh [2], Brendan I Cohn-Sheehy [2], John Q. Trojanowski [4], Mario F. Mendez [5], Harry V. Vinters [5], Dennis W. Dickson [6], Marilu Gorno-Tempini [3], Adam L. Boxer [3], Bruce L. Miller [3], Lea T. Grinberg [3], William W. Seeley [3], William J. Jagust [7]

[1] *Memory & Aging Center and Department of Neurology, University of California San Francisco Helen Wills Neuroscience Institute, University of California Berkeley Lawrence Berkeley National Laboratory*
[2] *Memory & Aging Center and Department of Neurology, University of California San Francisco Helen Wills Neuroscience Institute, University of California Berkeley*
[3] *Memory & Aging Center and Department of Neurology, University of California San Francisco*
[4] *Center for Neurodegenerative Research, University of Pennsylvania, Philadelphia*
[5] *David Geffen School of Medicine, University of California Los Angeles*
[6] *Dept. of Neuroscience, Mayo Clinic Jacksonville*
[7] *Helen Wills Neuroscience Institute, University of California Berkeley Lawrence Berkeley National Laboratory*

Objective: Pathological validation studies of amyloid imaging have been conducted largely in end-of-life subjects that may not represent clinical practice. We assessed the diagnostic accuracy of PIB-PET versus pathology in a consecutive series of patients from an academic dementia clinic, and compared with the performance of FDG-PET.

Methods: 37 patients (mean age 66.5±8.8, MMSE 21.1±6.8) underwent PIB (all) and FDG (34/37) PET. Clinical diagnoses included Alzheimer's disease (AD, N=10), frontotemporal dementia (FTD, N=24), mild cognitive impairment (N=2) and prion disease (N=1). PET scans were visually interpreted by two raters blinded to clinical diagnosis (PIB: positive or negative; FDG: AD or FTD). Pathologic diagnoses (2.9±1.8 years after PET; 36 autopsies and one biopsy) were based on standard research criteria.

Results: Pathologic diagnoses included: high-likelihood AD (N=9), FTD (N=24), mixed high-likelihood AD/FTD (N=3) and prion disease (N=1). PIB reads had a sensitivity of 100% (both raters) and specificity of 88%-92% for post-mortem high-likelihood AD. A single patient with clinical AD who was rated PIB-negative by consensus had FTD at autopsy, while consensus PIB+ cases with clinical FTD were found to have either primary AD (N=2) or mixed AD/FTD pathology (N=3). Cases with discordant visual reads had either CERAD frequent (2) or CERAD sparse but frequent diffuse plaques (1): none met high-likelihood AD criteria.

FDG reads had a sensitivity of 83%-92% and specificity of 77% for AD. Mixed AD/FTD cases were usually read as AD (Rater 1 2/3, Rater 2 3/3). Positive predictive values for high-likelihood AD: PIB 80%-86%, FDG 67%-69%; negative predictive values: PIB 100%, FDG 89%-94%. Overall accuracy (excluding mixed high-likelihood AD/FTD): PIB 91%-94%, FDG 81% ($p>0.35$).

Conclusions: Amyloid PET had high sensitivity and negative predictive value for the pathologic diagnosis of AD. Positive test interpretation was complicated by mixed pathology. Amyloid imaging surpassed FDG in predicting underlying neuropathology.

Keywords: *Pathology, PIB, FDG, Frontotemporal dementia, Alzheimer's disease*

Presented by: Rabinovici, Gil D.

SESSION 9: KEYNOTE LECTURE

Senile plaques: Classification, distribution, clinical correlation and Amyloid imaging

Thomas G. Beach

Banner Sun Health Research Institute, Sun City, AZ

Senile plaques have been intensively studied in postmortem brains for more than 100 years and the resultant knowledge has not only helped us understand the etiology and pathogenesis of Alzheimer's disease (AD), it has pointed to possible modes of prevention and treatment that are being actively tested. Within the last 10 years, it has become possible to image plaques in living subjects. This is arguably the single greatest advance in AD research since the identification of the Ab peptide as the major plaque constituent. The limitations and potentialities of amyloid imaging are still not completely clear but are perhaps best glimpsed through the perspective gained from the accumulated postmortem histological studies, including some very recent clinical trials in which almost 200 subjects have had both amyloid imaging during life as well as extensive histological examination after death. The original morphological classification of plaques into classical, neuritic, cored and diffuse has been supplemented by ongoing detailed biochemical analyses and increasingly detailed mapping of plaque brain distribution. All of this information continues to be tested by clinicopathological correlation and it is through this means that we will best be able to employ the powerful tool of amyloid imaging.

Presented by: Beach, Thomas G..

SESSION 10: Memory Complaints/JADNI

CHAIRS: Reisa Sperling (Massachusetts General Hospital/Harvard Medical School) and Christopher Rowe (Austin Health)

Subjective memory complaints are related to default network disruption in clinically normal older adults with high amyloid burden

Patrizia Vannini [1], Rebecca Amariglio [1], Andrew Ward [2], Sarah Wigman [3], Willem Huijbers [3], Koene Van Dijk [4], Aaron Schultz [2], Tamy-Fee Meneide [2], Trey Hedden [5], Dorene Rentz [1], Keith Johnson [2], Reisa Sperling [1]

[1] Center for Alzheimer Research and Treatment, Department of Neurology, Brigham and Women's Hospital, Harvard Medical School, Boston, MA 02115
[2] Athinoula A. Martinos Center for Biomedical Imaging, Department of Neurology, Massachusetts General Hospital, Harvard Medical School, Charlestown, MA 02129,USA
[3] Center for Alzheimer Research and Treatment, Department of Neurology, Brigham and Women's Hospital, Harvard Medical School, Boston, MA 02115.
[4] Athinoula A. Martinos Center for Biomedical Imaging, Department of Psychiatry, Massachusetts General Hospital, Harvard Medical School, Charlestown, MA 02129,USA
[5] Athinoula A. Martinos Center for Biomedical Imaging, Department of Radiology Massachusetts General Hospital, Harvard Medical School, Charlestown, MA 02129,USA

Memory is one of the earliest cognitive domains affected in Alzheimer's disease (AD). Early in the course of AD, an individual may be aware of these subtle memory deficits before the people around them start to notice. Recent fMRI studies show that a specific set of brain regions, collectively called the default mode network (DMN), is important for both episodic memory and self-awareness. The DMN may also be especially vulnerable to early AD pathology. One striking possibility is that altered self-awareness in older adults represents an early indicator of progressive decline towards AD due to disconnection of specific DMN regions. Here, we used resting-state fMRI to investigate whether altered self-awareness of memory ability is related to DMN dysfunction and biomarker evidence of amyloid (Aβ) pathology in preclinical AD.

Methods: Clinically normal (CN) older adults (n=170, mean age = 74) were administered two subjective memory questionnaires (MFQ and E-Cog), which were combined to estimate a composite score of subjective memory appraisal. The integrity of the DMN was estimated by analyzing functional connectivity between a priori defined regions including the medial prefrontal (MPFC), posterior cingulate (PCC), lateral parietal (LPC) and the entorhinal cortex (EC) as estimated by resting-statefunctional MRI. Subjects were classified into low and high amyloid burden groups using a Gaussian mixture model approach.

Results: We found that more subjective memory complaints were associated with decreased functional connectivity in the DMN (r=-0.16, p=0.018). More importantly, we found a significant interaction (F(1,169)=5.52, p=0.02) between amyloid and functional connectivity between the EC and PCC, such that in the high amyloid group, more subjective memory complaints were associated with lower functional connectivity.

Interpretation: Our results suggest that in CN individuals with high amyloid burden, self-reported memory changes are related to functional disconnection of DMN regions. This suggests that subjectivememory complaints may offer insight into early behavioral and pathological changes in AD.

Keywords: *subjective memory impairment, default network, resting state fMRI, amyloid*

Presented by: Vannini, Patrizia

Amyloid burden and neurodegeneration independently contribute to greater subjective cognitive concerns in clinically normal older individuals

Rebecca Amariglio [1], Elizabeth Mormino [2], Patrizia Vannini [1], Gad Marshall [1], Keith Johnson [2], Reisa Sperling [1], Dorene Rentz [1]

[1] *Brigham and Women's Hospital*
[2] *Massachusetts General Hospital*

Emerging evidence suggests that subjective cognitive concerns (SCC) may herald initial cognitive decline at the preclinical stage of Alzheimer's disease (AD). Nonetheless, it remains unclear if amyloid (Ab) burden and neurodegeneration (ND) are independently associated with SCC in clinically normal individuals.

Here, we sought to investigate the unique contribution of high Ab burden (preclinical stage 1) plus ND (preclinical stage 2) in predicting SCC in clinically normal (CN) older individuals. Findings were contrasted against individuals without AD biomarker positivity (stage 0) and individuals with evidence of ND, but low Ab burden (SNAP).

We studied 181 CN older individuals from the Harvard Aging Brain Study. Ab status was determined with PIB-PET imaging and ND was measured using two a priori imaging markers: hippocampus volume and glucose metabolism extracted from AD-vulnerable regions. A subjective cognitive concerns composite was calculated using three validated questionnaires. Linear regression models with Ab and ND status were used to predict SCC, controlling for age, education, and gender. SCC were also examined across preclinical groups based on joint Ab and ND status.

SCC was not related to age, gender or education. Both Ab ($p=0.001$) and ND ($p=0.029$) were independently associated with greater SCC. Examination across preclinical groups revealed that SCC was greater in stage 2 compared to stage 0 ($p<0.001$), stage 1 ($p=0.12$) and SNAP ($p=0.06$). Furthermore, Stage 0 had lower SCC than both SNAP ($p = 0.04$) and stage 1 ($p=0.09$). There was no difference between Stage 1 and SNAP ($p=0.87$).

We demonstrate independent and additive contributions of Ab and ND status in predicting SCC, such that individuals that are positive on both biomarkers show the greatest SCC while individuals positive for a single biomarker show intermediate levels of SCC. This pattern is consistent with heightened risk of subsequent progression in preclinical stage 2.

Keywords: *preclinical Alzheimer's disease, subjective cognitive concerns*

Presented by: Amariglio, Rebecca

Longitudinal amyloid deposition with ^{11}C-PiB in Japanese ADNI study

Kenji Ishii [1], Muneyuki Sakata [1], Keiichi Oda [1], Jun Toyohara [1], Kiichi Ishiwata [1], Michio Senda [2], Kengo Ito [3], Ryozo Kuwano [4], Takeshi Iwatsubo [5], Study Group for Japanese Alzheimer's Disease Neuroimaging Initiative [6]

[1] *Team for Neuroimaging Research, Tokyo Metropolitan Institute of Gerontology*
[2] *Molecular Imaging Research Group, Foundation for Biomedical Research and Innovation*
[3] *Department of Brain Science and Molecular Imaging, National Institute for Longevity Sciences*
[4] *Center for Bioresources, Brain Research Institute, Niigata University*
[5] *Department of Neuropathology and Neuroscience, Tokyo University Graduate School of Medicine*
[6] *JADNI*

Detailed longitudinal change of amyloid ß deposition in terms of each stage of Alzheimer's disease (AD) and with respect to the status of ApoE genotype have not been understood well. We examined the longitudinal change of ^{11}C-Pittsburgh compound B (PiB) PET imaging from the follow up data of Japanese ADNI Subjects.

Among 545 elderly subjects who were enrolled in the Japanese ADNI study, 170 subjects participated in ^{11}C-PiB PET study. We analyze the data from 106 subjects who completed the follow up visits (3 years for NL/MCI, 2 years for AD) including 46 cognitively normal (NL), 41 mild cognitive impairment (MCI), and 19 possible AD.

The ^{11}C-PiB PET images acquired 50-70 min post injection were co-registered to individual MRI data of same visit, and automated VOI analysis were performed using DARTEL template, standard set of volumes of interest, and cerebrospinal fluid volume correction. The regional (precuneus, frontal, temporal and parietal cortices) uptake was evaluated in reference to that of the cerebellar cortex. The mean cortical uptake (mcSUVR) was calculated as the average of composite VOIs regarded as the representative value of individual global cortical amyloid deposition. The longitudinal mcSUVR were evaluated based on the clinical categories of the baseline visit and the possession of ApoE4 gene.

The number of subjects of ApoE4 +/- was 15/21 in NL, 24/17 in MCI and 8/11 in AD. The mcSUVR was significantly larger in ApoE4 carrier subgroups of NL ($p < 0.005$), and MCI ($p < 0.001$) than that in ApoE4 non-carrier subgroups, but not those of AD. The averaged annual change of mcSUVR in ^{11}C-PiB positive subjects was 2.3%. In each subgroup except for AD without ApoE4, steady increase of mcSUVR was observed, however, only AD without ApoE4 showed decline by follow up, presumably reflecting the dominant effect of atrophy.

Keywords: *longitudinal, amyloid deposition, ApoE, PiB*

Presented by: Ishii, Kenji

Higher Aβ burden in subjective memory complainers: A flutemetamol sub-study in AIBL

Christopher C Rowe [1], Vincent Doré [2], Pierrick Bourgeat [2], Rachel Buckley [3], Robyn Veljanoski [1], Olivier Salvado [2], Robert Williams [1], Kevin Ong [1], Alan Rembach [3], Lance Macaulay [4], David Ames [5], Colin L Masters [3], Victor L Villemagne [1]

[1] *Department of Nuclear Medicine & Centre for PET, Austin Health, Melbourne, VIC, Australia*
[2] *CSIRO Preventative Health Flagship: The Australian e-Health Research Centre, Brisbane, QLD, Australia*
[3] *The Florey Institute of Neuroscience and Mental Health, The University of Melbourne, VIC, Australia*
[4] *CSIRO Preventative Health Flagship: Materials Science and Engineering, Melbourne, VIC, Australia*
[5] *National Ageing Research Institute, Melbourne, VIC, Australia*

Background: The underlying pathological process, diagnostic utility and prognostic value of subjective memory complaints (SMC) in relation to Alzheimer's disease (AD) remains unclear. The relationship between SMC and Aβ burden as assessed by ^{18}F-flutemetamol was explored in healthy elderly controls (HC) with and without SMC and compared to participants with mild cognitive impairment (MCI) and AD patients.

Methods: 187 AIBL participants who had not been previously imaged were evaluated: 134 HC (age 74.4±5.6), 42 MCI (age 73.9±6.2) and 11 mild AD patients (age 74.8±8.6). HC were further classified according to the presence (HC-SMC, n=80) or absence of SMC (non-memory complainers HC-NMC, n=54). All participants underwent a comprehensive neuropsychological examination, and a 3D T1 MP-RAGE MRI. ^{18}F-flutemetamol-PET images were acquired from 90-110 mins post-injection of ^{18}F-flutemetamol and regional and global cortical SUVR were calculated using the pons as reference region. A SUVR cut-off of 0.62 was used to define scans as low (Aβ-) or high (Aβ+) Aβ burden.

Results: About 91% of AD, 55% of MCI, and 22% of HC were deemed Aβ+. Despite normal neuropsychological scores, HC-SMC had significantly higher ^{18}F-flutemetamol retention (0.54±0.14 vs. 0.49±0.10, respectively, p=0.026) and significantly higher prevalence of Aβ+ cases (33% vs. 7%, respectively, p=0.0006) than HC-NMC.

Conclusions: Subjective memory complaint indicated increased risk of preclinical AD in this study population. Longitudinal follow-up of this cohort continues.

Keywords: *Alzheimer's disease, subjective memory complaints*

Presented by: Rowe, Christopher C

Poster Presentations *(Alphabetized by presenting author)**

POSTER SESSION

P41 Early functional changes in the language network in response to increased amyloid beta deposition in healthy older adults

Katarzyna Adamczuk [1], An-Sofie De Weer [1], Natalie Nelissen [1], Patrick Dupont [1], Koen Van Laere [2], Rik Vandenberghe [3]

[1] *Laboratory for Cognitive Neurology, KU Leuven, Belgium*
[2] *Nuclear Medicine and Molecular Imaging, KU Leuven and UZ Leuven, Belgium*
[3] *Laboratory for Cognitive Neurology, KU Leuven, Belgium; Neurology Department, UZ Leuven, Belgium*

Background: Word finding symptoms are frequent early in the course of Alzheimer's disease. The posterior superior temporal sulcus (STS) is among the earliest language areas affected in amnestic MCI and early-stage probable AD (Vandenbulcke et al., 2007; Nelissen et al., 2007).

Objectives: Is amyloid load in cognitively intact older adults associated with functional brain changes in the language network (and in particular STS)?

Methods: Fifty-seven community-recruited right-handed adults (mean age=65, SD=5.5, range 52-74) underwent ^{18}F-flutemetamol PET, volumetric and functional MRI, and neurolinguistic evaluation. The fMRI design contained two factors: task (associative-semantic versus visuoperceptual judgment) and input-modality (written words versus pictures). Standardized uptake value ratios (SUVR) were calculated with cerebellar reference region. As primary outcome analysis, we conducted a linear regression analysis between SUVR in a composite volume of interest ($SUVR_{comp}$) and activity levels obtained from the contrast of the associative-semantic minus the visuoperceptual control condition for words and pictures (cluster-level $P<0.05$ corrected for the whole brain search volume).

Results: Amyloid $SUVR_{comp}$ was positively correlated with fMRI response in left posterior STS (cluster level $P_{corrected}=0.007$, 62 voxels, -57, -45, 9, Spearman r=0.33). This correlation was also significant when only the word conditions were contrasted (cluster level $P_{corrected}=0.031$, 44 voxels, -57, -45, 9, Spearman r=0.38) but not for pictures (cluster level $P_{corrected}>0.7$). Reaction times during an offline lexical decision task negatively correlated with the mean fMRI responses in this region (Spearman r=-0.39, P=0.0032).

Conclusion: In cognitively intact older adults, amyloid load is associated with functional changes in left posterior STS, an area involved in lexical-semantic processing. Increased activity with higher amyloid load in cognitively intact individuals together with decreased activity in MCI and early AD is reminiscent of the activity pattern seen in medial temporal cortex during episodic memory tasks (Sperling, 2007; Reiman et al., 2012) in the different stages of AD.

Keywords: *amyloid, PET, fMRI, normal aging, cognition*

Presented by: Adamczuk, Katarzyna

To locate a poster by number, view Program at page 10.

P7 Patterns of Av-45 uptake using VOIs based multivariate analysis in elderly peoples

Djilali Adel [1], Anne-Sophie Salabert [1], Florent Aubry [2], Julien Delrieu [3], Thierry Voisin [3], Sophie Gillette [3], Anne Hitzel [4], Bruno Vellas [3], Pierre Payoux [1]

[1] Inserm, imagerie cérébrale et handicaps neurologiques UMR 825. Nuclear Medicine department, Toulouse University Hospital, Toulouse, France. Paul Sabatier University, Toulouse University, France.
[2] Inserm, imagerie cérébrale et handicaps neurologiques UMR 825. Paul Sabatier University, Toulouse University, France.
[3] Department of Geriatric Medicine, Toulouse University Hospital. Paul Sabatier University, Toulouse University, France.
[4] Nuclear Medicine department, Toulouse University Hospital, Toulouse, France. Paul Sabatier University, Toulouse University, France.

AV45 is an ^{18}F-labeled amyloid-tracer that has been introduced for Alzheimer Disease (AD) diagnosis. AV45-PET in elderly subjects has not been documented yet. This work aimed to evaluate patterns of ß-amyloid deposits in elderly volunteers who don't meet the criteria of AD or dementia using principal component analysis (PCA).

Methods: AV-45 ancillary study is based on the Multidomain Alzheimer Preventive Trial (MAPT) survey including 271 subjects. MAPT Study is a 3-years, randomized trial enrolling elderly volunteers (>70years), on the basis of at least one of this criteria: subjective memory complaint spontaneously expressed (with a MMSE>24), limitation in one instrumental activity of daily living, and slow walking-speed (speed≤0.8m/s).PET-scans were spatially normalized with AV-45 template provided by Avid-Radiopharmaceutical using SPM8. A semi-automated quantitative analysis was applied, and the cortical-to-cerebellar signal ratio was compute in 80 VOIs (Brodmann areas). Briefly PCA is a data-driven technique that takes a linear combination of the values and that maximize the overall variance. PCA was applied on 80 VOIs. Principal components (PCs) and their correlation with age were investigated.

Results: 91 subjects were quoted as amyloid positive by visual assessment. Cattel's scree-test identified 3 PCs that contributing for 81.2% of total variance. The first PC comprised mainly the medial temporal (BA:21,22,39,48) involved in memory, and prefrontal cortices (BA10,11,47). The PC2 involved BA35,38,30,29,34, and the third mainly occipital (BA18,19) and prefrontal cortices (BA10,11,45,25). No correlation between PCs and age was found in this elderly population.

Discussion/Conclusion: Three PCs explained the major part of the amyloid-burden variability in non-demented elderly subjects. The pattern of amyloid-burden is linked with area involved in memory processes. Surprisingly, no correlation between age and PCs was found in elderly (70 to 91 yo). So PCs should be explained by others cognitive scores and further studies should be leaded to improve comprehension of such phenomenon.

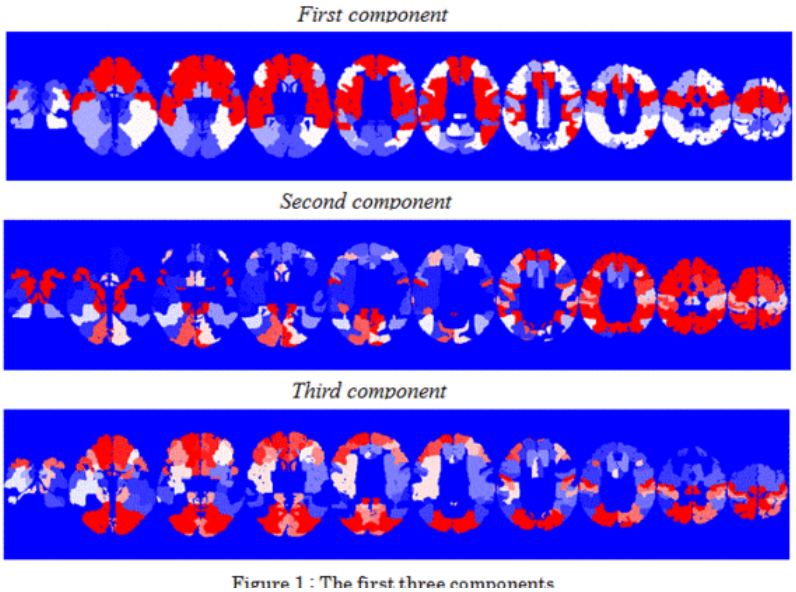

Figure 1 : The first three components

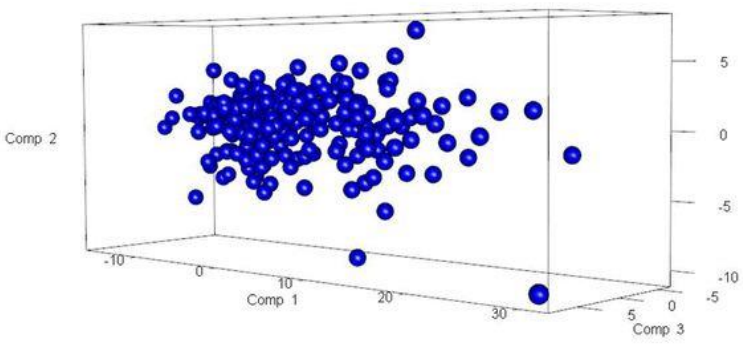

Figure 2: Subjects representation in the three components

Keywords: *PET, Amyloid, multivariate analysis*

Presented by: Adel, Djilali

P53 Prevalence of amyloid burden in elderly subjects in a PET-AV45 multicenter study

Djilali Adel [1], Anne Hitzel [2], Julien Delrieu [3], Thierry Voisin [3], Sophie Gillette-Guyonnet [3], Bruno Vellas [3], Pierre Payoux [1], et al.

[1] Inserm, imagerie cérébrale et handicaps neurologiques UMR 825; Nuclear Medicine department, Toulouse University Hospital, Toulouse, France. Paul Sabatier University, Toulouse University, France;
[2] Nuclear Medicine department, Toulouse University Hospital, Toulouse, France. Paul Sabatier University, Toulouse University, France;
[3] Department of Geriatric Medicine, Toulouse University Hospital, Toulouse, France. Paul Sabatier University, Toulouse University, France;

Objectives: The purpose of this study is to evaluate the prevalence of ß-amyloid burden in elderly people who don't meet criteria of dementia or Alzheimer disease, as assessed by AV45-PET scans, and the concordance between visual assessment and SUVr quantification.

Methods: A multicenter study from the Multidomain Alzheimer Preventive Trial (MAPT), acquisitions of 15 min, and 50 min after a bolus injection of AV-45 was performed. The study enrolling elderly volunteers aged of 70years and over with an MMSE>24. The images were visually assessed by three trained observers on a binary scale (+ / -) blinded of clinical data. Then a semi-automatic quantification was performed on six cortical regions (Clark et.al.) to obtain SUVr taking the cerebellum as reference region. The SUVr is the cortical average over six regions (temporal, parietal, frontal, precuneus, anterior-cingulate and posterior-cingulate).

Results: 271 subjects (162F, 109M) aged of 76.6 ± 4.6 years were included. 33.2% of subjects were amyloid positive (Aβ+) based on visual assessment. The mean SUVr was significantly higher ($p<0.0001$) in Aβ+ group (1.34±0.17) compared to Aβ- (1.088±0.1). There is no statistical signifiance in SUVr between females and males (1.173±0.17 and 1.168±0.17). Then higher AV45 uptake is not associated with a greater age in elderly subjects 77.14±4.5 versus 76.44±4.3 for Aβ+ and amyloid negative (Aβ-) subjects respectively ($p<0.21$). It follows no correlation between age and SUVr in this population. The visual assessment and the SUVr were concordant with an area under the curve AUC=0.90.

Conclusions: The prevalence of amyloid deposits in elderly no-demented subjects was not so high and was not linked with aged or gender. The quantification by SUVr, it agree with visual assessment and could help the diagnosis of amyloid positivity.

Presented by: Adel, Djilali

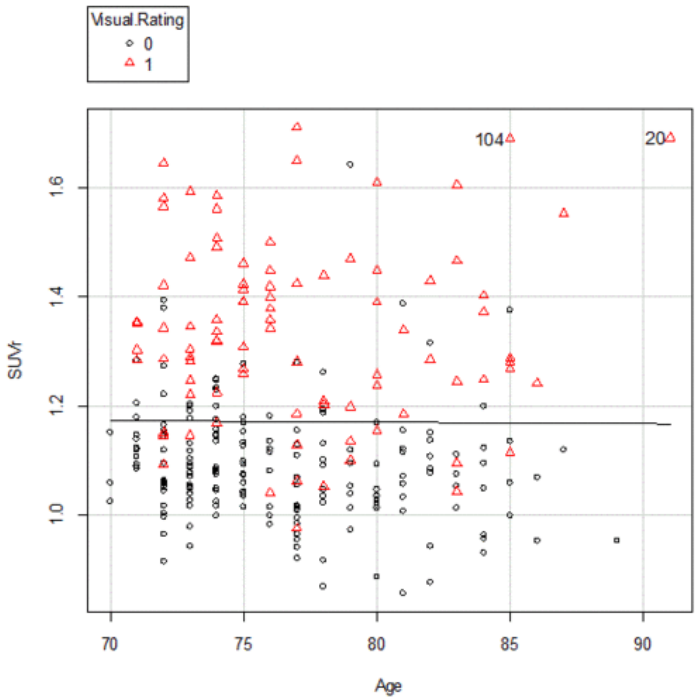

Figure 1: Scatter plot of SUVr versus age, Red: amyloid positive subjects, Black: amyloid negative subjects

P42 Imaging amyloid in adults with Down's syndrome using PiB-PET

Tiina Annus [1], Liam R. Wilson [1], Shahid Zaman [1], Young T. Hong [2], Tim Fryer [2], Franklin Aigbirhio [3], Rob Smith [2], Anthony J. Holland [4]

[1] Cambridge Intellectual and Developmental Disabilities Research Group Department of Psychiatry University of Cambridge Douglas House 18b Trumpington Road Cambridge CB2 8AH United Kingdom
[2] Wolfson Brain Imaging Centre Department of Clinical Neurosciences University of Cambridge School of Clinical Medicine Box 65 Cambridge Biomedical Campus Cambridge, CB2 0QQ
[3] Department of Clinical Neurosciences Wolfson Brain Imaging Centre Department of Clinical Neurosciences University of Cambridge School of Clinical Medicine Box 65 Cambridge Biomedical Campus Cambridge, CB2 0QQ
[4] Cambridge Intellectual and Developmental Disabilities Research Group Department of Psychiatry University of Cambridge Douglas House 18b Trumpington Road Cambridge CB2 8AH United Kingdom

Introduction: Down's syndrome (DS) is associated with the trisomy of chromosome 21, which is believed to significantly increase their risk of developing Alzheimer's disease (AD). It is hypothesised that the presence of an extra copy of the amyloid precursor protein (APP) gene leads to increased formation of β-amyloid (Aβ) plaques, neuronal death and clinical AD. The present study aims to extend the findings of a pilot study by Landt et al. (2011) by investigating the relationship between distribution and load of Aβ with age and dementia in DS.

Methods: Forty-two adults with DS aged 25-65 underwent an MRI scan and 90-minute dynamic PET scan using Pittsburgh Compound-B (PiB). The BP_{ND} maps were created using simplified reference tissue model (Gunn et al, NeuroImage 1997) with superior grey matter of cerebellum as reference tissue. T-1-template was created using DARTEL toolbox in SPM8. Regions of interest (ROIs) were manually drawn on the template and applied to the warped BP_{ND} map to obtain regional BP_{ND} values. Dementia was diagnosed using CAMDEX informant interview.

Results: Adults with DS without dementia (DS-AD, n=30), with early signs of dementia (DS+E, n=5) and with dementia (DS+AD, n=6) demonstrated highest PIB binding in striatum and lowest in hippocampus. A significant positive correlation of BP_{ND} values with age was seen for all ROIs. Significantly higher PiB retention was observed in all ROIs in DS+AD, when compared to DS-AD, and in none of the ROIs, when compared to DS+E. Individuals with DS+E demonstrated significantly higher BP_{ND} values in all ROIs apart from occipital lobe and hippocampus, when compared to DS-AD.

Conclusion: A significant positive relationship between PiB-binding and age was observed in all groups. PiB binding in ROIs apart from occipital lobe and hippocampus in DS+E suggests the course of amyloid spread, culminating in positive binding in all ROIs in DS+AD.

Keywords: *Down's syndrome, dementia, Alzheimer's disease, PiB,*

Presented by: Annus, Tiina

P37 Exploring the best methods to detect longitudinal change in amyloid imaging

Suzanne Baker [1], Shawn Marks [2], Susan Landau [2], William Jagust [3]

[1] *Lawrence Berkeley National Lab*
[2] *Helen Wills Neuroscience Institute, UC Berkeley*
[3] *Helen Wills Neuroscience Institute, UC Berkeley & Lawrence Berkeley National Lab*

This project explored alternative methods of analyzing longitudinal PIB data. We looked at DVR versus SUVR (50-70min) and the effect of reference region: cerebellar gray (cereg), whole cerebellum (cere), whole cerebellum+pons (cere+p), whole cerebellum+eroded hemispheric white (cere+w), and whole cerebellum+pons+eroded hemispheric white (cere+p+w). 28 older healthy control subjects had two 90 minute PIB scans within 3±0.9 years. Cingulate, frontal, parietal and temporal cortex were the target regions used for comparison between methods. Despite the high correlation between DVR and SUVR values from both visits within reference region, the annual percent change (a%c) measured by DVR versus a%c measured by SUVR within reference region is less correlated (Figure1), although highest correlations were found using cere or cere+p. Reference regions including white matter should minimize white matter effects on cortical signal and thereby reduce the correlation between white matter a%c and target a%c. Figure 2 shows r^2 between white matter a%c versus SUVR target ROIs a%c using various reference regions. Adding cerebellar white to the reference region decreases the a%c correlation with white matter a%c; adding eroded hemispheric white to the reference region further decreases this correlation. This decrease in correlation implies a decrease in white matter in the target signal. However, the higher correlations with hemispheric white a%c (in comparison to cerebellar white a%c) shows target signal in the hemispheric white matter still exists despite the erosion of the ROI, suggesting that including hemispheric white matter in the reference region should be done with caution. The ideal reference region would have sufficient white matter to divide out white matter signal in the cortex, but minimize white matter contaminated with cortical signal. Whole cerebellum or cerebellum+pons may be the best option as a reference region due to the DVR/SUVR correlation, removing white matter signal and not cortical signal.

Keywords: *longitudinal, reference region, DVR, SUVR*

Presented by: Baker, Suzanne

P17 Comparison of reference regions for [18F]Florbetapir PET SUVR computation

Arnaud Charil [1], Felix Carbonell [1], Alex Zijdenbos [1], Alan Evans [2], Robert Koeppe [3], Jeff Sevigny [4], Ping Chiao [4], Barry Bedell [2]

[1] *Biospective Inc., Montreal, QC, Canada*
[2] *Biospective Inc. & Montreal Neurological Institute, McGill University, Montreal, QC, Canada*
[3] *University of Michigan, Ann Arbor, MI, USA*
[4] *Biogen Idec, Cambridge, MA, USA*

Background: Amyloid PET is increasingly utilized in research studies and clinical practice. Quantitative assessment of beta-amyloid burden is typically based on the standardized uptake value ratio (SUVR), which is derived from the ratio of radiotracer uptake in target and reference brain regions. The cerebellar gray matter is commonly used as a reference region for amyloid PET. However, this particular reference region may not be optimal for all tracers. As such, we have performed a systematic study to determine the optimal reference region(s) for [18F]florbetapir scans.

Methods: [18F]florbetapir PET and 3D T1-weighted MR images were obtained from the ADNI database (n=454 subjects), as well as from subjects participating in an ongoing Phase IB clinical Alzheimer's disease study sponsored by Biogen Idec. Reference regions included cerebellar gray matter (cbGM), cerebellar white matter (cbWM), whole cerebellum (cbFull), pons, cbFull+pons, deep white matter (dWM), and dWM+cbFull+pons. Target regions-of-interest (ROIs) included frontal, parietal, lateral temporal, sensorimotor, anterior and posterior cingulate cortices, as well as a composite ROI including all of these cortical regions. The target ROI SUVR measures were generated using Biospective's fully-automated PIANO™ image processing software. Probability density functions, correlation analysis, and discriminant analysis were employed to compare SUVR measures using the different reference regions.

Results: Our results demonstrated that reference regions which did not include the cbGM were advantageous for [18F]florbetapir studies. This observation was consistent across the datasets and study groups.

Conclusions: Several amyloid PET tracers currently exist and it is vital to determine the optimal reference region for SUVR-based measures for each particular tracer. We employed multiple, complementary metrics, and utilized both ADNI and clinical trial data for this study. Our results suggest that cbGM may not be the optimal reference region for assessment of beta-amyloid plaque burden based on [18F]florbetapir PET scans.

Keywords: *SUVR, Florbetapir, Reference Region, ADNI, Clinical Trial*

Presented by: Bedell, Barry

P27 Statistically-driven, automated subject classification based on amyloid PET scans

Felix Carbonell [1], Arnaud Charil [1], Alex Zijdenbos [1], Alan Evans [2], Jeff Sevigny [3], Ping Chiao [3], Barry Bedell [2]

[1] *Biospective Inc., Montreal, QC, Canada*
[2] *Biospective Inc. & Montreal Neurological Institute, McGill University, Montreal, QC, Canada*
[3] *Biogen Idec, Cambridge, MA, USA*

Background: Classification of subjects as Amyloid-Positive (Aβ+) or Amyloid-Negative (Aβ-) based on amyloid PET scans is increasingly utilized in research studies and clinical practice. While qualitative, visual assessment is currently the gold-standard approach, automated classification techniques are inherently unbiased, reproducible, and efficient. The objective of this work was to evaluate the performance of a recently developed statistical approach for the automated classification of subjects with different levels of cognitive impairment using amyloid PET scans.

Methods: [18F]florbetapir PET and 3D T1-weighted MR images and were obtained from three cohorts, specifically ADNI healthy control (HC) subjects (Cohort 1), ADNI MCI subjects (Cohort 2), and prodromal/mild Alzheimer's disease (AD) subjects from an ongoing Phase IB clinical study sponsored by Biogen Idec (Cohort 3). SUVR maps were generated using Biospective's fully-automated PIANO^{TM}image processing software. Subjects were classified into Aβ+ and Aβ- groups based on visual evaluation of [18F]florbetapir PET scans. These classifications were used to initialize an iterative, voxelwise, regularized discriminant analysis to optimize the selection of a set of regions-of-interest (ROIs) and a threshold for automated classification of Aβ+ and Aβ- subjects in each cohort. The resulting ROIs and thresholds were cross-validated between cohorts.

Results: The automated classifier demonstrated high accuracy, specificity, and sensitivity. The optimal ROIs included areas of the default mode network (DMN), such as the precuneus and medial frontal cortex.

Conclusions: We have validated an automated approach for classification of subjects as Aβ+ or Aβ- using three different subject cohorts. This strategy represents an improvement over current methods that rely on either subjective, visual evaluation of amyloid PET images or quantitative measures based on pre-defined anatomical ROIs. Ultimately, fully-automated subject classification may complement or supplant visual reads in clinical practice and for eligibility assessment in AD clinical trials.

Keywords: *Subject Classification, Florbetapir, Discriminant Analysis, ADNI, Clinical Trial*

Presented by: Bedell, Barry

P56 Body mass index is associated with verbal episodic memory in cognitively normal older individuals with low fibrillar amyloid-beta measured by [^{11}C]-PiB

Murat Bilgel [1], Yi-Fang Chuang [2], Yang An [2], Jerry Prince [3], Dean Wong [3], Madhav Thambisetty [2], Susan Resnick [2]

[1] National Institute on Aging, NIH, Baltimore, MD, 21224, USA; Johns Hopkins University School of Medicine, Baltimore, MD, 21205, USA
[2] National Institute on Aging, NIH, Baltimore, MD, 21224, USA
[3] Johns Hopkins University School of Medicine, Baltimore, MD, 21205, USA

Background: Previous studies have implicated body mass index (BMI) as a predictor of verbal memory. In order to determine whether this association is present independent of brain amyloid levels, we performed linear regression analyses restricted to high and low amyloid individuals.

Method: Associations between verbal episodic memory measured by the California Verbal Learning Test (CVLT) immediate recall trials on list A, concurrent BMI, and Pittsburgh Compound B (PiB) retention were studied in a cross-sectional sample consisting of cognitively normal subjects (N=68), ages 61 to 92 (mean age= 77±7) from the Baltimore Longitudinal Study of Aging (BLSA). Subjects were split into low PiB and high PiB groups based on mean cortical distribution volume ratio (DVR) (using a threshold of DVR=1.09, the two groups had N=48 and 20, respectively).

Results: Linear regression models controlling for age, sex, race, education, APOE e4 status, and cardiovascular conditions (including myocardial infarction and congestive heart failure) showed that CVLT immediate recall score is inversely related to concurrent BMI (β=-0.8909, p=0.025) in cognitively normal persons with low PiB retention. No other covariate was associated with CVLT except for age (β=-0.6474, p=0.021) in the low PiB group. These findings remained significant after adjustment for mean cortical DVR. On the other hand, BMI was not associated with CVLT immediate recall score in the high PiB subjects neither in the unadjusted nor adjusted models.

Conclusions: Higher BMI is associated with lower verbal immediate recall performance in individuals with no or minimal levels of brain amyloid-beta. The lack of this association in individuals with high amyloid-beta suggests that brain amyloid levels may alter the effects of factors reported to be associated with cognitive function.

Keywords: *Verbal memory, body mass index*

Presented by: Bilgel, Murat

P51 [18F]Flutemetamol blinded image interpretation: assessment of the electronic training program for Japanese readers

Chris Buckley [1], Brian J McParland [1], Jan Wolber [1], Paul Sherwin [2], Michelle Zanette [2], Gill Farrar [1]

[1] *GE Healthcare; Amersham, UK*
[2] *GE Healthcare; Princeton, NJ*

Objective: Previously (*Sherwin, HAI 2013*) reported the validation of an Electronic Training Program (ETP) for interpreting [18F]flutemetamol (VIZAMYL™) PET images, using US readers. The successful use of the ETP with Japanese-board trained readers in the Phase II study in Japan is reported.

Methods: Japanese subjects, AD (n = 20), aMCI (n=20) and healthy controls (n=25) were dosed with 185 MBq of Flutemetamol F 18 Injection and underwent brain PET. Images (n=65) were interpreted blind by 10 readers (5 Japanese-board trained, 5 non-Japanese board trained), each trained using the ETP, who classified each image as positive or negative for brain amyloid. Agreement across all five readers in the two groups was determined and reported as Fleiss' kappa. Results were also compared to the European Phase II study (*Vandenberghe et al., Ann Neurol 2010;68:319–329*) and the previous ETP study (*Sherwin et al., HAI 2013*). Intra-reader reproducibility (IRR) was also determined by re-reading images from 7 subjects (10%) selected randomly from the 65 subjects.

Results: Among the 5 Japanese readers, there was complete agreement for 61 (94%) of 65/70 images read, (kappa = 0.94). Among the 5 non-Japanese readers, there was complete agreement for 62 (95%) of 65 images read, (kappa = 0.96). The performance of each group of readers is consistent with the EU Phase II data (kappa 0.96; Vandenberghe 2010) which used an in-person training method. These results are slightly higher than the Phase 3 read study (n=276, kappa = 0.83; *Sherwin et al., HAI 2013*) which included a wider spectrum of subjects, including end-of-life subjects. Intra-reader agreement ranged from 86% to 100% (median 100%) and was similar to those of the European Phase II study (97.5%) and the Phase 3 study (93% to 100%).

Conclusion: The ETP is effective in training Japanese readers. This further validates the use of electronic media for the training of readers in the routine interpretation of [18F]flutemetamol images.

Keywords: *[18F]flutemetamol, VIZAMYL™, blinded image evaluation, electronic training program, kappa score.*

Presented by: Buckley, Chris

P45 Disclosure of amyloid imaging results in cognitively normal individuals

David Johnson [1], Vidoni Eric [2], Magdalena Leszko [1], Rebecca Bothwell [2], Jeffrey Burns [2]

[1] *University of Kansas*
[2] *University of Kansas Medical Center*

Introduction: Disclosing amyloid imaging results to cognitively normal (CN) older adults has begun in the setting of prevention trials. Disclosing amyloid status to CN individuals remains debatable, in particular in the clinical setting, given an imprecise understanding of its clinical significance, lack of effective therapeutic options, and unknown psychological risk.

Methods: The KU Alzheimer's Prevention Program Exercise (APEX) trial is among the coming wave of AD prevention trials. We disclose amyloid status using a genetics counseling approach with pre- and post-scan counseling conducted by clinicians. We assess the effect of disclosure on anxiety, depression, perception of risk, and health behaviors at baseline and at 6-weeks and 6-months post-disclosure, similar to the REVEAL study. Measures include the Beck Anxiety Inventory (BAI), Center for Epidemiologic Studies Depression Scale (CES-D), Impact of Genetic Testing for AD (IGT-AD) and surveys of health behaviors.

Results: APEX will screen a total of 400 CN older adults (CDR 0) with amyloid PET to identify 100 participants with cerebral amyloid for a one-year exercise trial. As of November 2013, a total of 24 participants have been screened with 4 individuals (17%) having elevated cerebral amyloid, as determined by visual reads informed by quantitative analyses. Our preliminary analyses suggest disclosing a positive amyloid status to CN individuals does not negatively influence anxiety (mean BAI 5.3 (4.4) at baseline vs 5.3 (2.6) at 6 weeks) or depression (mean CES-D 3.0(1.4) at baseline vs. 2.3(1.2) at 6-weeks). There was no apparent adverse psychological impact (mean IGT-AD 16.3(4.9), similar values to the REVEAL study). Amyloid positive participants reported greater intent to change their daily diet and exercise.

Conclusion: Our preliminary experience suggests that disclosing amyloid imaging results to CN adults with pre- and post-disclosure counseling has a low risk of psychological harm and may motivate an individual to adopt healthier lifestyle behaviors.

Keywords: *disclosure, psychology, ethics, amyloid status*

Presented by: Burns, Jeffrey

P34 Differential temporal patterns of Amyloid-β and functional imaging markers across mutation types in autosomal dominant Alzheimer's disease: Findings from the DIAN Study

Jasmeer Chhatwal [1], Aaron Schultz [1], Keith Johnson [2], Tammie Benzinger [3], Clifford Jack [4], Beau Ances [5], Caroline Sullivan [1], Stephen Salloway [6], John Ringman [7], Robert Koeppe [8], Daniel Marcus [3], Paul Thompson [9], Andrew Saykin[10], John Morris [5], Reisa Sperling [11], et al.

[1] *Department of Neurology, Massachusetts General Hospital, Harvard Medical School, Boston MA*
[2] *Departments of Neurology and Radiology, Brigham and Women's Hospital, Massachusetts General Hospital, Harvard Medical School, Boston MA*
[3] *Department of Radiology, Section of Neuroradiology, Washington University School of Medicine, St. Louis, MO*
[4] *Department of Radiology, Mayo Clinic, Rochester MN*
[5] *Department of Neurology, Washington University School of Medicine, St. Louis MO*
[6] *Department of Neurology, Butler Hospital, Brown University School of Medicine, Providence, RI*
[7] *Department of Neurology, Easton Center for Alzheimer's Disease Research, University of California - Los Angeles, Los Angeles, CA*
[8] *Department of Radiology, University of Michigan School of Medicine, Ann Arbor, MI*
[9] *Lab of Neuro Imaging, UCLA School of Medicine, Los Angeles, CA*
[10] *Department of Radiology, IU Center for Neuroimaging, Indiana University School of Medicine, Indianapolis, IN*
[11] *Brigham and Women's Hospital, Massachusetts General Hospital, Department of Neurology, Center for Alzheimer's Research and Treatment, Harvard Medical School, Boston MA*

Rationale: Imaging biomarkers will play a key role in upcoming Alzheimer's disease (AD) prevention clinical trials, including trials in autosomal-dominant AD (ADAD). Accordingly, we examine whether subjects harboring mutations in Presenilin-1 (*PSEN1*), Presenilin-2 (*PSEN2*), or Amyloid Precursor Protein (*APP*) show differential temporal or spatial patterns of imaging biomarker change in ADAD.

Methods: Focusing on ADAD subjects who were at or younger than their estimated age of symptom onset at their baseline visit, we examined both main effects of mutation type and interactions between mutation type and estimated years to symptom onset (EYO) using regional imaging biomarker values as the outcome. These relationships were examined in cross-sectional PiB and FDG-PET, functional connectivity MRI (fcMRI), and MRI-derived structural measures. Preselected Freesurfer ROIs were used for FDG, PiB and structural data. Template-based rotation was used to assess fcMRI networks.

Results: Significant mutation type effects were observed in PiB binding in several midline structures (posterior cingulate, precuneus, anterior cingulate). With the exception of significant, differential FDG hypometabolism in *PSEN1* carriers in the precuneus, no significant effects of mutation type were apparent in other FDG and structural measures within pre-selected cortical ROIs. Similarly, no significant mutation type or interaction effects were observed in the Default Mode, Dorsal Attention, Motor, or Visual Networks.

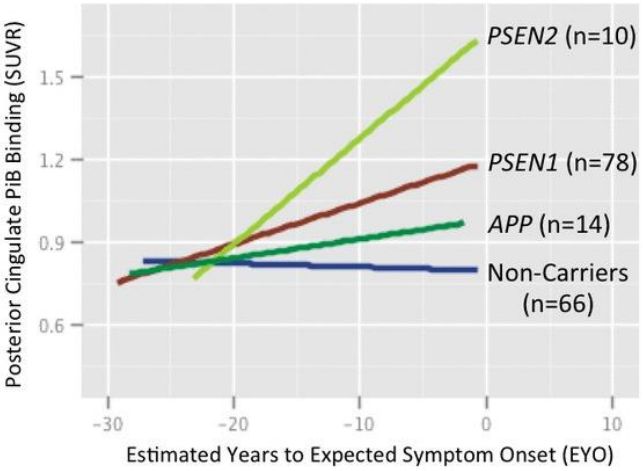

Conclusion: Mutation type may be an important consideration when using regional amyloid and FDG-PET measures as secondary outcomes in ADAD clinical trials. Though the patterns observed here in cross-sectional data will need to be verified in longitudinal data, plotting PiB binding against EYO suggests that *PSEN2* carriers may show a greater rate of midline fibrillar amyloid deposition as compared to *PSEN1* carriers, whereas *APP* carriers may show a lower rate. These differences hint at underlying genotypic variation in the kinetics of amyloid production, processing, and clearance that may our pathophysiologic understanding of ADAD.

Keywords: *functional connectivity, amyloid, autosomal dominant AD*

Presented by: Chhatwal, Jasmeer

P15 Comparison of PIB-PET data to Florbetapir-PET data acquired from different patient cohorts and the role of age in the discriminative power of amyloid imaging

Konstantinos Chiotis [1], Stephen F. Carter [2], Agneta Nordberg [3]

[1] Alzheimer Neurobiology Center, Karolinska Institutet; Sweden
[2] Alzheimer Neurobiology Center, Karolinska Institutet; Sweden, Wolfson Molecular Imaging Center, University of Manchester, Manchester; UK
[3] Alzheimer Neurobiology Center, Karolinska Institutet; Sweden, Department of Geriatric Medicine, Karolinska University Hospital Huddinge; Sweden

Introduction: Several 11C- and 18F-PET radiotracers, which bind with high affinity to fibrillar amyloid, have been developed and are applied clinically into different patient cohorts.

Objectives: To investigate the comparability of two amyloid PET tracers (11C-PIB/18F-Florbetapir), when applied in two different patient cohorts and to explore the effect of age in the discriminative properties of amyloid imaging.

Methods: 11C-PIB-PET data from 51 healthy controls (HC), 72 mild cognitive impairment (MCI) and 90 Alzheimer's disease (AD) patients deriving from the DIMI EU project (Nordberg et al.2013) were analysed using a PIB-PET population template and atlas (mean age 68.5±7.8 years). 18F-Florbetapir-PET data were analysed by applying the same methodology in a matched for age (mean age 69.4±6.9 years), gender and MMSE-score population (51 HC,72 MCI and 84 AD), deriving from the Alzheimer's Disease Neuroimaging Initiative (ADNI). An additional ADNI population (246 HC,344 MCI and 138 AD), with a Florbetapir scan, was split in two age groups matched for MMSE-score and gender distribution, with mean ages of 70.9±3.5 and 80.9±3.9 years.

Results: Regional values of PIB and Florbetapir retention were strongly correlated in the young matched groups across the different brain regions investigated (r=0.829,p=0.00). However, a narrower range and lower cut off was observed for the Florbetapir data (0.99-2.06,1.34) compared to PIB (1.09-2.67,1.42). The lower discriminative power that Florbetapir produced, with Sensitivity(SE)/Specificity(SP)=86/82 in comparison with 91/90 for PIB, was investigated between the two age groups deriving from the ADNI population. The older subjects displayed much lower SE/SP in comparison to the younger group (72.5/78.9 and 89.9/85.5 respectively).

Conclusions: This study demonstrates the comparability of amyloid imaging in two unrelated, but matched, relatively young populations using two different fibrillar amyloid PET tracers. Moreover, the low discriminative ability of amyloid imaging in older patients may suggest a limited clinical usefulness in an older patient population.

Keywords: *Florbetapir, PIB, ADNI, comparison, age*

Presented by: Chiotis, Konstantinos

P59 The value of early F18-Florbetapir scan information as an estimate of regional cerebral blood flow and comparison to F18-FDG measures of cerebral metabolism

Michael Devous , Abhinay Joshi , Michael Navitsky , Michael Pontecorvo , Daniel Skovronsky , Mark Mintun

Avid Radiopharmaceuticals Philadelphia, PA

Background: Neuroimaging assessments of amyloid plaque and of non-specific neurodegeneration, such as that provided by FDG, may be complementary in the evaluation of neurodegenerative disorders. We explored whether scanning in the first 5 min after florbetapir injection could be used as a surrogate marker of regional cerebral blood flow (rCBF) and assessed the degree to which these images concurred with FDG images of cerebral glucose metabolism (rCGM).

Methods: Florbetapir and FDG PET images from ADNI2 were analyzed for 70 subjects diagnosed as Alzheimer's Disease (AD, N=6), Mild Cognitive Impairment (MCI, N=15), subjective memory complaints (N=31) and cognitively normal (N=18). Subjects had a dynamic PET acquisition from 0-20 min after injection of 370 (±10%) MBq florbetapir. On a separate day all subjects underwent a dynamic (6x5 min) FDG scan (185 MBq ±10%) starting 30 min after injection. Integrated images of the first 5 min of scanning were created for Florbetapir using a trapezoidal method and for all 30 min of the FDG scan. After spatial normalization to MNI space, whole-brain normalized values were calculated for both Florbetapir area under the curve (AUC) and FDG images. Correlation analysis was performed between FDG and florbetapir data from ROIs and on a voxel-wise basis.

Results: For ROI analyses, the average correlation r value was 0.91 with an average slope of 0.81. For voxel-wise correlations, the average r value was 0.84 and the average slope was 0.78. Visual inspection of the "rCBF"/rCGM image pairs revealed substantial concordance among areas of both normal and reduced neuronal metabolism.

Conclusions: ROI and voxel-wise analyses between 0-5 min florbetapir data and 30 min FDG images showed high mean correlations. Further work appears warranted to evaluate the utility of early florbetapir as a surrogate for the functional information seen in an FDG scan.

Keywords: *florbetapir, early scan, FDG, rCBF, rCGM*

Presented by: Devous, Michael

P4

Amyloid imaging changes diagnosis and treatment in patients with progressive cognitive impairment: Multicenter evaluation of 3-month post-scan outcomes

P. Murali Doraiswamy [1], Andrew Siderowf [2], Michael Pontecorvo [2], Stephen P. Salloway [3], Adam S. Fleisher [4], Carl H. Sadowsky [5], Anil K. Nair [6], Ming Lu [2], Anupa K. Arora [2], Daniel M. Skovronsky [2], Mark A. Mintun [2], Michael Grundman [7], AV45-A17 Study Group [8]

[1] *Duke University*
[2] *Avid Radiopharmaceuticals, Inc.*
[3] *Butler Hospital*
[4] *Department of Neurosciences, University of California, San Diego; Banner Alzheimer's Institute*
[5] *Nova Southeastern University*
[6] *Department of Neurology, Alzheimers Disease Center, Quincy Medical Center*
[7] *Global R&D Partners, LLC; Department of Neurosciences, University of California, San Diego*
[8] *AV45-A17 Study Group*

Background: We previously reported that clinicians may change their diagnosis and intended management of patients with cognitive decline based on the results of amyloid imaging.

Objective: To determine whether amyloid imaging could influence actual diagnosis and management.

Methods: In our initial study, 229 patients with progressive cognitive decline and an uncertain diagnosis were recruited to 19 clinical sites. The site physician provided a provisional diagnosis, an estimate of his/her diagnostic confidence, and a management plan both before and after receipt of the florbetapir F18 PET results. In this follow-up study, the clinical charts of participants for the three months following the initial study were reviewed to determine whether the diagnosis reported before amyloid imaging changed and whether study physicians carried out their intended management plan.

Results: Records for 172/229 (75.1%) of participants in the initial study had at least 3 months of clinical follow-up and were available for review. The diagnosis recorded pre-scan was changed in the clinical charts in 46/81 (57.0%) of cases when the florbetapir scan was negative, including24/59 (96.0%) of cases where the pre-scan diagnosis was AD. When the scan was positive, the actual diagnosis changed in 45/91 (49.0%) of cases. Compared to the pre-scan management plan, amyloid imaging results led to a decrease in cholinesterase or memantine use in 20/43 (46.5%) subjects with a negative scan, and the addition of a cholinesterase inhibitor or memantine in 7/57 (12.3%) of cases with a positive scan.

Conclusions: In this multi-center study, we found that evaluation with florbetapir F18 PET altered actual diagnosis and management in a manner consistent with changes in intended management observed in our prior study, possibly avoiding unnecessary treatment. While limited by retrospective methods, the results indicate that amyloid imaging may meaningfully impact how physicians diagnose and treat cognitively impaired patients.

Keywords: *Clinical management,Diagnosis,Amyloid imaging,Clinical trial*

Presented by: Doraiswamy, P. Murali

P35 Practice effects relate to flutemetamol uptake, but not FDG or hippocampal volume: Moving cognition earlier in Jack's curves

Kevin Duff , Norman Foster , Richard King , John Hoffman

University of Utah

Background: Jack et al. (2013) have suggested a temporal ordering of biomarker positivity for Alzheimer's disease, with amyloid deposition occurring before neuronal degeneration and cognitive impairment. However, additional support for this model is needed.

Methods: The current study examined short-term practice effects across one week as a new measure of cognitive functioning and its relationship to amyloid burden (via ^{18}F-flutemetamol PET imaging) and neuronal degeneration (via metabolism on FDG-PET and hippocampal volumes on MRI) in 25 non-demented older adults.

Results: Short-term practice effects significantly correlated with ^{18}F-flutemetamol uptake (r=-0.45, p=0.02), but was more modestly related to FDG-PET metabolism (r=0.33, p=0.11). There was no relationship between practice effects and hippocampal volume on MRI (r=0.04, p=0.85).

Conclusions: In this very mildly impaired sample, short-term practice effects were more strongly related to amyloid deposition (^{18}F-flutemetamol) than with either marker of neuronal degeneration (FDG-PET or MRI). If the temporal ordering of biomarkers in Alzheimer's disease proposed by Jack et al. (2013) is correct, then short-term practice effects may be a more sensitive indicator of cognitive functioning in prodromal Alzheimer's disease.

Keywords: *cognition, amyloid, imaging*

Presented by: Duff, Kevin

P54 Alpha-synuclein imaging: Identifying small molecules that bind to aggregated Alpha-synuclein

Dale Mitchell [1], Kevin Nash [1], David Hardick [1], David Cronk [1], Paul Kotzbauer [2], Zhude Tu [2], Jinbin Xu [2], Robert Mach [3], Jamie Eberling [4], N. Scott Mason [5], William Klunk [5], Chester Mathis [5]

[1] *BioFocus*
[2] *Washington University*
[3] *University of Pennsylvania*
[4] *Michael J. Fox Foundation*
[5] *University of Pittsburgh*

The ability to image alpha-synuclein deposition in the brain would be a game-changing achievement for the Parkinson's disease (PD) field. The accumulation of aggregated alpha-synuclein is a pathological hallmark of PD and a priority target for drug development given its hypothesized contribution to neurodegeneration. Alpha-synuclein pathology also contributes to other conditions, such as Lewy body dementia. *In vivo* imaging of alpha-synuclein pathology could be useful as a biomarker of the presence of disease and disease progression, and as a pharmacodynamic tool for drug development.

A consortium was initiated in 2011 with the goal of developing an alpha-synuclein PET tracer. Two high throughput screens were utilized to identify small molecules that bind to aggregated alpha-synuclein using either the fluorescent ligand Thioflavin T or the radioligand [3H]-Chrysamine G. 100,000 compounds selected from the BioFocus screening libraries based on chemical diversity and lead-like properties were screened for their ability to bind to alpha-synuclein fibrils in both assay formats and identified hit compounds targeting different binding sites.. Initial hit compounds were subjected to hit confirmation, potency studies and for selectivity over beta-amyloid and tau. Compounds for further investigation were prioritized based on selectivity and calculated properties for good CNS penetration. Competitive radioligand binding assays were conducted using the inhibition of [3H]-PiB with 300 nM and 30 nM (cold) concentrations of the compounds to further evaluate their binding to synthetic alpha-synuclein and beta-amyloid fibrils. Compounds that were confirmed for selectivity and affinity in these assays were subsequently radiolabeled and assessed for binding in PD and AD tissue. Two lead series were identified for further optimization and in vivo testing.

Keywords: *alpha-synuclein, Parkinson's, Lewy body*

Presented by: Eberling, Jamie

P1 Evaluation of F-18 radiolabeled cromolyn as a potential Aβ polymerization inhibitor and PET tracer

David R. Elmaleh [1], Timothy M. Shoup [1], Alan J. Fischman [2], Kazue Takahashi [3], Mykol Larvie [1], Erik Vogan [4]

[1] *Massachusetts General Hospital*
[2] *Shriners Hospitals for Children*
[3] *Pediatrics Services, Massachusetts General Hospital*
[4] *Harvard Institutes of Medicine Ctr Neurologic Diseases*

Objective: Multiple lines of evidence suggest that the accumulation of neurotoxic oligomeric aggregates of amyloid-beta is a central event in the pathogenesis of Alzheimer's disease. We have explored cromolyn and its fluorinated analog for potential use as both an amyloid imaging agent and as therapeutic agents. In this study we report the Ab-peptide polymerization inhibition results for these compounds and the synthesis and biodistribution of F-18 labeled cromolyn in mice. Additionally, we have used mathematical modeling to evaluate cromolyn's structural mode of interaction with abeta oligomers.

Method: The Ab-peptide inhibition assays were performed according to the method of Findeis. The progress of Ab polymerization was monitored by measuring turbidity as the apparent UV absorbance in a Bio-Rad microplate reader equipped with a 405-nm filter. Inhibition values are the relative polymerization slow down and are expressed as the relative increased time ratio of the polymerization to reach 50% of maximum signal. Biodistribution of F-18 labeled cromolyn was performed in normal mice at 5, 30, and 60 min. Cromolyn binding to model protofibrils formed from abeta residues 16 to 22 was examined using all-atom explicit-solvent molecular dynamics conducted at 320 K over 20 ns simulation.

Results: Polymerization inhibition assays reveal that cromolyn and its fluorinated derivative caused 6 to 8 fold inhibition at 5 and 50 nM concentration. Biodistribution of the fluorinated analog demonstrates brain accumulation which stayed constant for 5, 30 and 60 min at 0.95, 0.94 and 0.94 % DPG. Preliminary analysis of the binding model indicates that cromolyn binds across the surface of the beta strand in a manner similar to that of Thioflavin-T.

Conclusion: Cromolyn and its fluorinated derivative are potential PET imaging agent for early detection and treatment of Alzheimer's disease.

Mice biodistribution of radiolabeled cromolyn biodistribution shows 1% dose per gram brain accumulate.

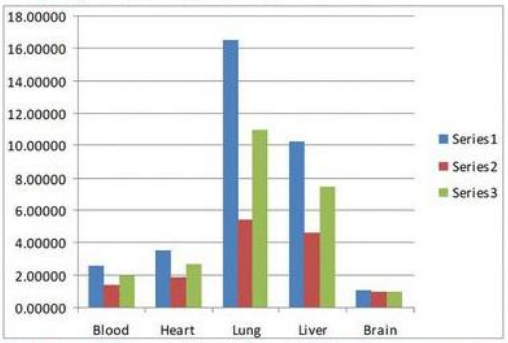

A 5,30,and 60 minute (series in graph) brain uptake shows 1% accumulation with little or no washout for the period measured.

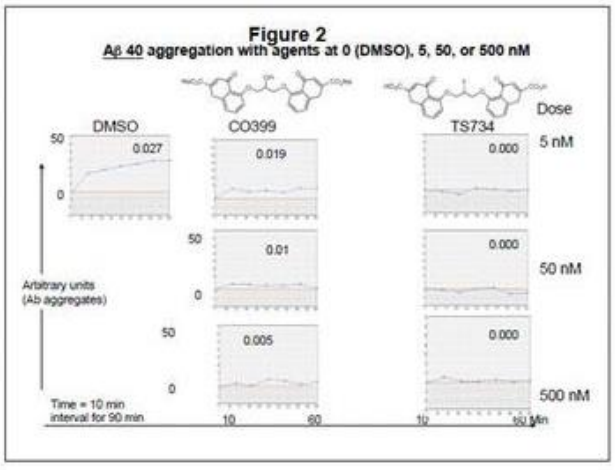

Preliminary analysis of the binding model indicates that cromolyn binding to the surface of beta sheet across the beta strand in a manner similar to Thioflavin-T

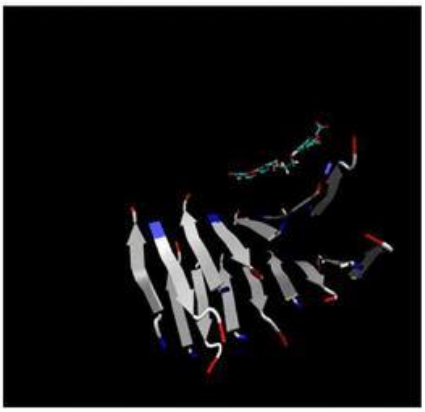

Keywords: *Cromolyn, F-18, Ab-peptide inhibition*

Presented by: Elmaleh, David R.

P62 Effects of age and amyloid on the encoding of visual scene detail

Jeremy Elman [1], Hwamee Oh [2], Cindee Madison [2], Suzanne Baker [1], Jacob Vogel [2], Sam Crowley [2], William Jagust [2]

[1] *Life Sciences Division, Lawrence Berkeley National Laboratory, Berkeley, CA 94720, USA*
[2] *Helen Willis Neuroscience Institute, University of California, Berkeley, CA 94720, USA*

Successful memory encoding is associated with increased and decreased activity across the brain. Both age and disease may be associated with behavioral impairments. However, cognitively normal elderly adults harboring increased levels of beta-amyloid (Aβ) demonstrate changes in brain activity without impaired memory function. It remains unclear whether the quality of memory in these subjects is spared and to what degree changes in activity represent deleterious versus compensatory processes.

Twenty-two young (mean age=23.6) and 49 older subjects (mean age=76.4) completed a visual scene encoding task during an fMRI scan, followed by two tasks to assess gist recall and detail memory. Gist memory was assessed with an old/new and high/low confidence response based on written descriptions of scenes. Subjects made true/false judgments about 6 written details for each scene to asses detail memory. Activity at encoding was back-sorted based on subsequent memory performance. Task-positive and negative networks were determined by contrasting high confidence hits with misses and activity was extracted to assess parametric changes associated with the number of details retrieved. Amyloid burden in the older subjects was examined using PIB-PET imaging and dichotomized into PIB+ and PIB- groups (N= 16 PIB+/33 PIB-).

Memory performance was similar among all groups. Age effects were apparent in multiple regions including the right hippocampus where young subjects showed greater overall activation and a steeper parametric increase of activity with number of encoded details. Interestingly, PIB+ subjects displayed sharper decreases in right inferior parietal (a task-negative region) activity associated with number of details encoded compared to PIB- subjects. In contrast, there was a sharper increase of activity across detail levels among PIB+ subjects in the right inferior LOC, a task positive region. While DMN activity was disrupted in PIB+ individuals, higher activation appeared to support memory formation and may reflect compensatory mechanisms underlying normal functioning in PIB+ subjects.

Keywords: *amyloid, memory, encoding, ageing*

Presented by: Elman, Jeremy

P32 Clinical presentation and imaging findings in complex ALS with AD-like cognitive impairment

Karim FARID [1], Stephen CARTER [1], Elena RODRIGUEZ-VIEITEZ [1], Ove ALMKVIST [1], Pia ANDERSEN [2], Anders WALL [3], Peter ANDERSEN [4], Agneta NORDBERG [5]

[1] Alzheimer Neurobiology Center, Department of Neurobiology, Care Sciences and Society, Karolinska Institutet, Stockholm, Sweden
[2] Department of Geriatric Medicine, Karolinska University Hospital Huddinge, Stockholm, Sweden
[3] Uppsala PET Center, Department of Radiology, Oncology and Radiation Sciences, Uppsala University, Uppsala, Sweden
[4] Department of Neurology, Umeå University, Umeå, Sweden
[5] Alzheimer Neurobiology Center, Department of Neurobiology, Care Sciences and Society, Karolinska Institutet, Stockholm, Sweden. Department of Geriatric Medicine, Karolinska University Hospital Huddinge, Stockholm, Sweden

Introduction: Deposition of fibrillar amyloid in brain is a well-known pathological hallmark of Alzheimer disease (AD). However, its presence in other forms of neurodegenerative diseases is unclear.

Aims: We here report clinical and imaging findings in a patient initially diagnosed as MCI due to AD and included in a multi-tracer PET study who later developed rapid progression of ALS-like impairments in the clinical follow-up.

Methods: A 60-year-old well-educated male was assessed for cognitive impairments. He underwent ^{11}C-PIB, ^{18}F-FDG and ^{11}C-deuterium-L-deprenyl (^{11}C-DED) PET imaging in addition to CSF analysis and neuropsychological assessments.

Results: Neuropsychological examination revealed episodic memory impairments. CSF p-Tau, total-Tau were increased but Aß$_{42}$ was within normal range. Individual patient's images as well as the comparison with age matched healthy controls showed a brain ^{18}F-FDG-PET hypometabolism in the left hippocampus and in the prefrontal cortices consistent with neurodegeneration and a ^{11}C-PiB-PET prefrontal, posterior cingulate and parietal cortices uptake consistent with amyloidal deposition. Furthermore, ^{11}C-DED-PET showed high brain binding consistent with increased astrocytosis. Two consecutive MRI scans showed a progressive right frontal/temporal cortical atrophy. One year later, the patient progressed in memory impairments, and was diagnosed as AD and shortly developed motor impairments and was diagnosed with ALS. After rapid progression, the patient died with pronounced motoric and bulbar symptoms 18 months later. Relatives denied autopsy why post-mortem analysis was not available and the exact pathological diagnosis remains unclear.

Conclusions: The case illustrates a complex pathology and clinical features suggestion that ALS may overlap with other neurodegenerative diseases. Further prospective multi-tracer studies should be conducted to better identify underlying disease mechanisms.

Keywords: *Amyotrophic lateral sclerosis; Fronto temporal dementia; Alzheimer disease; PET imaging*

Presented by: FARID, Karim

P36 Striatal 11C-PiB retention in AD, MCI and HC: the pathotololgical significance of high PIB retention in the putamen

Karim FARID [1], Ove ALMKVIST [1], Katharina BRUEGGEN [1], Stephen CARTER [2], Anders WALL [3], Karl HERHOLZ[4], Agneta NORDBERG [5]

[1] 1- Alzheimer Neurobiology Center, Department of Neurobiology, Care Sciences and Society, Karolinska Institutet, Stockholm, Sweden
[2] 1- Alzheimer Neurobiology Center, Department of Neurobiology, Care Sciences and Society, Karolinska Institutet, Stockholm, Sweden. 2- Wolfson Molecular Imaging Centre, University of Manchester, 27 Palatine Road, Manchester M20 3LJ, UK
[3] 1- Uppsala PET Center, Department of Radiology, Oncology and Radiation Sciences, Uppsala University, Uppsala, Sweden
[4] 1- Wolfson Molecular Imaging Centre, University of Manchester, 27 Palatine Road, Manchester M20 3LJ, UK
[5] 1- Alzheimer Neurobiology Center, Department of Neurobiology, Care Sciences and Society, Karolinska Institutet, Stockholm, Sweden 2- Department of Geriatric Medicine, Karolinska University Hospital Huddinge, Stockholm, Sweden

High fibrillar Aβ deposition in the cerebral cortex has been well established by ^{11}C-PiB-PET in sporadic Alzheimer´s disease (AD) patients. A high ^{11}C-PiB-PET retention was demonstrated in the striatum of PSN1 mutations carriers but is less studied in sporadic AD/MCI.

To better understand the relationship between the striatum and AD pathophysiology, we compared the caudate, putamen and neocortical ^{11}C-PiB-PET retention in 97 AD, 72 mild cognitive impairment (MCI) patients, 51 healthy controls (HC). The putamen and whole-cortex ^{18}F-FDG-PET uptake was also studied in 15 AD, 17 MCI and 6 HC from the same patients.

The putamen ^{11}C-PiB retention exceeded neocortical and caudate ^{11}C-PiB uptake in all subjects (p<0.05; HC and MCI ^{11}C-PiB-negative), (p<0.001; AD and MCI ^{11}C-PiB-positive).

The putamen ^{11}C-PiB retention was HC<AD (p=0.0001), HC<MCI ^{11}C-PiB-positive (p<0.0001), AD>MCI ^{11}C-PiB-negative (p<0.0001), AD>MCI ^{11}C-PiB-positive (p=NS).

The converter-MCI, all ^{11}C-PiB-positive (n=29/72), had higher baseline ^{11}C-PiB retention in the putamen>caudate>neocortex (p<0.0001).

The putamen ^{18}F-FDG uptake exceeded the whole-cortex uptake in all subjects (p<0.001) and was HC<AD (p=0.025), HC<MCI (p<0.001), AD<MCI (p=NS).

Striatum is highly connected to the cortex via several pathways. One possible explanation for the findings might be the functional connectivity that could be behind correlated Aβ plaque levels in functionally-related regions and is supported by research on "hub" vulnerability that has shown highly connected regions to be especially vulnerable to Aβ pathology. Furthermore, the putaminal ^{18}F-FDG increases could reflect a compensation mechanism of this highly connected structure and/or brain inflammation that has been previously described to precede neurodegeneration. Interestingly, we found that even in HC, the ^{11}C-PiB and the ^{18}F-FDG uptake in putamen>neocortex.

Fibrillar amyloid might be present in regions that are not directly related to pathological degeneration and progression of the disease. Moreover, these results emphasize the further understanding of the potential role of the putamen in the AD pathophysiology.

Keywords: *11C-PiB-PET, 18F-FDG-PET, Striatum, Putamen, Alzheimer Disease*

Presented by: FARID, Karim

P29 Advanced education mediates the impact of amyloid burden on reasoning in healthy older adult

Michelle E. Farrell , Gérard N. Bischof , Karen M. Rodrigue , Kristen M. Kennedy , Denise C. Park

University of Texas at Dallas

Objective: To determine whether education, as a proxy of cognitive reserve, differentially mitigates the impact of amyloid burden on four major cognitive constructs: processing speed, working memory, episodic memory and reasoning.

Methods: Subjects were selected from a group of 187 healthy older adults (>60 years of age) from the Dallas Lifespan Brain Study that underwent a comprehensive cognitive battery and a florbetapir amyloid PET scan. Participants were divided into three education groups: Higher (>Bachelor's, n=52), Intermediate (Bachelor's degree, n = 45) and Lower

Results: A 3 x 2 (Amyloid level x Education level) ANOVA revealed main effects of Amyloid ($p=0.05$) and Education ($p<0.001$) and an Amyloid x Education interaction ($p=0.013$) for reasoning. Lower-educated individuals exhibited decreasing reasoning scores with increasing amyloid burden ($R^2=0.083$, $\beta= -1.471$, $p=0.006$) whereas higher-educated individuals were unaffected by amyloid burden ($p=0.662$). The analyses of working memory, processing speed, and episodic memory yielded neither main effects nor interactions associated with amyloid burden.

Discussion: These findings provide evidence that when amyloid is detrimental to task performance, as in the case of reasoning, a high level of education confers resilience to the negative effects of amyloid. These results also add to growing evidence that amyloid deposition may have its strongest effects on higher level cognition.

Keywords: *amyloid, cognitive reserve, education, normal aging, healthy aging, reasoning*

Presented by: Farrell, Michelle E.

P25 Early-frame PiB PET perfusion and FDG PET glucose metabolism comparison in cognitively normal persons at three levels of genetic risk for Alzheimer's disease

Hillary Protas [1], Kewei Chen [1], Ji Luo [1], John Thompson Rausch [1], Robert Bauer III [1], Sandra Goodwin [1], Nicole Richter [1], Daniel Bandy [1], Richard Caselli [2], Adam Fleisher [1], Eric Reiman [1]

[1] *Banner Alzheimer's Institute;Arizona Alzheimer's Consortium*
[2] *Mayo Clinic;Arizona Alzheimer's Consortium*

Background: While Pittsburgh Compound B (PiB) positron emission tomography (PET) is commonly used for assessing fibrillar beta-amyloid deposition, its early frames can also be used for evaluating cerebral perfusion (pPiB). Recent reports showed a significant association between pPiB measured cerebral blood flow and fluorodeoxyglucose (FDG) measured cerebral metabolic rate for glucose in patients with Alzheimer's dementia (AD). This current study characterizes the relationship between regional pPiB and FDG PET measurements in cognitively normal apolipoprotein-E (APOE) ε4 homozygotes(HM), heterozygotes(HT) and noncarriers(NC).

Methods: Dynamic PiB-PET and FDG-PET scans were acquired with a between-scan interval of less than 6 months in 10 APOE-ε4 HM, 18 HT, and 21 NC, 64±6 years of age. pPiB images were computed from frames acquired 1.0-6.5 min, and FDG-PET images from frames acquired 30-60 min after injection, each normalized for the count variation using a cerebellar gray matter reference region. SPM8 was used to characterize and compare differences in regional PET measurements among the three groups. Voxel-wise linear regression was used to characterize the relationship between regional pPiB and FDG-PET measurements.

Results: In comparison with the HT and NC groups, the APOE-ε4 HMs had significantly lower pPiB and FDG PET measurements in the vicinity of the precuneus, posterior cingulate, parieto-temporal cortex, and prefrontal regions ($P<0.005$, uncorrected). There was a close correlation between voxel-based pPiB PET and FDG PET measurements for all subjects ($R^2=0.94\pm0.02$, max=0.97, min=0.84) and a close correlation between voxel-based pPiB-PET and FDG-PET differences among the HM, HT and NC groups ($R=0.71$, $p<1.1e-16$).

Conclusions: PiB-PET and FDG-PET measurements are roughly comparable in their ability to characterize regional differences between cognitively normal persons at differential risk for AD. Further studies are indicated to assess the power of pPiB in the tracking of preclinical AD and in the evaluation of preclinical AD treatments.

Keywords: *Perfusion, PiB, Glucose Metabolism*

Presented by: Fleisher, Adam

P49 Florbetapir-PET has greater clinical impact than FDG-PET in the differential diagnosis of AD and FTD

Pia M. Ghosh [1], Cindee Madison [2], Miguel Santos [3], Kristin Norton [4], Suzanne Baker [4], Adam L. Boxer [3], Howard J. Rosen [3], Zachary A. Miller [3], Marilu Gorno-Tempini [3], Bruce L. Miller [3], William J. Jagust [5], Gil D. Rabinovici [1]

[1] *University of California San Francisco Dept. of Neurology, Memory & Aging Center, Helen Wills Institute, University of California Berkeley, Lawrence Berkeley National Laboratory*
[2] *Helen Wills Institute, University of California Berkeley*
[3] *University of California San Francisco Dept. of Neurology, Memory & Aging Center*
[4] *Lawrence Berkeley National Laboratory*
[5] *Helen Wills Institute, University of California Berkeley, Lawrence Berkeley National Laboratory*

Objective: To prospectively compare the clinical impact of amyloid and FDG PET in discriminating Alzheimer's disease (AD) and frontotemporal dementia (FTD).

Methods: Patients with suspected AD (N=24) or FTD (N=13) were assessed by behavioral neurology fellows and attending physicians at an academic dementia center (10 by fellows, 2 by attendings, 25 by both). Mean age was 63.6±7.6 and MMSE 21.3±6.6. All patients underwent florbetapir-PET, and 35/37 underwent FDG. Scans were visually read blinded to clinical information. Written reports of scan reads were released to clinicians sequentially using a balanced design (50% florbetapir disclosed first, balanced between fellows and attendings). Clinicians independently rated their top clinical diagnosis, diagnostic confidence and management plan (e.g. drug treatment, laboratory evaluations) prior to PET and following disclosure of each scan result.

Results: Florbetapir PET was positive in 63% of patients with suspected AD and negative in 85% of FTD patients. FDG reads agreed with the clinical diagnosis in 73% of AD and 69% of FTD patients. Florbetapir and FDG agreed in classifying 86% of patients (κ=0.72). There was no relationship between the order in which scans were disclosed and concordance with pre-PET diagnosis ($p>0.54$). Fellows changed their primary clinical diagnosis in 15% of cases after florbetapir disclosure and 0% after FDG disclosure ($p<0.001$). Attending physician diagnoses changed in 11% of patients following florbetapir and 4% after FDG results ($p=0.08$). Clinicians reported high diagnostic confidence in 37% of patients pre-PET, 45% post-FDG and 71% post-florbetapir ($p=0.004$ vs. FDG). Changes in management were more frequent after florbetapir (32%) than FDG disclosure (12%) but this was not significant ($p=0.67$). Clinicians reported that amyloid results were more helpful than FDG in 76% of cases.

Conclusions: Amyloid PET had greater clinical impact than FDG, and should be considered the PET scan of choice for the discrimination of AD and FTD.

Keywords: *Florbetapir, FDG, clinical impact, FTD, AD*

Presented by: Ghosh, Pia M.

P44 Source of cognitive complaint and amyloid binding in mild cognitive impairment

Katherine Gifford , Stephen Damon , Angela Jefferson

Vanderbilt University

Background A cognitive complaint is necessary for a mild cognitive impairment (MCI) diagnosis; however, it is poorly understood how complaint relates to biomarkers of Alzheimer's disease (AD) pathology in MCI. We assessed the presence and source of complaint (i.e., self or informant) in relation to regional amyloid binding in MCI.

Methods: MCI participants were analyzed from the Alzheimer's Disease Neuroimaging Initiative (n=66, 73±7 years, 45% female). Self- and informant-cognitive complaint was measured by the Everyday Cognition (ECog) questionnaire. Amyloid binding was captured with positron emission tomography (18)F-AV-45 (florbetapir) and quantitatively measured via the standard uptake value ratio (SUVr) across multiple cortical regions. Correlations related self- and informant-cognitive complaint scores to regional SUVRs.

Results: Informant-based total ECog score of global cognitive complaint was related to increased global (r=0.35, p=0.003), frontal (r=0.34, p=0.006), temporal (r=0.34, p=0.005), parietal (r=0.33, p=0.007), and precuneus regional SUVRs (r=0.39, p=0.001). Self-based total ECog score of global cognitive complaint was not related to differences in SUVR in any cortical region (all p-values>0.30). When limiting complaint to memory only (i.e., ECog memory subscale), informant-complaints were related to increased global (r=0.39, p=0.001), frontal (r=0.36, p=0.003), temporal (r=0.37, p=0.002), parietal (r=0.31, p=0.01), and precuneus regional SUVRs (r=0.44, p<0.001). Self-complaint from the ECog memory subscale was related to increased parietal SUVRs (r=0.29, p=0.01) and trends were noted for global (r=0.24, p=0.06), temporal (r=0.23, p=0.06), and precuneus regional SUVRs (r=0.22, p=0.07).

Conclusion: Findings highlight that in MCI, informant-complaint is modestly correlated with diffuse amyloid binding. This association is present with both a global cognitive complaint and a memory-specific cognitive complaint. However, only a memory-specific self-complaint is related to increased amyloid binding in selective regions. Results suggest informant-complaint may more closely capture the presence of AD pathology than self-complaint in MCI.

Presented by: Gifford, Katherine

P11 Striatal and extrastriatal dopamine transporter levels relate to cognition in Lewy body diseases

Marta Marquie , Joseph Locascio , Dorene Rentz , Alex Becker , Trey Hedden , Keith Johnson , John Growdon , Stephen Gomperts

Massachusetts General Hospital

Objective: The biological basis of cognitive impairment is believed to be multifactorial. We investigated the contribution of dopamine deficiency to cognition in Lewy body disorders (Parkinson Disease [PD] and dementia with Lewy bodies [DLB]) with dopamine transporter (DAT) imaging.

Methods: We acquired ^{11}C-altropane PET and MRI in 19 nondemented subjects with PD, 10 DLB, and 17 healthy control subjects (HCS). We analyzed DAT concentration in putamen, caudate, anterior cingulate (AC), orbitofrontal and prefrontal regions, using the Standardized Uptake Volume Ratio with partial volume correction, and we related DAT concentration and global cortical thickness to neuropsychological performance.

Results: DAT concentration in putamen and in caudate were similar in PD and DLB groups and lower than in HCS. Adjusting for putamen DAT concentration, as a measure of severity of motor disease, caudate DAT concentration was lower in DLB than in PD. Reduced caudate DAT concentration in DLB was associated with worse Clinical Dementia Rating Scale - sum of boxes (CDR-SB) scores and visuospatial skills. Higher AC DAT concentration was associated with lower putamen DAT concentration in DLB and with higher putamen DAT concentration in PD. Higher AC DAT concentration in DLB correlated with greater impairment in semantic memory and language.

Conclusions: Caudate and extrastriatal dopamine dysfunction contribute in opposing directions to cognitive impairment in dementia with Lewy bodies.

Keywords: *Altropane dopamine transporter Parkinson*

Presented by: Gomperts, Stephen

P2

Is there a binary relationship of mean brain Amyloid concentrations to cognitive, functional, metabolic and volumetric MRI variables in the ADNI cohort?

Mohammed Goryawala [1], Malek Adjouadi [1], David Loewenstein [2], Warren Barker [3], Ranjan Duara [3]

[1] *Center for Advanced Technology and Education, Florida International University*
[2] *Psychological Services and Neuropsychology Laboratory, Mount Sinai Medical Center*
[3] *Wien Center For Alzheimer's Disease & Memory Disorders, Mount Sinai Medical Center*

Objective: To determine vulnerability of cognitive, functional, cerebral metabolic rate of glucose (CMRglu) and brain volume variables to fibrillar amyloid burden, in relation to APOE genotype and disease stage in the ADNI Cohort.

Methods: Subjects were cognitively normal (CN) (n= 125), eMCI (n= 114), LMCI (n = 91) and AD (n=55) individuals by APOE e4 genotype status (e4+ (n=136) versus e4- (n=211)) in the ADNI 2 cohort. Piecewise Linear Models were used to assess the concurrent relationships between mean brain standardized uptake value ratios (SUVRs) of [18F]-florbetapir uptake, MMSE, auditory verbal learning test (AVLT), CDR sum of boxes (CDRsb) scores, regional CMRglu values and brain volumes on MRI, as a function of e4 status. Inflection points for SUVR scores in relationship to each of these regression curves were identified by computing points on the linear models at which the second derivative changes sign.

Results: The association of SUVR scores with each variable was stronger for e4+ than e4- subjects ($p<0.01$), with the strongest correlations being with entorhinal cortex volume (R^2 for e4+ =0.19), CDRsb (R^2 for e4+ =0.18), mean CMRglu (R^2 *for e4+= 0.15*), and Hippocampal volume (R^2 for e4+=*0.16).* Inflection points were identifiable for all the variables, and were at higher SUVR scores in e4+ *(* μ=1.286, stddev = 0.12) than e4- *(* μ=1.064, stddev = 0.06) subjects (*p<0.001*). The SUVR at the inflection points among cognitive *(* μ=1.270, stddev = 0.13), atrophy *(* μ=1.230, stddev = 0.16) and CMRglu *(* μ=1.201, stddev = 0.20) variables were different.

Conclusions: The relationships between SUVR scores and scores for cognitive, functional, CMRglu and MRI volumetric variables show a wide range of SUVR scores among e4+ versus e4- subjects. The concept of being amyloid "positive" or "negative" does not appear to be valid.

Keywords: *Fibrillar β-amyloid, Apolipoprotein E, cerebral metabolic rate of glucose (CMRglu), cognitive scores, volumetric brain analysis*

Presented by: Goryawala, Mohammed

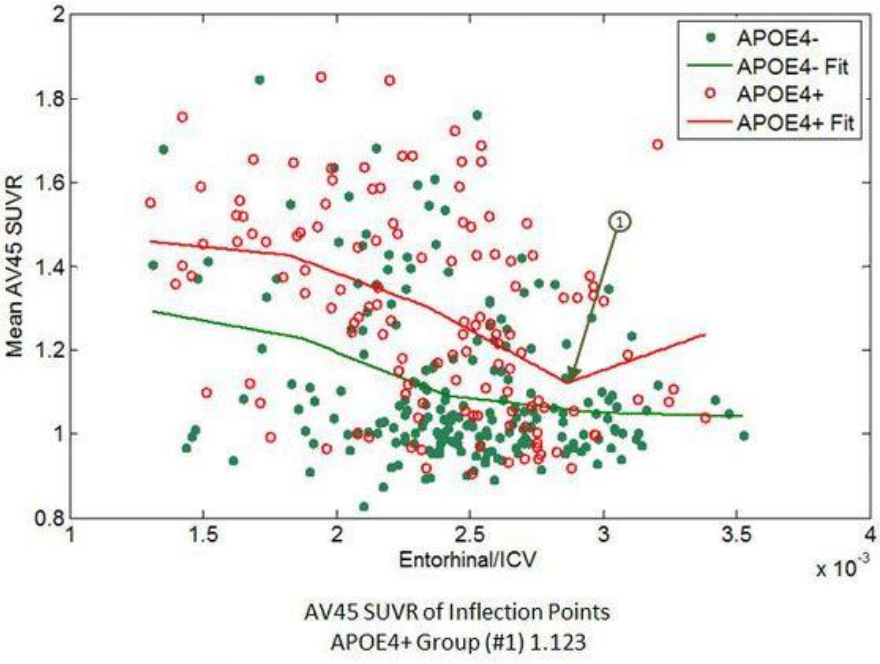

Figure 1: Fibrillar amyloid burden mean AV45 SUVR versus Normalized Entorhinal Cortex Volume showing mean AV45 SUVR for the inflection points of among APOE4- and APOE4+ subjects.

P60

Relationship of regional cerebral volumes to mean brain Amyloid concentration, APOE genotype and disease stage in the ADNI 2 cohort

Mohammed Goryawala [1], David Loewenstein [2], Warren Barker [3], Ranjan Duara [3], Malek Adjouadi [1]

[1] *Center for Advanced Technology and Education, Florida International University*
[2] *Psychological Services and Neuropsychology Laboratory, Mount Sinai Medical Center*
[3] *Wien Center for Alzheimer's Disease and Memory Disorders*

Objective: Regional cerebral glucose metabolism (rCMRglu) in healthy normal was found to be associated with APOE4 genotype (e4) but not with amyloid burden (Jagust and Landau, J Neurosci. 2012; 32: 18227–18233). Therefore, we explored the relationships between ***regional cerebral atrophy***, brain amyloid burden, e4 and disease stage.

Methods: Regional brain volumes (RBV), mean standardized uptake value ratios (SUVR) of [^{18}F] florbetapir uptake and e4 status were studied concurrently among cognitively normal (CN) (n= 154), eMCI (n= 133), LMCI (n = 124) and AD (n=65) subjects in the ADNI 2 cohort, using CDR– Sum of Boxes (CDRsb) to measure disease stage. The relationship between the imaging variables as a function of APOE genotype and CDRsb scores was assessed using GLM.

Results: Mean SUVR increased (p<0.001) and RBV decreased, especially in the hippocampus (*p<0.001*), entorhinal cortex (*p<0.001*), with corresponding ventricular enlargement (*p<0.001*) as a function of disease stage (CDR-SB). When disease stage was included in the model, e4 status was related to mean SUVR *(p<0.001*) and not to RBV, except for ventricular size (*p<0.05*). When disease stage was not included in the model mean SUVR scores were more strongly associated with RBV among e4+ subjects than in e4- subjects (*p<0.01*). The highest correlations between SUVR and RBV were in the entorhinal cortex (R^2 *= 9.5%, p <0.001*) among e4- subjects and the middle-temporal cortex (R^2 *= 16.0%, p< 0.001)* for e4+ subjects.

Conclusions: In contrast to the reported lack of association, in CN subjects, between SUVR and rCMRglu (Jagust and Landau, 2012) when e4 status was taken into account, here we did find localized relationships between SUVR and RBV, independent of e4 status and disease stage. Across the disease stages there is more widespread relationship between regional atrophy in relation to SUVR scores, which is further modified by e4 status.

Keywords: *[18F] florbetapir PET imaging, regional cerebral atrophy, brain amyloid burden, APOE4 genotype*

Presented by: Goryawala, Mohammed

Table 1: Generalized Linear Models for Mean Brain Amyloid Concentration and Regional Cerebral Volumes with respect to APOE Genotype and Disease Stage (CDRsb)

Response Variable	Model R square	Model Terms	p-value
Mean AV45 SUVR	35.18%	APOE4	<0.001
		CDRsb	<0.001
Ventricular Volume	11.73%	APOE4	<0.05
		CDRsb	<0.001
Hippocampus Volume	23.39%	APOE4	ns*
		CDRsb	<0.001
Whole Brain Volume	14.33%	APOE4	ns*
		CDRsb	<0.001
Entorhinal Cortex Volume	28.04%	APOE4	ns*
		CDRsb	<0.001
Fusiform Volume	18.02%	APOE4	ns*
		CDRsb	<0.001
Middle Temporal Volume	23.51%	APOE4	ns*
		CDRsb	<0.001
Intracranial Volume (ICV)	4.45%	APOE4	ns*
		CDRsb	ns*

**ns = not significant at p = 0.05 level.*

Table 2: Generalized Regression Models of Mean Brain Amyloid Concentration SUVR with respect to Regional Cerebral Volumes

Model Term	Model R^2 APOE4 Genotype	
	APOE4-	APOE4+
Ventricular Volume	3.12%	7.83%
Hippocampus Volume	4.30%	13.85%
Whole Brain Volume	6.31%	11.70%
Entorhinal Cortex Volume	9.50%	14.44%
Fusiform Volume	6.72%	8.49%
Middle Temporal Volume	4.74%	16.02%
Intracranial Volume (ICV)*	0.02%	0.01%

**For ICV the regression models are found to be insignificant at p=0.05 level.*

P23 Genetic resilience to Tau- and Amyloid-related neurodegeneration

Timothy Hohman , Mary Ellen Koran , Tricia Thornton-Wells

Vanderbilt University Medical Center

A subset of individuals present at autopsy with the pathological features of Alzheimer's disease (AD) having never manifest the clinical symptoms. Biomarker advances provide the opportunity to investigate such neuroresilience by leveraging measures of amyloid and tau pathology. We sought to identify genetic variants that modify the relation between AD biomarkers and neurodegeneration using data from 690 subjects enrolled in the AD Neuroimaging Initiative (ADNI). We first performed mixed-model regression to fully characterize the relation between the presence of pathology (none, amyloid only, tau only, both) and longitudinal change in lateral inferior ventricle (LILV) volume. Next, we used a genome-wide association study interaction analysis to identify genes that modify this relationship between pathology and atrophy correcting for multiple comparisons. In posthoc analyses we stratified across the ADNI-1 and ADNI-2/GO cohorts to validate identified effects.

Both the presence of amyloid-pathology alone and the combined presence of amyloid and tau was related to ventricular dilation. In genetic interaction analyses we identified two SNP-amyloid (rs7849530, rs4866650) interactions that modified the association between amyloid-positivity (in the absence of tau positivity) and neurodegeneration (**Figure 1)**. These effects were validated across both ADNI cohorts. In each case, the minor allele was associated with increased ventricular dilation in the presence of amyloid pathology. Interestingly, both of these intergenic SNPs are within 50 KB of SNPs previously implicated in AD. Next, we identified one SNP (rs12261764) that modified the relationship between tau pathology (irrespective of amyloid positivity) and neurodegeneration (**Figure 2)**. The minor allele of this SNP was associated with less ventricular dilation (less atrophy) in those with pathology, and more dilation in those without pathology. However, only the protective effect within tau-positive individuals was validated **(Figure 3)**. These findings highlight the potential utility of gene-environment interactions in identifying novel genetic factors relevant to disease risk and resilience.

Keywords: *Resilience, MRI, Genetics, Genetic Interaction, CSF*

Presented by: Hohman, Timothy

P21 Specificity of [^{3}H]T808, [^{3}H]THK-5105 and [^{3}H]AV-45 (florbetapir) binding to aggregated tau and amyloid plaques in human AD tissue *in vitro*

Michael Honer , Henner Knust , Luca Gobbi , Dieter Muri , Edilio Borroni

F. Hoffmann-La Roche Ltd., Basel, Switzerland

Objectives: Amyloid-beta (Aβ) plaques and neurofibrillary tangles (NFT) are key histopathological features in Alzheimer's disease (AD). Their shared beta sheet secondary structure together with their co-existence in AD brains poses major challenges for the development of Aβ- or tau-specific radiotracers. Several radioligands for specific imaging of Aβ plaques and NFTs have recently been published. In this study, the *in vitro* specificity of [^{3}H]T808, [^{3}H]THK-5105 and [^{3}H]AV-45 (florbetapir) was tested by refined autoradiographic techniques along with immunohistofluorescence analysis.

Methods: Radioligand binding to brain tissue sections of early and late stage AD patients as well as tau-overexpressing Tg4510 mice and Aβ-expressing B6.152H mice was analyzed by macro- and microautoradiographies and co-staining of Aβ plaques and NFTs on the same tissue section using Aβ- and tau-specific antibodies.

Results: [^{3}H]AV-45 (florbetapir) revealed specific binding to Aβ plaques as present in human AD and Aβ-expressing transgenic mouse brain tissue. On the contrary, binding of [^{3}H]T808 to AD brain sections was found to be tau-specific, clearly lacking binding to Aβ plaques in AD tissue but also missing binding to NFTs as present in Tg4510 mice. Under the experimental conditions used [^{3}H]THK-5105 showed binding to both Aβ plaques and NFTs in human AD brain and was only positive on Aβ-expressing B6.152H mouse brain sections.

Conclusions: Co-localization studies of radioligand binding and antibody staining on the same tissue section provide a powerful technique to investigate the specificity of tracer binding to human AD tissue on the macroscopic and microscopic level while the use of transgenic mouse models for specificity assessment of novel radiotracers has to be challenged.

Keywords: *PET, autoradiography, T808, AV-45, THK-5105*

Presented by: Honer, Michael

P9 Arterial stiffness is associated with amyloid accumulation over two years in very elderly adults

Timothy Hughes 1, Lewis Kuller 2, Emma Barinas-Mitchell 2, Eric McDade 3, William Klunk 4, Ann Cohen 4, Chester Mathis 5, Steven DeKosky 6, Julie Price 5, Oscar Lopez 3

[1] *Department of Internal Medicine, Wake Forest School of Medicine, Wake Forest University.*
[2] *Department of Epidemiology, Graduate School of Public Health, University of Pittsburgh*
[3] *Department of Neurology, School of Medicine, University of Pittsburgh*
[4] *Department of Psychiatry, School of Medicine, University of Pittsburgh*
[5] *Department of Radiology, School of Medicine, University of Pittsburgh*
[6] *Office of the Dean and Department of Neurology, School of Medicine, University of Virginia*

Importance: Recent studies show that cerebral amyloid deposition is associated with blood pressure and measures of arterial stiffness in non-demented subjects.

Objective: To examine the association of measures of arterial stiffness and change in amyloid deposition over time.

Methods: In this longitudinal study of brain aging, 91 non-demented subjects age 83+ participating of Program Project Grant at the University of Pittsburgh were examined baseline and 81 returned for follow-up imaging. Changes in β-amyloid (Aβ) deposition were determined by positron emission tomography (PET) using the Pittsburgh compound B twice two years apart. Aβ-positivity was assessed using the sparse K-means approach and a standardized uptake value ratio of 1.64 over 6 regions. Arterial stiffness was assessed by pulse wave velocity (PWV) using a noninvasive and automated waveform analyzer at the time closest to the second PET scan. All measures were performed under standardized conditions. PWV was measured in the central (carotid-femoral (cfPWV) and heart femoral (hfPWV)), peripheral (femoral-ankle (faPWV)), and mixed (brachial-ankle (baPWV)) vascular beds.

Results: The proportion of Aβ-positive subjects increased from 45% at baseline to 75% at follow-up. Systemic arterial stiffness as measured by baPWV was significantly higher among Aβ-positive participants at baseline and follow-up. Each standard deviation increase in central stiffness (cfPWV ($p=0.004$) and hfPWV ($p=0.018$)) was associated with increases in Aβ deposition over time.

Conclusions: This study showed that amyloid deposition increases with age in non-demented individuals, and that arterial stiffness is strongly associated with the progressive deposition of Aβ amyloid in the brain, especially in this age group. The observed changes in Aβ deposition over time were associated with generalized arterial stiffness indicating that there is an active relationship between these two processes.

Keywords: *arterial stiffness, amyloid deposition, aging, hypertension*

Presented by: Hughes, Timothy

P61 Estimation of the number of physicians specializing in treating adult dementia patients in the US: Applying appropriate use criteria to medicare claims data

Noam Y. Kirson [1], Urvi Desai [1], Alice Kate G. Cummings [1], Howard G. Birnbaum [1], Craig A. Hunter [2]

[1] *Analysis Group, Inc., Boston, MA*
[2] *Eli Lilly and Company, Indianapolis, IN*

Background: Experts have developed rigorous appropriate use criteria (AUC) for the use of beta amyloid PET imaging. In part, these AUC emphasize that beta amyloid imaging should only be utilized by "dementia experts" who have extensive and documented expertise in diagnosis and management of cognitively-impaired patients. The number of physicians meeting the AUC is unknown.

Methods: Using de-identified administrative claims data for Medicare beneficiaries (5% random sample), physicians were defined as dementia experts if they met the following criteria: 1) physician specialty of psychiatry, neurology or geriatric medicine; and 2) ≥25% of their medical claims in 2011 were associated with patients diagnosed with dementia (ICD-9 CM: 290.x, 294.1, 331.x). Three alternative definitions were used to estimate the share of claims associated with dementia patients, ranging from inclusion of only claims directly associated with a dementia diagnosis code to all claims associated with patients ever diagnosed with dementia. The number of dementia specialists in the US was extrapolated from the sample using national estimates of practicing physicians. Board certification information was unavailable.

Results: Less than 19,000 physicians in the Medicare database met AUC (~50% of all identified psychiatrists/neurologists/geriatricians), with that number reaching as low as 2,740 using the most restrictive definition (~8%). The corresponding extrapolation to the national level ranges from ~28,700 to ~4,400. Using the broader definitions, psychiatrists (~45%) and neurologists (~47%) accounted for most specialists identified, with geriatricians (~8%) representing a much smaller proportion.

Conclusion: This analysis suggests there is approximately one dementia expert for every 1,700–18,000 Medicare beneficiaries. Nearly 5.2 million Medicare beneficiaries are already diagnosed with Alzheimer's disease (AD), a number projected to increase to 7.7 million by 2030. Given this, further agreement on how to operationalize the AUC within Medicare could be valuable to patient management and future research.

Keywords: *AUC, Medicare, dementia specialist*

Presented by: Hunter, Craig A.

P46 Modeling intra-brain Amyloid-ß propagation via an epidemic spreading framework

Yasser Iturria Medina [1], Roberto C. Sotero [1], Alan C. Evans [2]

[1] *Montreal Neurological Institute, Montreal, QC, Canada*
[2] *Montreal Neurological Institute, and Biospective Inc., Montreal, QC, Canada*

Background: Amyloid-ß (Aß) proteins are a key component in aging and associated neurodegenerative disorders, such as Alzheimer´s disease (AD). The prion-like hypothesis explains the AD neurodegenerative progression by the intercellular transfer of Aß proteins[1], under the perspective that these behave like infectious agents that propagate from a few initial host regions to other brain regions. However, characterizing the mechanisms underlying intra-brain Aß proteins propagation/deposition, still represents a major challenge to the molecular pathological approaches[2,3,4] devoted to the study of AD.

Methods: We hypothesized that intra-brain Aß propagation follows an epidemic spreading behavior, whose complex dynamics can be explained by the competitive interaction between Aß propagation agents and the system´s Aß clearing response. Then, we developed a stochastic epidemic spreading model whose contact network is defined by the anatomical connectivity matrix of the brain[5]. The validity/applicability of the proposed hypothesis and model is explored using 756 individual PET datasets from ADNI.

Results/Conclusions: The proposed epidemic spreading behavior model reproduced, from a remote "non-infectious" state, the advanced Aß deposition patterns of healthy and pathologic brains (explaining ~30 % variance of individual intra-brain Aß deposition patterns). Furthermore, and overcoming previous molecular pathological approaches[2,3,4], our model it is capable of clarify the specific biological mechanisms underlying Aß deposition. Specifically, our results strongly suggest that it is not an increased Aß production but a deficit on the Aß clearing processes, resulting in an abnormal deposition pattern, what could be mainly associated to AD development (see Fig.1). The proposed hypothesis/model bears potential implications for the biophysical analysis of misfolded protein neurodegenerative diseases and the assisted creation of therapeutic mitigation strategies.

References:
1. Frost, B, and Diamond, MI, 2010. Nat. Rev. Neurosci. 11, 155–159.
2. Seeley et al, 2009. Neuron, 62, 42–52.
3. Zhou et al., 2012. Neuron, 73, 1216–1227.
4. Raj et al., 2012. Neuron, 73, 1204–1215.
5. Iturria-Medina et al., 2007. Neuroimage, 36, 645-660.

Keywords: *Amyloid-ß, prion-like hypothesis, anatomical brain networks, epidemic spreading*

Presented by: Iturria Medina, Yasser

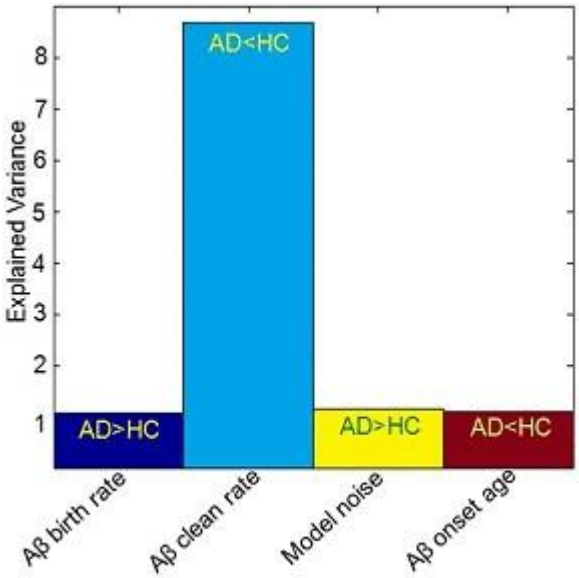

Fig 1. Explained variance of the model variables by the clinical diagnoses (HC, EMCI, LMCI and AD).

P63 The potential of florbetapir F 18 and an early scan PET protocol (0-20 minutes after injection) to evaluate for the presence of amyloid

Abhinay D. Joshi [1], Michael D. Devous Sr. [1], Michael J. Pontecorvo [1], Michael Navitsky [1], Ian Kennedy [1], Mark A. Mintun [1], Daniel M. Skovronsky [1], and Alzheimer's Disease NeuroImaging Intiative [2]

[1] *Avid Radiopharmaceuticals Inc. a wholly owned subsidiary of Eli Lilly and Company*
[2] *ADNI*

Background: Florbetapir quantification typically involves calculation of cortical SUVr values from images acquired 50-60 min after injection. We investigated an empirical method to evaluate amyloid binding of florbetapir using an acquisition only 0-20 min after injection.

Methods: Using florbetapir PET data from early phase development, an empirical approach was developed that used the dynamic 0-20 min to calculate a florbetapir amyloid binding estimate (FABE). We then evaluated the performance of this method with data from the ADNI2 database for 70 subjects diagnosed with Alzheimers Disease (n=6), early or late mild cognitive impairment (n=15), subjective memory complaints (n=31) and cognitively normal (n=18). Subjects had a dynamic PET acquisition from 0-20min (4x15sec, 4x30sec, 3x60sec, 3x120sec, 2x240sec) after injection of 370 MBq of florbetapir. A 10 min acquisition at 50 min after injection was also available for evaluation and was used to calculate standard SUVr values as ratio of cortex to entire cerebellum. The 0-20 min dynamic data was processed to create the FABE using Equation 1. Performance of FABE in classifying cases relative to SUVr was evaluated using ROC analysis and Kappa statistics. A correlation analysis was done as well.

$$\mathrm{FABE} = \frac{\int_0^5 \text{Average cortex (t)dt}}{\int_0^5 \text{Cerebellum(t)dt}} * \left[\frac{\mathrm{d}}{\mathrm{dt}}\mathrm{SUVr(t)}\right]_{8-20} \qquad [1]$$

Results: The range of FABE values was -3733 to 11697. Correlation between SUVr and FABE was r=0.79 ($p<0.001$). A pre-specified threshold (SUVr>1.10) was used to define florbetapir positivity. The optimal threshold for FABE using the ROC curve and Youden index was determined as FABE=210. With this threshold, 96% (67/70) of cases were classified into the same category (positive or negative) as with the standard SUVR method and the kappa between the two measures was 0.91 (95% CI: 0.80 to 1.00).

Conclusion: An empirical method of processing florbetapir PET data from 0-20 min after injection appears to correlate with conventional calculations of SUVr and agree with SUVr threshold-determined positive and negative classifications.

Keywords: *Florbetapir, AV45, PET, AD, early scan*

Presented by: Joshi, Abhinay D.

P58 Comparing concordance of different SUVR calculation methods with florbetapir visual reads

Gregory Klein [1], Ping Chiao [2], Jerome Barakos [3], Derk Purcell [3], Mehul Sampat [1], Joonmi Oh [1], Jeff Sevigny [2], Joyce Suhy [1]

[1] *Synarc, Inc.*
[2] *Biogen Idec*
[3] *California Pacific Medical Center*

Introduction: Visual assessment of florbetapir PET brain scans requires contrasting cortical gray matter with respect to neighboring white matter to obtain binary amyloid status. Quantitative classification approaches based on standard uptake value ratio (SUVR) may perform differently because of differences in co-registration techniques, selection of cortical and reference regions, and determination of thresholds. We evaluate a number of quantitative classification approaches with respect to visual assessment.

Methods: Two independent central readers performed visual assessments of florbetapir PET images for the first 250 subjects screened in a Phase 1b clinical trial. SUVR values of each dataset were computed using three analysis methods: a Freesurfer (FS) analysis in native space, a PET-only analysis in Talairach space (PO), and a hybrid PET/MRI method in Talairach space (HPM) using the same regions as the PO method, but using MRI instead of the PET to obtain the co-registration. Regional SUVRs were evaluated with three reference regions: whole cerebellum (WC), cerebellar grey (CG) and pons or brainstem. SUVR thresholds were determined in two ways: (1) using published thresholds for WC and CG, or via regression analysis for pons and brainstem, and (2) empirical analysis giving highest agreement with visual reads. Discordance between visual assessment and each quantitative approach was separately computed.

Results: Visual assessment is generally more conservative than the quantitative approaches, producing more amyloid negative results. Visual/quantitative discordance ranged from 6.0% to 11.6%, and no method was clearly superior using joint statistics, though the PO method performance was lower due to co-registration issues. Observations of individual discordant cases revealed that the WC reference region appears to be abnormal in some cases, and that a pons or brainstem reference may be preferred.

Conclusions: Concordance of visual reads and SUVR methods is highest for methods using MRI data. The brainstem reference region may provide superior performance.

Keywords: *Visual Reads, SUVR, Florbetapir*

Presented by: Klein, Gregory

Table 1 Discordance of SUVR results with Visual Reads. Top shows results using published SUVR thresholds (discordance % / threshold). Bottom shows (discordance / threshold) for empirically selected SUVR threshold methods.

	Whole Cerebellum	Cerebellar Grey	Pons	Brainstem
Freesurfer	8.0 / 1.10	8.4 / 1.28	-	8.0 / 0.79
PET-only	11.6 / 1.10	-	11.2 / 0.71	-
Hybrid PET/MRI method	6.8 / 1.1	-	8.8 / 0.75	-

	Whole Cerebellum	Cerebellar Grey	Pons	Brainstem
Freesurfer	7.2 / 1.11	7.6 / 1.29	-	6.0 / 0.87
PET-only	8.0 / 1.15	-	8.0 / 0.75	-
Hybrid PET/MRI method	6.4 / 1.15	-	8.0 / 0.73	-

P67 Early age of onset is associated with greater neuroinflammation in Alzheimer's disease

William Charles Kreisl [1], Chul Hyoung Lyoo [1], Meghan McGwier [1], Joseph Snow [2], Kimberly Jenko [1], Winston Corona [3], Cheryl Morse [1], Sami Zoghbi [1], Victor Pike [1], Francis McMahon [3], R. Scott Turner [4], Robert Innis [1]

[1] *Molecular Imaging Branch, National Institute of Mental Health*
[2] *Office of the Clinical Director, National Institute of Mental Health*
[3] *Human Genetics Branch, National Institute of Mental Health*
[4] *Memory Disorders Program, Georgetown University*

Background: Individuals with early-onset Alzheimer's disease (EOAD) demonstrate greater neurodegeneration than late-onset AD (LOAD) patients of equal clinical severity. PET imaging studies show no difference in Pittsburgh Compound B (PIB) binding between EOAD and LOAD patients, suggesting that factors other than fibrillar amyloid contribute to the more aggressive course seen with EOAD. Our recent PET study found that EOAD patients have greater binding with [^{11}C]PBR28 - a radioligand for the inflammatory biomarker translocator protein (TSPO). However, in this study patients were not matched for clinical severity.

Methods: PIB-positive EOAD (n = 20, age of onset = 56 ± 5 years) and LOAD (n = 8, age of onset = 72 ± 6 years) patients were matched by clinical severity. [^{11}C]PBR28 binding was compared using univariate ANOVA with TSPO genotype as a fixed factor. Regional brain volumes were determined using Freesurfer.

Results: EOAD patients had greater [^{11}C]PBR28 binding than LOAD patients in prefrontal cortex, superior and inferior parietal lobule, precuneus, occipital cortex, and temporal cortex ($p < 0.05$). [^{11}C]PBR28 binding inversely correlated with age-of-onset in superior and inferior parietal lobule and precuneus ($r > -0.39$, $p < 0.05$). EOAD patients had greater atrophy than LOAD patients in the superior and inferior parietal lobule ($p < 0.05$). Groups did not differ in Mini Mental State Exam score or Clinical Dementia Rating Scale score. However, EOAD patients had worse performance on Block Design than LOAD patients (raw score 11.1 ± 11 *vs.* 25.8 ± 14, $p = 0.02$).

Conclusion: Among AD patients, earlier age-of-onset is associated with greater focal neuroinflammation. This relationship is strongest in the parietal cortex where EOAD patients also reveal greater atrophy and worse performance on functionally-related cognitive tasks. A more robust neuroinflammatory response to upstream pathological events may explain the more aggressive clinical course of EOAD.

Keywords: *Early onset Alzheimer's disease, inflammation*

Presented by: Kreisl, William Charles

P31 The association between glucose metabolism in Alzheimer's disease-vulnerable regions and cognitive reserve is modified by amyloid status within clinically normal individuals

Molly LaPoint [1], Elizabeth Mormino [1], Rebecca Amariglio [2], Aaron Schultz [1], Trey Hedden [3], J. Alex Becker [4], Keith Johnson [5], Reisa Sperling [6], Dorene Rentz [2]

[1] Athinoula A. Martinos Center for Biomedical Imaging, Department of Radiology, and Department of Neurology, Massachusetts General Hospital, Harvard Medical School, Boston, MA
[2] Center for Alzheimer Research and Treatment, Department of Neurology, Brigham and Women's Hospital, and Department of Neurology, Massachusetts General Hospital, Harvard Medical School, Boston, MA
[3] Athinoula A. Martinos Center for Biomedical Imaging, Department of Radiology, Massachusetts General Hospital, Harvard Medical School, Boston, MA
[4] Department of Radiology, Massachusetts General Hospital, Harvard Medical School, Boston, MA
[5] Departments of Radiology and Neurology, Massachusetts General Hospital, Harvard Medical School, Boston, MA
[6] Center for Alzheimer Research and Treatment, Department of Neurology, Brigham and Women's Hospital, Athinoula A. Martinos Center for Biomedical Imaging, and Department of Neurology, Massachusetts General Hospital, Harvard Medical School, Boston, MA

Objective: To investigate the association between cognitive reserve (CR) and glucose metabolism in clinically normal (CN) individuals with high and low beta-amyloid (Aβ) deposition.

Methods: We studied 162 CN subjects from the Harvard Aging Brain study. All completed PIB-PET and FDG-PET. A CR factor score was created using a confirmatory factor analysis that included years of education, occupation score (adapted from the Hollingshead Two-Factor Index of Social Position), average lifetime cognitive activity (Cognitive Activities Scale), and premorbid verbal IQ (AMNART). We tested the interaction between the CR factor score and Aβ status on patterns of glucose metabolism in temporoparietal regions previously shown to be vulnerable in Alzheimer's disease (AD). Age, gender, and total gray matter were used as covariates.

Results: There was no difference in CR between the Aβ+ and Aβ- subjects. Overall, Aβ+ subjects showed lower FDG metabolism than Aβ- subjects. The interaction between Aβ status and the CR factor score in predicting FDG-PET was significant (p=0.006). Further examination revealed that within Aβ- individuals, *higher* CR was associated with *higher* FDG, whereas within Aβ+ individuals, *higher* CR was associated with *lower* FDG.

Conclusion: This pattern suggests that high CR may modify the relationship between Aβ and glucose metabolism in AD-vulnerable regions, such that CN individuals who are Aβ+ yet have high CR exhibit lower FDG-PET, possibly indicating an ability to maintain clinical function despite greater AD pathology. It is also possible that Aβ+ individuals with low CR and low glucose metabolism were excluded from the study because they are more likely to progress to clinical impairment sooner than their high-CR counterparts.

Keywords: *FDG, PIB, cognitive reserve*

Presented by: LaPoint, Molly

P48

Quantification and accuracy of clinical [11C]-PiB PET/MRI: The effect of MR-based attenuation correction

Ian Law [1], Flemming L. Andersen [1], Adam E. Hansen [1], Steen G. Hasselbalch [2], Claes Ladefoged [1], Sune H Keller [1], Søren Holm [1], Lotte Højgaard [1]

[1] *The Department of Clinical Physiology, Nuclear Medicine and PET, Rigshospitalet, Denmark.*
[2] *Memory Disorders Research Group,Rigshospitalet, Denmark.*

Aims: The Dixon-Water-Fat segmentation (DWFS) method is a standard attenuation correction (AC) method in PET/MRI and has demonstrated a systematic and spatially variable quantitative bias in the brain compared to PET/CT. The aim of this study was to measure the regional and absolute bias of DWFS-AC in combined PET/MR images of the brain using [11C]-PiB and evaluate the impact on the clinical reading of these images.

Methods: Twenty-eight healthy volunteers, 6 MCI, 4 AD, and 6 clinical dementia cases (26 M, 18 F, median age: 68 y (51-78 y)) underwent a simultaneous PET/MRI (Siemens mMR) acquisition 40 min pi of (170-709) MBq [11C]-PiB. A single 30 min frame was reconstructed twice (OSEM-3D, 21it4sub, 5 mm Gauss) with the only difference being the AC calculation. AC was performed using either DWFS or a head CT scan acquired independently on the same day. Activity concentration was sampled on AC-PET from symmetrically delineated ROI's in cortical areas, deep white matter, and the caudate nuclei. Ratios of region-to-cerebellar grey matter (SUVr) were calculated. Bland-Altman analysis was used to compare AC methods.

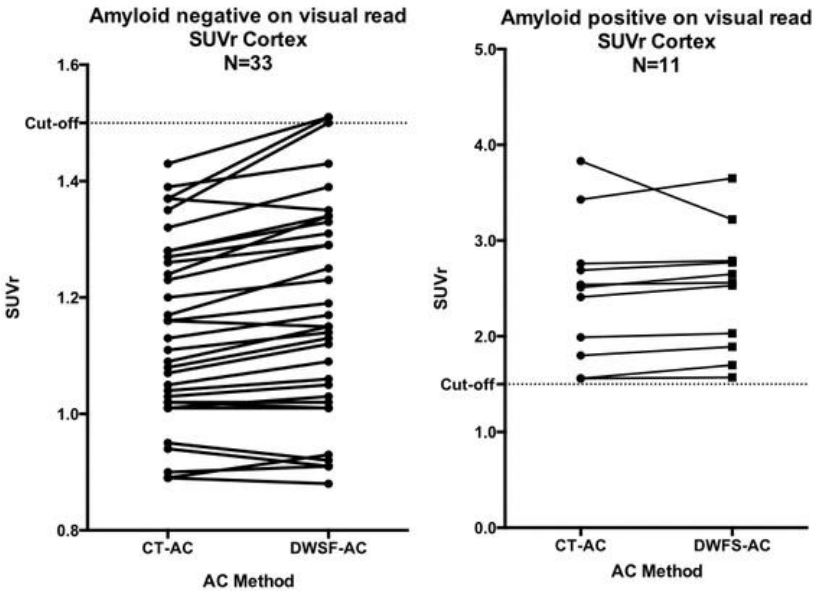

Results: Using CT-AC as the gold standard compared to DWFS-AC the average activity concentration (Bq/mL) in all ROI's was biased by -18 % (-7 to -34 %), and the SUVr's were biased by +0.11 in the caudate nuclei and +0.04 in lateral cortical ROI's. Although the visual categorization of both, amyloid-positive (n=11) and -negative (n=33) scans was unaffected by DWFS-AC, 2 healthy subjects were quantitatively reclassified as amyloid positive.

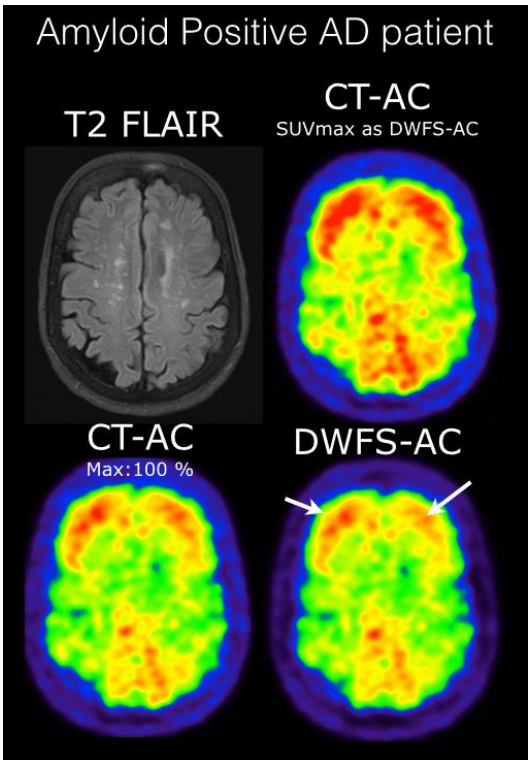

Conclusion: A visual and quantitative evaluation of MR-AC using DWFS in the brain with [11C]-PiB show a noticeable radially variable bias. Although robust on visual reading, the quantitative diagnostic criteria (SUVr) using this biomarker with DWFS-AC may need to be modified.

Keywords: *PiB, Attenuation correction, PET/MRI,*

Presented by: Law, Ian

P13 Relationship between Amyloid burden and clinical course across AD pathophysiologic stages

Richard Margolin [1], Jianing Di [2], Randolph Andrews [3], Steven Salloway [4], Reisa Sperling [5], Leslie Shaw [6], HR Brashear [2], Enchi Liu [2], Mark Schmidt [2], Dawn Matthews [3]

[1] *CereSpir, Inc.*
[2] *Janssen Pharmaceuticals R&D*
[3] *ADM Diagnostics LLC*
[4] *Butler Hospital, The Warren Alpert Medical School of Brown University*
[5] *Departments of Neurology and Radiology, Massachusetts General Hospital, Harvard Medical School; Center for Alzheimer Research and Treatment, Department of Neurology, Brigham and Women's Hospital, Harvard Medical School*
[6] *Department of Pathology and Laboratory Medicine, Institute on Aging, Center for Neurodegenerative Disease Research, University of Pennsylvania Medical School*

Background. Amyloid PET is used to assess fibrillar Aβ burden across AD stages and employed in therapeutic trials. Using SUVRs, individuals are commonly divided into amyloid-positive (amy+) and negative (amy-) groups. In two Phase 3 trials of experimental treatments in AD dementia, differences in clinical characteristics between amy+/- groups were identified in placebo-treated subjects: amy- subjects generally scored better at baseline and declined less than amy+ subjects. The same pattern was observed for demented and MCI subjects in an observational study (ADNI) and was more robust in MCI. Longitudinal divergence between amy+/- groups was suggested on some instruments. The present analysis extends previous work to assess the pattern in subtypes of MCI (EMCI/LMCI) and earlier stage disease.

Methods. We examined initial and longitudinal performance in ADNI subjects with ≥1 amyloid PET scan, using available ADAScog/11, MMSE, RAVLT, CDR-SB and FAQ data. Subjects in the dementia cohort, the MCI cohort, and MCI sub-cohorts were categorized as amy+/- based on tracer-specific cutpoints applied to their initial PET scan. Diagnosis was as recorded at that scan. The effect of APOE4 carrier status was evaluated. Data analysis used an MMRM including age and baseline score.

Results. Of 153 dementia subjects, 12% were amy-. Of 537 MCI subjects, 44% were amy- (EMCI: 52%, LMCI 34%). In both demented and MCI cohorts, amy- scored better at baseline and progressed less. Demented amy- scored significantly better on only ADAScog; MCI amy- scored better on all measures. Similarly, demented amy- declined less on only ADAScog; MCI amy- scored better on almost all measures.

Conclusions. Amy- subjects perform better at baseline and decline less on cognitive and functional measures at all clinical stages; the difference seems most robust in MCI. Inclusion of slowly progressive amy- subjects in therapeutic trials may degrade statistical power and reduce potential study success, especially in early stage disease.

Keywords: *amyloid, burden, positive, negative*

Presented by: Margolin, Richard

P12 Aβ accumulation is associated with hippocampal hypometabolism in cognitively normal older adults regardless of Aβ level

Shawn Marks , Jacob Vogel , Cindee Madison , William Jagust

Helen Wills Neuroscience Institute, University of California, Berkeley, CA

Some older normal individuals show elevated PIB retention indicative of brain β-amyloid (Aβ) deposition, while others do not have high levels of PIB but show evidence of longitudinal increases (accumulation). We sought to characterize the cognitively normal Aβ accumulator with respect to other Alzheimer's disease biomarkers, regardless of Aβ positivity.

A total of 36 cognitively normal older adults from the Berkeley Aging Cohort Study were imaged at two time points using PIB-PET and accumulation was quantified as change per year. Overall, accumulation was significantly greater than zero (as assessed by 1-sample t-test) and there were no differences in accumulation between those identified as Aβ positive or negative at baseline. Anatomically, significant increases were seen in the precuneus and medial frontal/orbitofrontal cortex. Aβ accumulators were labeled as those individuals with change greater than one half standard deviation above the group mean. Change measures (continuous and by accumulator group) were used to assess relationships with brain structure and function. A significant negative relationship was found between the continuous measure of Aβ change and voxelwise baseline glucose metabolism, such that those individuals with the largest Aβ increases displayed hypometabolism bilaterally in the hippocampus (Figure 1). Metabolism in the same left hippocampal region was significantly associated with episodic memory performance at baseline. Significant longitudinal hippocampal volume loss was observed in Aβ accumulators relative to non-accumulators.

Recent longitudinal studies have emphasized the conversion to amyloid positivity; however, these findings show that Aβ accumulation occurs in cognitively normal older adults and is related to underlying neurodegenerative processes, irrespective of Aβ positivity. This suggests that the trajectory of an individual's accumulation may be more meaningful than Aβ deposition at a single time point.

Keywords: *Longitudinal PIB-PET, Glucose Metabolism, Hippocampus*

Presented by: Marks, Shawn

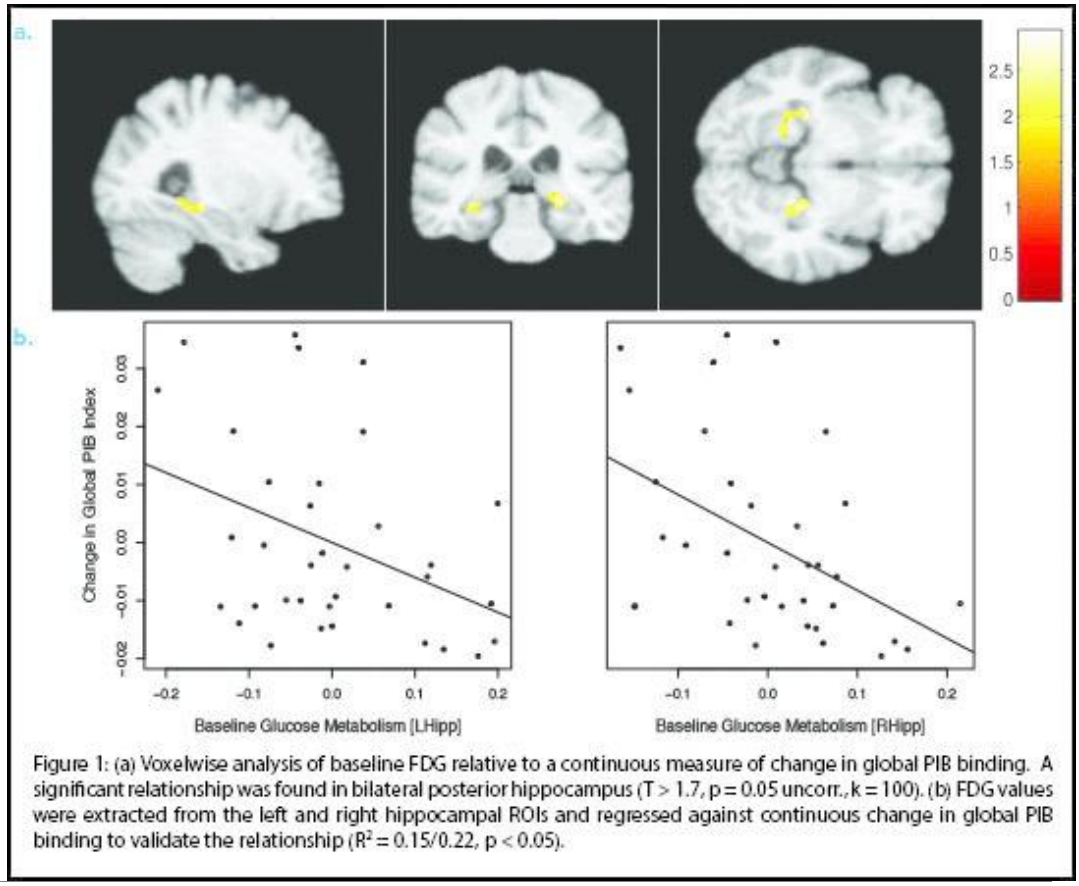

Figure 1: (a) Voxelwise analysis of baseline FDG relative to a continuous measure of change in global PIB binding. A significant relationship was found in bilateral posterior hippocampus ($T > 1.7$, $p = 0.05$ uncorr., $k = 100$). (b) FDG values were extracted from the left and right hippocampal ROIs and regressed against continuous change in global PIB binding to validate the relationship ($R^2 = 0.15/0.22$, $p < 0.05$).

P18 Is there an asymmetric distribution of in vivo Amyloid in primary progressive aphasia?

Adam Martersteck [1], Christopher Murphy [2], Christina Wieneke [1], Kewei Chen [3], Ji Luo [3], Pradeep Thiyyagura [3], M.-Marsel Mesulam [4], Emily Rogalski [1]

[1] *Cognitive Neurology and Alzheimer's Disease Center, Northwestern University (NU) Feinberg School of Medicine, Chicago, IL, USA*
[2] *The University of Arizona College of Medicine, Phoenix, AZ, USA*
[3] *Banner Alzheimer's Institute, Phoenix, AZ, USA*
[4] *Cognitive Neurology and Alzheimer's Disease Center, Northwestern University (NU) Feinberg School of Medicine, Chicago, IL, USA NU Feinberg School of Medicine, Department of Neurology, Chicago, IL, USA*

Background: Primary progressive aphasia (PPA) is a clinical dementia syndrome caused by neurodegenerative disease often characterized by asymmetric atrophy in the language-dominant (usually left) hemisphere. The most common neuropathologies found in PPA are Alzheimer's disease (AD; ~40%) or a form of frontotemporal lobar degeneration (~60%). PPA patients with postmortem AD show a leftward predominance of neurofibrillary tangles, but not beta-amyloid plaques in neocortical areas compared to the symmetric pathology of patients with dementia of the Alzheimer's type. This study will determine whether *in vivo* amyloid imaging shows a clinically concordant asymmetric pattern in a well-characterized cohort of amyloid positive PPA patients.

Methods: Twenty-one PPA subjects with florbetapir imaging were screened for amyloid positivity by calculating cerebral-to-cerebellar standard uptake value ratios (SUVRs) using a gray-matter mask consisting of six bilateral volumes of interest (VOIs) in the frontal, temporal, parietal, anterior cingulate, posterior cingulate, and precuneus. Amyloid positivity was defined as SUVR $\geq$ 1.10. Laterality scores were examined for each VOI pair to determine if there was a leftward asymmetry among the amyloid positive subjects.

Results: Thirteen subjects were amyloid positive. Their mean age was 68.7 (± 5.7) years and they had an average WAB-AQ of 82.0 (± 10.7). Overall florbetapir retention only showed significant leftward asymmetry for the parietal and anterior cingulate VOIs ($p<0.007$ after Bonferroni correction).

Conclusions: These results show that amyloid imaging can show clinically concordant asymmetric distributions in PPA. The marked asymmetry of amyloid in the parietal lobe is consistent with cortical atrophy patterns seen in the early stages of PPA. Previous studies of PPA using PiB have rarely reported lateralized PET amyloid uptake. No quantitative florbetapir imaging studies have been reported in PPA. It will be important to determine if disease stage, atrophy, amyloid agent, and other factors influence the estimated distribution of amyloid *in vivo*.

Keywords: *dementia, Primary Progressive Aphasia, laterality, florbetapir*

Presented by: Martersteck, Adam

P52 CogState computerized testing and neurodegenerative and amyloid imaging: Implications for secondary preventive trials

Michelle Mielke , Heather Wiste , Stephen Weigand , Prashanthi Vemuri , Val Lowe , Mary Machulda , Rosebud Roberts , Kejal Kantarci , David Knopman , Bradly Boeve , Clifford Jack , Petersen Ronald

Mayo Clinic, Rochester, MN

Background: Inexpensive, non-invasive screening tools of brain amyloidosis and neurodegeneration are needed for secondary preventive Alzheimer's disease (AD) trials enrolling cognitively normal (CN) individuals. We examined the association between performance on the CogState computerized cognitive battery and AD neuroimaging measures and compared it to the association between standard neuropsychological tests and neuroimaging measures.

Methods: We included CN Mayo Clinic Study of Aging (MCSA) participants, aged 51-70, who had undergone MRI (n=324), FDG PET (n=259), and/or PiB PET (n=261), the CogState computerized assessment, and standard cognitive battery within 6 months. CogState tests included: Detection (DET) – simple reaction time; Identification (IDN) – choice reaction time; One Card Learning (OCL) – visual learning; One Back test (ONB) – working memory/attention; and the Groton Maze Learning Test (GMLT) – spatial working memory. Linear regression assessed the relationship between each test and continuous measures of PiB PET SUVR, hippocampal atrophy, and FDG PET metabolism in an "AD signature region" (both partial volume corrected and non-corrected), controlling for age, sex, and education. We also examined the relationship between the neuroimaging measures and domain-specific z-scores (memory, language, executive function, visuospatial) using the MCSA standard neuropsychological battery.

Results: A slower reaction time for CogState IDN (p=0.04) and ONB (p=0.006), and lower memory (p=0.001) and attention (p=0.03) z-scores, were associated with FDG hypometabolism without partial volume correction. Fewer moves per second on the GMLT (p=0.001) and lower OCL accuracy (p=0.02) were associated with smaller hippocampal volumes. No CogState tests or cognitive z-scores were associated with PIB at $p<0.05$.

Conclusion: Results suggest this computerized assessment may be a useful indicator of neurodegenerative pathology among CN individuals. Notably, associations between standard cognitive testing and neuroimaging were not much different than that between CogState and neuroimaging. The brief CogState tests might serve an equivalent function as traditional cognitive testing for clinical trials in CN subjects.

Presented by: Mielke, Michelle

P47 Longitudinal Amyloid measurement for clinical trials: A new approach to overcome variability

Dawn Matthews [1], Boris Marendic [1], Randolph Andrews [1], Ana Lukic [1], Steven Einstein [2], Enchi Liu [2], Richard Margolin [3], Mark Schmidt [4], for the Alzheimer's Disease Neuroimaging Initiative [5]

[1] *ADM Diagnostics LLC, Chicago, Illinois*
[2] *Janssen Research and Development, South San Francisco, California*
[3] *CereSpir, New York, New York*
[4] *Janssen Research and Development, Beerse, Belgium*
[5] *ADNI*

Background. Longitudinal amyloid imaging studies amyloid imaging exhibit high within-subject variability and disparate results depending upon the reference region used for SUVr measurement. We took a new approach to understand these discrepancies and address the need for methods that reduce variability.

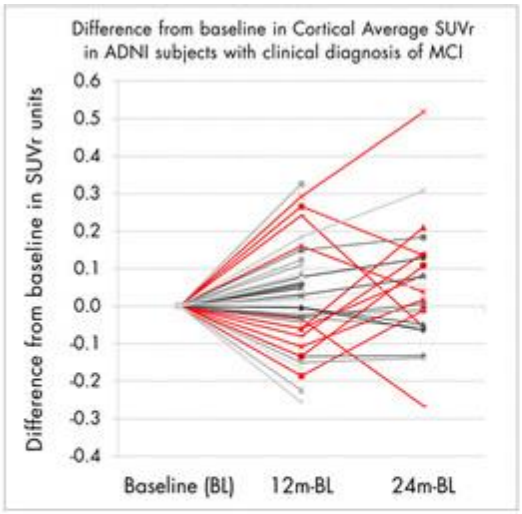

Figure 1. Longitudinal change in cortical average SUVr of ADNI-1 MCI subjects measured using 11C-PiB and ADNI gray cerebellum reference region. Directional changes and subjects exceeding typical ranges are highlighted.

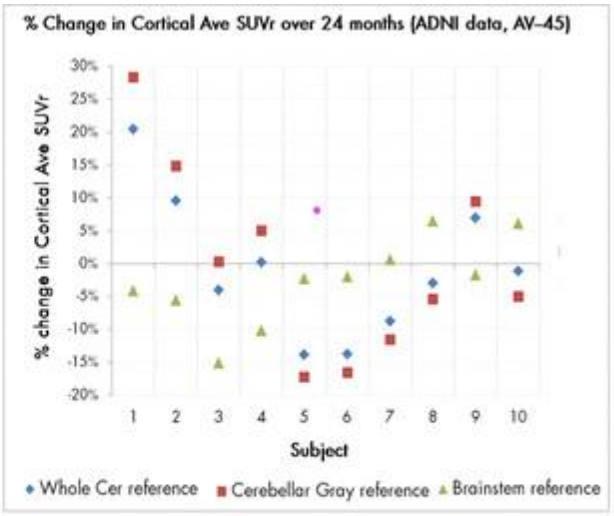

Figure 2. Disparities in 24m change in cortical average SUVr across whole cerebellum, gray cerebellum, and brainstem reference regions for 10 ADNI subjects imaged with florbetapir.

Methods. We examined longitudinal changes in cortical average SUVr in 84 ADNI-GO/2 subjects imaged with florbetapir and 70 ADNI-1 subjects imaged using 11C-PiB. Most SUVr analyses have used reference regions such as cerebellum or pons. We hypothesized that signal may be different in the inferior planes encompassing these regions compared to planes closer to the center of the axial field of view due to factors including scanner detector performance and scatter correction. We first evaluated the way in which signal varied in several regions while traversing transaxial slices of the brain. We then explored whether more centrally located regions that should not accumulate amyloid could serve as alternate references, reducing inferior slice variability. Cortical (altGM) and white matter (WM) approaches were compared.

Results. 24m mean change in florbetapir SUVr was similar across all references (1-2%) but variability was substantially reduced using alternate references (altGM -3 to 6%, WM -11-9%) compared to gray cerebellum (-17%-28%), whole cerebellum (-14%-20%), and pons (-15%-16%). Similarly, 12m %change in 11C-PiB SUVrs was 1-3% across all references but variability was reduced with alternate references compared to gray cerebellum and pons. Longitudinal change in amyloid+ florbetapir subjects became significant only with alternate references ($p<0.00009$, $p<0.002$), and most significant in 11C-PiB subjects ($p<0.00002$) with alternate references, which showed fewer directional changes. Slice-by-slice analysis provided insight to reference region disparities.

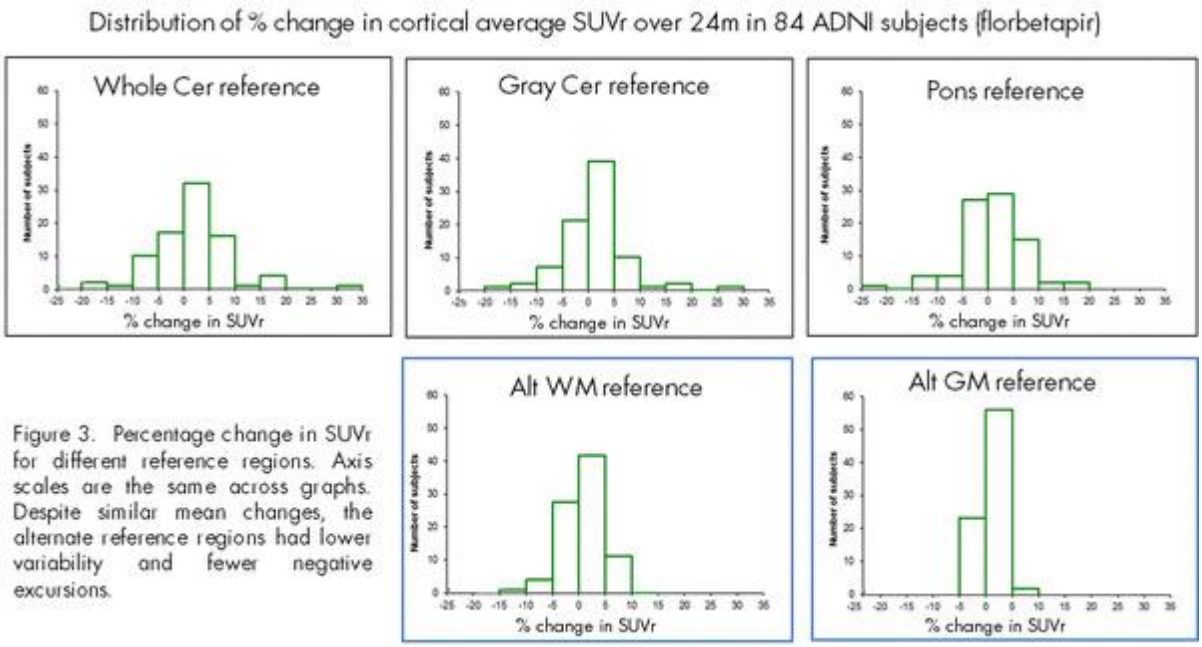

Figure 3. Percentage change in SUVr for different reference regions. Axis scales are the same across graphs. Despite similar mean changes, the alternate reference regions had lower variability and fewer negative excursions.

Conclusions. Our analyses suggest transaxial fluctuation in longitudinal PET signal changes arising from factors likely related to the scanner rather than amyloid. Our alternate reference region approach helps to address acquisition-related variability, benefitting measurement accuracy and statistical power.

Keywords: *imaging, florbetapir, variability, longitudinal, trials*

Presented by: Matthews, Dawn

P16 Prediction of Amyloid-beta hepatic clearance using sandwich cultured primary rat hepatocytes

Loqman Mohamed , Amal Kaddoumi

Department of Basic Pharmaceutical Science, College of Pharmacy, University of Louisiana at Monroe, Monroe, Louisiana

Failure in amyloid beta (Aβ) systemic clearance across the liver has been suggested to play a role in Aβ brain accumulation and thus contributes largely to the pathology of Alzheimer's disease (AD). The purpose of this study was to in vitro characterize the transport mechanisms of $A\beta_{40}$ across the liver using sandwich cultured primary rat hepatocytes (SCHs) and determine its biliary clearance (Cl_{bile}) and biliary excretion index (BEI%). ^{125}I-$A\beta_{40}$ BEI% was time dependent and reached steady state at 30min with an average value of 29.8% and Cl_{bile} of 1.47ml/min/kg of body weight. The role of low density lipoprotein-receptor related protein-1 (LRP1) in mediating the basolateral uptake of ^{125}I-$A\beta_{40}$ in SCHs was assessed using receptor-associated protein (RAP, 2μM). Significant reduction in ^{125}I-$A\beta_{40}$ BEI% and Cl_{bile} with RAP was observed, demonstrating a major contribution of LRP1 in mediating hepatic uptake of intact ^{125}I-$A\beta_{40}$ via transcytosis. Furthermore, activity studies suggested lower role of receptor for advanced glycation end products (RAGE) in ^{125}I-$A\beta_{40}$ hepatic uptake. Verapamil (50μM) and valspodar (20μM) significantly reduced ^{125}I-$A\beta_{40}$ BEI% indicating a role for P-glycoprotein (P-gp) in the biliary excretion of ^{125}I-$A\beta_{40}$ in SCHs. LRP1 and P-gp mediated ^{125}I-$A\beta_{40}$ biliary excretion was inducible and increased BEI% by 26% following rifampicin pretreatment. In conclusion, our findings demonstrated that beside LRP1, P-gp and to a lesser extent RAGE are involved in ^{125}I-$A\beta_{40}$ hepatobiliary disposition and support the use of enhancement of ^{125}I-$A\beta_{40}$ hepatic clearance via LRP1 and P-gp induction as a novel therapeutic approach for the prevention and treatment of AD.

Keywords: *Amyloid-beta, P-glycoprotein, LRP1, hepatic sandwich culture, biliary clearance.*

Presented by: Mohamed, Loqman

P64 Identifying cost-effective predictive rules of Amyloid-β level by integrating neuropsychological tests and plasma-based marker

Shuai Huang [1], Amanda Smith [2], Mona Haghighi [3], Brent Small [4], Dave Morgan [2]

[1] *Industrial and Management Systems Engineering & Byrd Alzheimer's Institute, University of South Florida*
[2] *Byrd Alzheimer's Institute, University of South Florida*
[3] *Industrial and Management Systems Engineering, University of South Florida*
[4] *School of Aging Studies, University of South Florida*

Background: Detecting participants who are positive for Aβ pathology is germane in designing prevention trials by enriching for those cases that are more likely to be amyloid positive. Existing brain amyloid measurement techniques, such as the Pib-PET and CSF, are not reasonable first-line approaches limited by either feasibility or cost.

Method: We compared different methods for integrating the Neuropsychological measurements and blood-based markers to predict the amyloid-β level.

Results: Using the ADNI cohort, we successfully extracted predictive rules of amyloid-β level.

Conclusion: Our study demonstrated that the integration of the Neuropsychological measurements and blood-based markers significantly improved the prediction accuracy. The prediction model has led to several simple rules, which have a great potential of being naturally translated into clinical settings such as enrichment screening for Alzheimer's prevention trials of anti-amyloid treatments.

Keywords: *amyloid prediction, Neuropsychological, plasma*

Presented by: Morgan, Dave

P14

Associations between beta-amyloid, markers of neurodegeneration, and cognition in clinically normal individuals from the Harvard Aging Brain Study

Elizabeth Mormino [1], Rebecca Betensky [2], Trey Hedden [3], Aaron Schultz [1], Rebecca Amariglio [1], Dorene Rentz [1], Keith Johnson [4], Reisa Sperling [4]

[1] Department of Neurology, Massachusetts General Hospital, Massachusetts General Hospital, Harvard Medical School, Boston, Massachusetts 02114
[2] Department of Biostatistics, Harvard School of Public Health, Boston, Massachusetts 02115
[3] Department of Radiology, Massachusetts General Hospital, Harvard Medical School, Boston, Massachusetts 02114
[4] Department of Neurology, Massachusetts General Hospital, Massachusetts General Hospital, Harvard Medical School, Boston, Massachusetts 02114; Department of Radiology, Massachusetts General Hospital, Harvard Medical School, Boston, Massachusetts 02114; Cen

Objective: To determine the strength of the association between beta-amyloid (Ab) and neurodegeneration (ND), as well as the relationship between these factors and cognitive decline in clinically normal subjects (CNs).

Methods: Data was examined from 191 CNs (age=74.5±6.0). Ab status was determined with PIB-PET, and ND was measured using hippocampus volume and glucose metabolism from Alzheimer's disease (AD) vulnerable regions. The associations between Ab and each marker of ND was assessed. Cut-offs for each ND marker were derived based on an AD sample, and CNs were considered ND+ if below the cut off for either ND marker. CNs were categorized into preclinical AD stages based on Ab and ND, and longitudinal decline was contrasted across groups (episodic memory and executive function composite scores, as well as Logical Memory delayed recall; follow-up=1.86±0.70).

Findings: Ab+ CNs showed significantly increased ND compared to Ab- CNs (however, these associations were small: r-values<0.20, <4% of the variance). Categorizing CNs revealed 47% in preclinical stage 0 (Ab-/ND-), 11% stage 1 (Ab+/ND-), 15% stage 2 (Ab+/ND+) and 24% SNAP ("Suspected Non-AD pathology"; Ab-/ND+). Stage 2 showed greater decline compared to other groups across multiple measures, whereas no other pair-wise contrast was significant.

Interpretation: Small associations between Ab and ND suggest that additional factors may contribute to the variance in markers of ND. It is also possible that the association between Ab and ND is weaken by a survival bias, such that Ab+/ND+ CNs are more likely to progress to mild cognitive impairment and thus less likely to be included in the CN sample. Consistent with this speculation, we found that stage 2 was most at risk for decline. Regardless of whether Ab and ND pathways are linked in the initial phase of AD, the presence of both factors is critical in assessing risk of decline among CNs.

Keywords: *aging, preclinical AD, neurodegeneration, beta-amyloid*

Presented by: Mormino, Elizabeth

P55 Beta-amyloid has a greater impact on memory in females than males across the clinical spectrum

Elizabeth Mormino [1], Reisa Sperling [2]

[1] Department of Neurology, Massachusetts General Hospital, Massachusetts General Hospital, Harvard Medical School, Boston, Massachusetts 02114
[2] Department of Radiology, Massachusetts General Hospital, Harvard Medical School, Boston, Massachusetts 02114; Center for Alzheimer Research and Treatment, Department of Neurology, Brigham and Women's Hospital, Harvard Medical School, Boston, Massachusetts

Objective: Although Alzheimer's disease (AD) is more prevalent in females, recent biomarker studies of AD development have not addressed mechanisms that may underlie this risk. We sought to determine whether female's heightened risk may be related to 1) a greater propensity to accumulate Aβ and/or 2) greater cognitive impairment for a given level of Aβ.

Methods: We analyzed data for 639 clinically normal (CN), 539 mild cognitive impairment (MCI), and 175 AD patients, collapsed across HABS, ADNI and AIBL. Subjects were included if they had amyloid imaging (HABS/AIBL=PIB; ADNI=AV45) and neuropsychological (Logical Memory delayed recall) data available. Logistic regression was used to assess whether gender was associated with Aβ positivity. Multiple regression models were conducted to determine the association between Aβ status and memory, and how this association may vary by gender. All analyses were conducted separately within each diagnosis, controlling for cohort, age,*APOE4* and education.

Results: We did not find evidence for a greater proportion of Aβ+ female subjects compared to males. Examination of memory scores revealed worse performance in Aβ+ female CNs than Aβ- female CNs (p=0.06), whereas there was no association between Aβ status and performance in CN males. In MCI, there was an effect of Aβ in both females and males (p-values<0.001), with high Aβ MCI females additionally showing worse memory than high Aβ MCI males (p=0.02). Finally, Aβ+ AD females showed lower scores than Aβ+ AD males (p=0.05, see Figure).

Conclusion: Although females were not more likely to be Aβ+, females tended to show worse memory for a given level of Aβ than their male counterparts. It is possible that additional gender-specific factors interact with Aβ to influence this heightened vulnerability, such as hormonal changes and/or higher levels of inflammation.

Keywords: *gender, memory, beta-amyloid*

Presented by: Mormino, Elizabeth

P28 PiB-PET significantly differs across neuropathologic classification of Alzheimer-type pathology and tangle predominant dementia

Melissa E. Murray [1], Dennis W. Dickson [1], Emily S. Lundt [2], Stephen D. Weigand [2], Scott A. Przybelski [2], Lennon G. Jordan [2], Joseph E. Parisi [2], David S. KNopman [2], Bradley F. Boeve [2], Kejal Kantarci [2], Ronald C. Petersen [2], Clifford R. Jack, Jr. [2], Val J. Lowe [2]

[1] *Mayo Clinic Jacksonville*
[2] *Mayo Clinic Rochester*

Background: Mild-to-moderate AD pathology is classified based upon severity of neurofibrillary tangles (NFTs) and amyloid-β plaques as "senile change" or "pathologic aging", while advanced AD can be classified into three distinct subtypes based upon predominance of cortical versus limbic NFTs. Limbic predominant AD (LP-AD) is an atypical AD subtype characterized by high numbers of limbic NFTs compared to cortex. In contrast, hippocampal sparing AD has greater involvement of cortex versus limbic regions, while typical AD shows expected involvement without NFT predominance. LP-AD differs neuropathologically from tangle predominant dementia (NFT-D), by plaque distribution and type. Clinical differentiation, however, is difficult given similarities in amnestic syndrome, older age-of-onset, and focal hippocampal atrophy.

Methods: Of the 40 autopsied subjects who underwent antemortem PiB- and FDG-PET imaging, 31 had a range of Alzheimer-type pathology. Using thioflavin-S microscopy, NFTs and plaques were counted in hippocampal and cortical regions for neuropathologic classification of Alzheimer-type pathology as (Table 1): normal, senile change, pathologic aging, and AD. NFT counts were used for AD subtyping of typical and LP-AD (Table 1). Criteria for NFT-D includes high numbers of hippocampal extracellular NFTs, sparse cortical NFTs, and absent neuritic plaque pathology. Global PiB measures were referenced to cerebellum (cutoff≥1.50), and FDG measures to pons (cutoff≤1.31).

Results: Global PiB differed across Alzheimer-type pathologic classifications ($p<0.001$), but FDG values did not ($p=0.101$) (Table 2). Both LP-AD subjects were PiB-positive (1.85 and 2.2), but the Braak=IV subject had a normal FDG (1.46) and the Braak=VI subject had an abnormal FDG (0.9). The NFT-D subject did not meet PiB-positivity cutoff (1.26), but had an abnormal FDG (1.05).

Table 1: Neuropathologic classification of Alzheimer type pathology

	β-amyloid plaques/ 100x magnification*	Neurofibrillary tangle (NFT) description
Normal	0	Braak NFT stage < IV
Senile change	< 30	Braak NFT stage < IV
Pathologic aging	≥ 30	Braak NFT stage < IV
Alzheimer's disease		Braak NFT stage ≥ IV
Limbic predominant AD	≥ 30	NFTs: Hippocampus >> Cortex
Typical AD		NFTs: Hippocampus > Cortex
Hippocampal sparing AD		NFTs: Hippocampus << Cortex

Braak neurofibrillary tangle stage, according to Braak & Braak, Acta Neuropathologica 1991; *Neocortical amyloid-β plaque cutoffs were derived according to Khachaturian criteria (Archives of Neurology 1985)

Conclusions: Global PiB differed across neuropathologically-defined groups of Alzheimer-type pathology, but FDG may be confounded by coexisting pathologies - emphasizing the need for more specific biomarkers (*e.g.* tau imaging ligands). Our results suggest molecular imaging of amyloid-β will allow distinction of AD from NFT-D – a likely candidate of the suspected non-Alzheimer's pathology (SNAP) group.

Table 2: PiB- and FDG-PET across neuropathologic classification of Alzheimer-type pathology and tangle predominant dementia

Pathologic class	Sample size	PiB-PET	FDG-PET
Normal	3	1.29 (1.28-1.37)	1.41 (1.22-1.52)
Senile change	3	1.47 (1.34-1.51)	1.16 (1.2-1.29)
Pathologic aging	11	1.74 (1.53-1.97)	1.33 (0.99-1.43)
Alzheimer's disease	13	2.12 (1.82-2.54)	0.88 (0.76-1.26)
Limbic predominant AD	2	2.03 (1.85-2.23)	1.16 (0.87-1.46)
Typical AD	11	2.12 (1.84 (2.55)	0.88 (0.68-1.23)
Hippocampal sparing AD	0	---	---
Neurofibrillary tangle predominant dementia	1	1.26	1.05

Keywords: *Atypical Alzheimer's disease, neurofibrillary tangles, amyloid plaques, neuropathology, memory*

Presented by: Murray, Melissa E.

P10 Brain Amyloid deposition influences the Cognition-Mobility Interface (COMBINE) in cognitively normal older adults

Neelesh Nadkarni [1], Beth Snitz [2], Annie Cohen [3], Stephanie Studenski [1], Subashan Perera [1], Oscar Lopez [2], Robert Nebes [3], William Klunk [3]

[1] *Department of Medicine (Geriatric Medicine and Gerontology), University of Pittsburgh School of Medicine, Pittsburgh, PA*
[2] *Department of Neurology, University of Pittsburgh School of Medicine, Pittsburgh, PA*
[3] *Department of Psychiatry, University of Pittsburgh School of Medicine, Pittsburgh, PA*

Background: Gait slowing precedes cognitive decline in Alzheimer's disease. Cognition and mobility rely on common brain resources that are prone to amyloidosis. The **co**gnition-**mo**b**i**lity **in**terfac**e** (**COMBINE**), assessed by measuring costs on gait when performing cognitive tasks while walking, acts as a "stress test" of underlying brain resources. Greater brain amyloid burden could affect the COMBINE, manifesting as a decrement in gait speed and therefore greater dual-task costs on gait speed.

Aim: To study whether the COMBINE is related to brain amyloid burden in cognitively normal elders.

Methods: Gait speed during single-task walking (ST) and costs on gait speed while walking and dialing a phone (dual-task cost) were measured on an automated walkway. Participants were divided based on their amyloid burden, determined on Pittsburgh B (PiB) PET, into high-amyloid (PIB+) and low-amyloid (PiB-) groups, using established PiB standardized uptake value ratio (SUVR) cutoffs. ST gait speed and dual-task costs were compared between groups. Regional PiB correlates of the dual-task costs were explored in the entire sample.

Results: The two groups (4 PiB+, 6 PiB-) were comparable in age (76 years), education, cognitive status (MMSE: 29), processing speed (DSST: 52 vs 60), physical performance (SPPB: 11) and grip strength. ST gait speed was comparable between groups (1.2 vs 1.1 m/sec, p=0.2); however, the dual-task cost was significantly greater in the PiB+ than PiB- group (p=0.02, Figure 1). Dual-task costs significantly correlated with global PiB SUVR (r=0.65, p=0.04) and regional PiB SUVR in the frontal (r=0.67, p=0.03), anterior ventral striatum (r=0.75, p=0.01), anterior cingulate (r=0.71, p=0.02), posterior cingulate (r=0.72, p=0.02) and thalamus (r=0.69, p=0.03). ST gait speed did not correlate significantly with any global or regional PiB SUVR.

Conclusions: Brain amyloid burden may influence the COMBINE, which appears to be related to the severity of amyloid deposition in regions relevant to cognition and mobility.

Keywords: *mobility, cognition, amyloid, PiB, dual-task, gait*

Presented by: Nadkarni, Neelesh

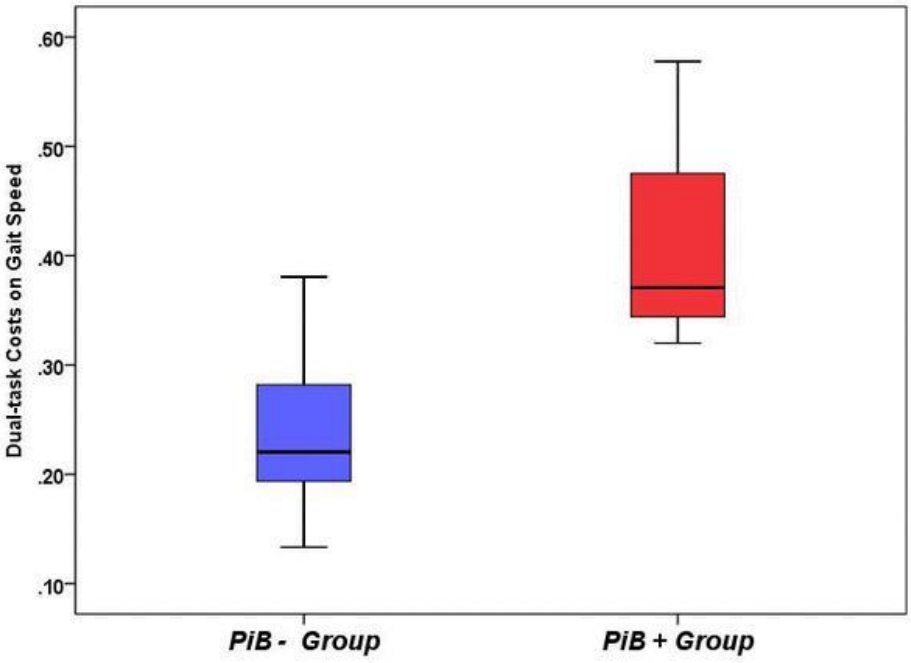

Figure 1: Dual-task costs on gait speed while walking and dialing a phone relative to single-task gait speed in low-amyloid (PiB-) and high-amyloid (PiB+) groups.

P22 Astrocytosis, amyloid deposition and gray matter density in parahippocampus of MCI patients

Il Han Choo [1], Stephen F Carter [2], Michael Schöll [3], Agneta Nordberg [4]

[1] Karolinska Institutet, Alzheimer Neurobiology Center, Stockholm.Sweden Department of Neuropsychiatry, School of Medicine, Chrosun University, Gwangju, Republic of Korea
[2] Karolinska Institutet,Alzheimer Neurobiology Center, Stockholm, Sweden Wolfson Imaging Center, Manchester University, Manchester, United Kingdom
[3] Karolinska Institutet, Alzheimer Neurobiology Center, Stockholm,Sweden
[4] Karolinska Institutet, Alzheimer Neurobiology Center, Stockholm, Sweden Department of Geriatric Medicine,Karolinska University Hospital Huddinge, Stockholm.Sweden

Introduction: The Alzheimer disease (AD) pathology is characterized by deposition of fibrillar amyloid, neurofibrillar tangles as well as activation of astrocytes and microglia, atrophy, dysfunctional synapse and cognitive impairments. Recent autoradiography studies have shown a different laminar distribution of astroglia and fibrillar Aß in cortex and hippocampus autopsy AD brains (1). In addition PET studies have shown an increased astrocytosis measured by ^{11}C-d-deprenyl (DED) in patients with mild cognitive impairment (MCI) in comparison to AD patients and controls (2).

Aims: to test the hypothesis that neuronal inflammation is an early phenomena in AD pathology related to Aß plaque deposition.

Methods: 20 patients with AD or mild cognitive impairment (MCI) underwent ^{11}C-PIB, ^{18}F-FDG and ^{11}C-deuterium-L-deprenyl (^{11}C-DED) PET imaging in addition to MRI scans, CSF biomarker analysis and neuropsychological assessments.

Results: A positive correlation was observed between PIB PET retention and DED binding in the parahippocampus of AD patients ($p<0.014$) while a negative correlation between gray matter density and DED binding was observed in PIB+ MCI patients. A negative correlation was observed between CSF Aß42 levels and PIB retention in parahippocampus of MCI+AD patients ($p<0.003$) while a positive correlation between total Tau and PIB retention in AD. CSF total tau also negatively correlated with decrease in gray matter density in MCI patients ($p<0.001$). No significant correlation was observed with FDG PET and any of the other PET, MRI or CSF biomarkers. Conclusions: High astrocytosis in the parahippocampus of PIB+ MCI patients suggest an early preclinical influence on neuronal loss. The lack of correlation between astrocytosis and CSF tau levels but positive correlation between astrocytosis and fibrillar amyloid deposition indicate that the parahippocampal astrocytosis is related to amyloid pathology.

1. Marutle et al. J Neuroinflammation 2013 ; 10 : 90
2. Carter et al. J Nucl Med 2012 ; 53 :37-46.

Keywords: *Fibrillar amyloid , astrocytosis, gray matter density, parahippocampus, MCI,AD, PET, 11C-d-deprenyl, 11C-PIB, MRI, CSF biomarkers*

Presented by: Nordberg, Agneta

P65 Regional brain activity and functional connectivity during memory encoding are differentially affected by age and β-amyloid deposition in cognitively normal older adults

Hwamee Oh [1], Jeremy Elman [1], Suzanne Baker [2], Cindee Madison [1], Jacob Vogel [1], Sam Crowley [1], William Jagust [3]

[1] Helen Wills Neuroscience Institute, University of California- Berkeley, CA 94720, USA
[2] Life Sciences Division, Lawrence Berkeley National Laboratory, Berkeley, CA 94720, USA
[3] Helen Wills Neuroscience Institute, University of California- Berkeley, CA 94720, USA and Life Sciences Division, Lawrence Berkeley National Laboratory, Berkeley, CA 94720, USA

While β-amyloid (Aβ) is present in a large proportion of cognitively intact older adults, its effect on brain activity during normal aging is not yet well understood. We examined how brain activity and connectivity underlying successful episodic encoding change as a function of age and Aβ deposition using fMRI and [^{11}C] PIB PET. Twenty-two young (mean age=23.6, 12 males) and 49 cognitively normal older adults (mean age=76.5, 20 males) performed an episodic encoding task of visual scenes during fMRI scans, followed by a postscan recognition task where subjects made an old/new judgment with confidence ratings based on written descriptions of the gist of visual scenes and a true/false judgment on 6 written visual details of the scenes. 150 encoding trials were sorted based on gist accuracy and the number of details correctly recognized. Older adults were further classified as PIB negative (PIB−) Old and PIB positive (PIB+) Old.

Compared to PIB- older subjects, young subjects showed increased activation in visual association areas (VA), inferior frontal cortex and hippocampus bilaterally for successful gist memory. PIB- older adults, however, showed an increased activation in the lateral and medial parietal cortex and lateral and medial frontal cortex. In addition, PIB- older adults showed stronger connectivity between the right parahippocampal gyrus (rPHG), VA, and lateral frontal cortex for gist memory but reduced connectivity between rPHG, VA, and hippocampus for visual details. Compared to PIB- older adults, PIB+ older adults showed greater activation in left hippocampus, VA and medial frontal cortex but reduced connectivity between rPHG and hippocampus for gist memory. These results suggest that neural correlates of gist memory and memory for specific episodic details are differentially affected by age. In addition, the presence of Aβ is associated with hippocampal dysfunction seen as increased regional activity but reduced functional connectivity during memory process.

Keywords: *Normal Aging, β-amyloid, Memory system*

Presented by: Oh, Hwamee

P66 Prevalence of Amyloid in cognitively normal, MCI and demented subjects – A meta-analysis of Amyloid PET studies

Rik Ossenkoppele [1], Willemijn Jansen [2], Bart van Berckel [1], Pieter Jelle Visser [3]

[1] *VU University Medical Center, Amsterdam, the Netherlands*
[2] *Maastricht University, Maastricht, the Netherlands*
[3] *VU University Medical Center, Amsterdam, the Netherlands & Maastricht University, Maastricht, the Netherlands*

Introduction: The advent of PET ligands that bind to amyloid-β have caused a major paradigm shift in diagnostic thinking. With almost a decade of experience, this is the time for a thorough meta-analysis of amyloid imaging studies to date.

Objectives: 1) to estimate the prevalence of amyloid in cognitively normal, MCI and demented subjects; 2) to relate this prevalence to age and APOE genotype.

Methods: First, MEDLINE databases were searched for "PET", "Amyloid", "Amyloid-beta", "PIB", "Flutemetamol", "Florbetapir" or "Florbetaben". Abstracts were screened and if the study appeared appropriate, corresponding authors were approached for individual subject data (i.e. amyloid PET status, APOE genotype, age, sex, education, MMSE and CDR). We applied random effects models to estimate the prevalence of amyloid.

Results: Clinical and demographic characteristics are presented in table 1. The prevalence of amyloid was 25.1% in cognitively normal subjects (n=1348), 53.0% in MCI (n=1055), 87.6% in AD dementia (n=1146) and 22% in non-AD dementia (n=510) (Figure 1). In cognitively normal subjects and MCI patients, older age and APOE ε4 carriership were associated with higher prevalence of amyloid ($p<0.05$; Figure 2A+B). In AD dementia patients, amyloid PET scans were more often negative in older and APOE ε4 negative patients ($p<0.05$, Figure 2C). Patients with a clinical diagnosis of VaD appeared more often amyloid PET positive with increasing age ($p<0.05$, Figure 2D), while this was not the case for DlB, FTD or dementia-other patients (e.g. CBD or PDD).

Conclusions: The major risk factors for the onset of AD, ageing and APOE ε4 genotype, were associated with higher prevalence of amyloid pathology in cognitively normals and MCI patients. In non-AD dementias, this ageing effect was observed only in VaD. APOE ε4 negative and older AD patients were more often amyloid-negative on PET.

Keywords: *Amyloid-PET, meta-analysis, prevalence, APOE, ageing.*

Presented by: Ossenkoppele, Rik

P19 Longitudinal quantification of brain amyloidosis in a rat model of Alzheimer's disease using [18F]NAV4694

Maxime J. Parent [1], MinSu P. Kang [1], Sonia Do Carmo [2], Antonio Aliaga [3], Cornelia Reininger [4], Jean-Paul Soucy [3], Serge G. Gauthier [1], A. Claudio Cuello [2], Pedro Rosa-Neto [1]

[1] *Translational Neuroimaging Laboratory, McGill Centre for Studies in Aging, Montreal Canada*
[2] *Department of Pharmacology, McGill University, Montreal Canada*
[3] *Montreal Neurological Institute, McGill University, Montreal Canada*
[4] *Navidea Biopharmaceuticals, Dublin OH, USA*

Background: Alzheimer's disease (AD) transgenic rat models allow in-vivo multiparametric acquisitions including CSF, plasma and imaging biomarkers as well as behavioral measures, without limitations imposed by the smaller size of mice. Here, we present imaging data on the McGill-R-Thy1-APP AD rat, which harbors amyloidosis due to a double APP mutation (Swe/Ind).

Aims and Hypothesis: We aimed to quantify brain fibrillary amyloid accumulation in the McGill-R-Thy1-APP using the amyloid imaging agent [^{18}F]NAV4694, which displays a favorable kinetic and biodistribution profile. We hypothesize an age-dependent [^{18}F]NAV4694 binding increase in Tg rats.

Methods: [^{18}F]NAV4694 PET (precursor provided by Navidea Biopharmaceuticals Inc.) was acquired at 10 and 16 months in 16 McGill-R-Thy1-APP rats (8 Tg, 8 wildtype ; WT). BP_{ND} maps were obtained from 60 minute dynamic acquisitions following [^{18}F]NAV4694 (11.99 ± 2.55MBq at 78.11 ± 34.06 TBq/mmol) tail-vein injection; pons was chosen as a reference region. Voxel-level group and age effects were estimated using a repeated measures general linear model.

Results: No differences were observed between Tg and WT at 10 mo. At 16 months, Tg rats showed higher [^{18}F]NAV4694 binding in the anterior cingulate cortex (t = 4.72), thalamus (t = 2.87) and hippocampus (t = 2.7) (Fig. 1). Compared to baseline, 16 mo Tg rats showed 5 to 46% [^{18}F]NAV4694 binding increases in various cortical areas (Fig. 2).

Discussion: [^{18}F]NAV4694 captured progressive global and regional amyloid plaque accumulation in 16 mo old McGill-R-Thy1-APP rat. Amyloidosis evolved from 10-16 months at an average rate of up to 7.73% per month. Highest amyloidosis regions overlap with the rat default mode network.

Significance: These results support the feasibility of using McGill-R-Thy1-APP and [^{18}F]NAV4694 PET as a platform for quantifying drug effects targeting amyloidosis. Animal models expressing a single AD pathophysiological feature associated with longitudinal study designs are crucial for developing of disease modifying therapies.

Keywords: *Transgenic rat, longitidunal, [18F]NAV4694*

Presented by: Parent, Maxime J.

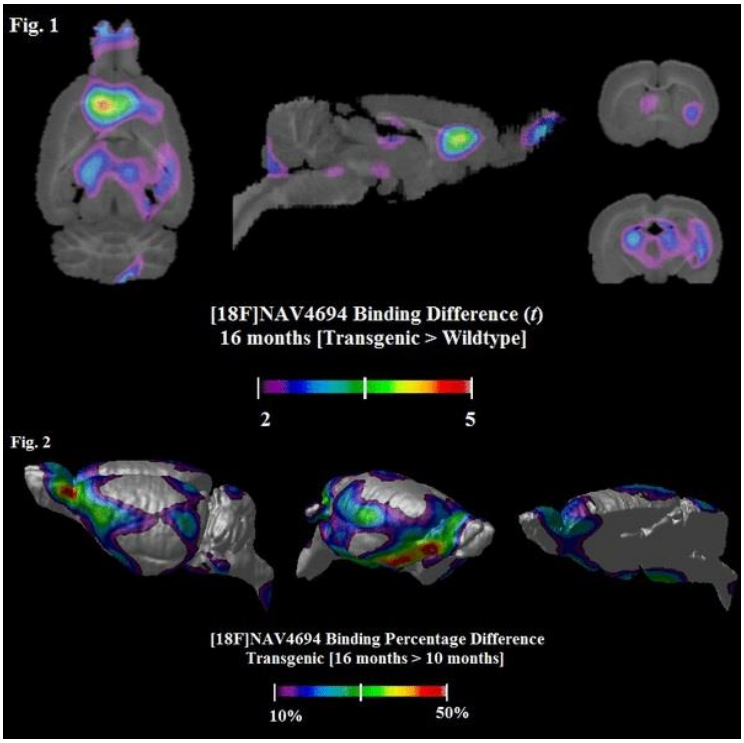

P30 Potential value of an interpretation method that incorporates quantitative estimate of cortical to cerebellar SUVr as an adjunct to visual interpretation of florbetapir PET scans

Michael Pontecorvo , Michael Devous Sr. , Anupa K. Arora , Marybeth Devine , Ming Lu , Andrew Siderowf , Stephen P. Truocchio , Catherine Devadanam , Abhinay D. Joshi , Christopher Breault , Stephen L. Heun , Daniel M. Skovronsky , Mark A. Mintun

Avid Radiopharmaceuticals, Inc.

Background: Commercial software is available for quantitation of amyloid PET images. We evaluated whether employing quantitation by FDA-cleared software as an adjunct to visual interpretation (VisQ method) improves accuracy of florbetapir scan interpretation in lower accuracy readers (those with <90% accuracy using visual techniques alone).

Methods: Twenty-two physicians were trained to use quantitation of florbetapir images as an adjunct to visual interpretation. Each reader then visually interpreted, without access to quantitation information, 46 florbetapir PET images from subjects autopsied within one year of PET scan (Clark et al, 2012) and 50 images selected from patients seeking diagnosis for cognitive decline (Grundman et al, 2012). Next, the readers reviewed all 96 images again, using MIMneuro 6.0.6 software to calculate a quantitative estimate (SUVr) of florbetapir activity and applied the VisQ method. For each case, the reader compared the SUVr to normal ranges. For scans in which the initial visual read and quantitative result were discordant, readers reassessed their original interpretation in light of the quantitation, reinspected images and verified ROI placement (a potential source of error in SUVr calculation) to resolve any discordance. They then provided a final VisQ interpretation.

Results: With visual interpretation, the mean accuracy (compared to pathology truth standard) on the 46 autopsy verified cases was 89.5%. 7 of the 22 readers were identified as lower accuracy visual readers. In these 7 readers, accuracy improved significantly with VisQ from a mean of 81.7% to 88.8% ($p=0.0029$). Across all 22 readers, accuracy improved from 89.5% to 93.8% ($p<0.0001$). Interreader agreement across all 96 cases increased ($p < 0.05$) from a Fleiss kappa of 0.72 to 0.79.

Conclusions: Accuracy and interreader reliability increased significantly after applying the VisQ method that incorporates quantitative estimates of florbetapir PET amyloid binding (SUVr).

Keywords: *Amyloid,florbetapir,quantitation,interpretation*

Presented by: Pontecorvo, Michael

P57 The Alzheimer's structural connectome: Patterns of cortical reorganization with increasing neuritic amyloid plaque burden

Jeff Prescott [1], Arnaud Guidon [2], P. Murali Doraiswamy [3], Kingshuk Choudhury [1], Chunlei Liu [2], Jeffrey Petrella [1]

[1] *Department of Radiology, Duke University Medical Center*
[2] *Brain Image Analysis Center, Duke University*
[3] *Departments of Psychiatry, Medicine and the Duke Institute for Brain Sciences, Duke University Medical Center*

Purpose: Evaluate differences in the structural connectome among patients with normal cognition, mild cognitive impairment (MCI), and Alzheimer's disease (AD), and determine the effect of increasing cortical amyloid deposition.

Materials and Methods*:* There were 102 subjects in the Alzheimer's Disease Neuroimaging Initiative 2 who met criteria for analysis. Subjects' T1 scans were automatically parcellated into regions of interest. Standardized uptake value ratios (SUVr) were calculated from florbetapir PET scans for composite cortical regions (frontal, cingulate, parietal, and temporal). Structural connectome graphs were created from DTI scans, and connectome organization was analyzed in each region using graph theoretic metrics. ANOVA of structural connectome metrics and florbetapir SUVr across diagnostic group was performed. Linear mixed effects models were fit to analyze the effect of florbetapir SUVr on the structural connectome metrics.

Results: Diagnostic group was associated with changes in weighted structural connectome metrics, with decreases from NC to MCI to AD demonstrated for strength in the bilateral frontal, right parietal, and bilateral temporal regions ($p < 0.05$); weighted local efficiency in the left temporal region ($p < 0.05$); and weighted clustering coefficient in the bilateral frontal and left temporal regions ($p < 0.05$). Increasing cortical florbetapir SUVr was associated with decreases in weighted structural connectome metrics; namely, strength ($p = 0.00001$), weighted local efficiency ($p = 0.00001$), and weighted clustering coefficient ($p = 0.0006$), independent of brain region.

Conclusions: Increasing amyloid burden is related to reorganization of the large-scale structural network architecture of the brain even in the preclinical stages of AD.

Keywords: *Structural connectome, Network theory, Florbetapir*

Presented by: Prescott, Jeff

P39 Mathematical modeling of amyloid-β disposition by brain endothelial cells

Hisham Qosa [1], Bilal Abuasal [1], Jeffrey Keller [2], Amal Kaddoumi [1]

[1] *College of Pharmacy University of Louisiana at Monroe*
[2] *Pennington Biomedical Research Center Louisiana State University.*

Alzheimer's disease has a characteristic hallmark of amyloid-β (Aβ) accumulation in the brain. This accumulation of Aβ has been related to its faulty cerebral clearance. Evaluation of kinetic parameters of Aβ uptake, efflux and degradation by endothelial cells of the blood-brain barrier (BBB) is essential to understand key steps involved in Aβ clearance across the BBB and its brain accumulation. Here, bEnd3 and hCMEC/D3 cells, as in vitro mouse and human BBB models, respectively, were used to establish a mathematical model to describe Aβ disposition by endothelial cells. Aβ disposition in brain endothelial cells involves several processes that simultaneously take place; therefore, the utilization of a mechanistic model to estimate $A\beta_{40}$ kinetic parameters in endothelial cells should provide a better approach than the conventional Michaelis-Menten. The mechanistic model depends on measurement of Aβ uptake and degradation at multiple time points with multiple Aβ concentrations at each time point. Based on our results from Aβ uptake and degradation studies in bEnd3 and hCMEC/D3 cells, these processes were best described by a mechanistic two-compartment model that could successfully describe Aβ disposition. The model structure consisted of saturable uptake and efflux processes in addition to linear intracellular degradation. The established model showed that: a) Aβ uptake process determines subsequent degradation and efflux processes, b) brain endothelial cells mediate Aβ degradation however the degradation rate is dependent on uptake rate and is higher in bEnd3 cells, and c) both cells mediate efficient efflux of intact Aβ. In conclusion, the established model offered a mathematical description of Aβ clearance across the BBB which could be improved to predict Aβ accumulation, aggregation and Aβ binding to different antibodies and imaging tracers in the brain.

Keywords: *amyloid, blood-brain barrier, disposition, mechanistic modeling*

Presented by: Qosa, Hisham

P43 Amyloid burden influences the relationship between hippocampal volume and default mode network connectivity in cognitively normal elderly

Aaron Schultz [1], Elizabeth Mormino [1], Willem Huijbers [2], Jasmeer Chhatwal [1], Andrew Ward [3], Sarah Wigman [4], Molly LaPoint [4], Trey Hedden [1], Keith Johnson [1], Reisa Sperling [4]

[1] Athinoula A. Martinos Center for Biomedical Imaging, Department of Radiology, Massachusetts General Hospital, Harvard Medical School, Boston, MA
[2] Department of Psychiatry, Massachusetts General Hospital/Harvard Medical School and the Athinoula A. Martinos Center for Biomedical Imaging
[3] Helen Wills Neuroscience Institute, University of California, Berkeley, CA Athinoula A. Martinos Center for Biomedical Imaging, Department of Radiology, Massachusetts General Hospital, Harvard Medical School, Boston, MA
[4] Center for Alzheimer Research and Treatment, Department of Neurology, Brigham and Women's Hospital, Harvard Medical School, Boston MA and the Athinoula A. Martinos Center for Biomedical Imaging

Rationale: Currently, preclinical Alzheimer's disease (AD) is often defined by evidence of fibrillar amyloid-β deposition. We hypothesized that within a cognitively normal group of elderly we would see differential relationships between markers of synaptic dysfunction and neuronal loss in individuals harboring a high amyloid burden (Aβ+) versus those who do not (Aβ-). In particular we investigated the cross-sectional relationship between default mode network functional connectivity (DMN-FC) and hippocampal volume (HV).

Methods: We examined cross-sectional relationships in neuroimaging data from 195 cognitively normal subjects (55 Aβ+ and 140 Aβ-) from the Harvard Aging Brain Study. DMN-FC measurements were made using Template Based Rotation, and HV measurements were made with Freesurfer v5.1. For Aβ we used a standard measure of cortical deposition of PiB, computed as DVRs with a cerebellar grey matter reference region.

Results: We found an interaction between amyloid status and HV when predicting DMN-FC ($F(1,190)=6.73$; $p=0.01$), such that there is a significant relationship between DMN-FC and HV only within the Aβ+ group (Aβ+: $r=0.459$, $p<0.001$; Aβ-: $r=0.031$, $p=0.717$). Modeling HV as a dichotomous variable we confirmed the interaction between Aβ and HV ($F(1,90)=8.75$, $p=0.003$), with the pattern of means showing lower DMN-FC in the Aβ+/small HV group as compared to the other three groups.

Conclusion: The presence of a relationship between DMN-FC and HV in only the Aβ+ group suggests that AD-type pathological changes drive alterations in both connectivity and structure, and that these changes are present prior to clinically defined impairment. We suggest that MR biomarkers can serve an important role in determining the approximate preclinical stage of AD in cognitively normal individuals with amyloid plaques.

Keywords: *Default Mode Network, functional connectivity, amyloid, preclinical Alzheimer's disease, hippocampal volume*

Presented by: Schultz, Aaron

P40

Update on the multicenter phase 3 histopathology study for ß-amyloid brain PET imaging

Osama Sabri [1], Andrew Stephens [2], Ana Catafau [2], Henryk Barthel [3], John Seibyl [4]

[1] *Department of Nuclear Medicine University of Leipzig, Leipzig, Germany For the Florbetaben Study Group*
[2] *Piramal Imaging, Berlin, Germany*
[3] *Department of Nuclear Medicine University of Leipzig, Leipzig, Germany*
[4] *MNI, New Haven, CT, USA*

Background: The pivotal histopathology phase 3 study of florbetaben was designed for an exact tissue-matched regional analysis of post-mortem brain tissue and imaging during life to detect and locate a pathological state. This is the first study demonstrating a direct correlation of amyloid deposition and tracer uptake in the identical anatomic region. In addition to assessment of specific regions, final neuropathological diagnosis was established by the onsite pathologist including the assessment of neuritic ß-amyloid plaque density according to CERAD criteria. A method for the visual assessment of florbetaben PET scans in clinical practice was validated. The results from the first 31 brains have been presented previously. After the initial analysis, brains of enrolled subjects that reached post-mortem continued to be collected and analyzed. We now present new results from the subject-level analyses with additional brain specimens.
Methods: 216 subjects were enrolled and underwent MRI and florbetaben PET scanning. All baseline PET scans were quantitatively assessed and read by three in-person trained readers using the method proposed for clinical practice. PET results were compared with presence/absence of neuritic β-amyloid plaque density according to CERAD criteria at the patient's autopsy and sensitivity & specificity was calculated. Subject-level quantitative analysis was performed and the composite SUVR was determined for each subject. A ROC curve analysis was performed to determine the optimal threshold for sensitivity / specificity calculation.
Results: In total 74 brain specimens became available and were assessed by onsite pathology. Sensitivity and specificity of the majority read of the subject-level visual assessment vs. histopathology was 97.9% and 88.9%, respectively. ROC curve analysis determined the optimal cut-off for sensitivity and specificity calculations to be 1.478. Using this quantitative analysis, a high sensitivity (89 %) and specificity (92 %) was obtained.
Conclusions: Previous results from 31 subjects were confirmed in a larger cohort. Visual and quantitative assessment is in good agreement.

Keywords: *florbetaben, histopathology, amyloid, PET*

Presented by: Seibyl, John

P24 TAU Tracer F^{18}-T807 inversely relates with brain functional hubs of elderly normals

Jorge Sepulcre [1], Sperling Sperling [2], Keith Johnson [3]

[1] Division of Nuclear Medicine and Molecular Imaging, Department of Radiology, Massachusetts General Hospital and Harvard Medical School, Boston, MA, USA; Athinioula A. Martinos Center for Biomedical Imaging, Charlestown, MA, USA
[2] Athinioula A. Martinos Center for Biomedical Imaging, Charlestown, MA, USA; Centre for Alzheimer Research and Treatment, Department of Neurology, Brigham and Women's Hospital and Harvard Medical School, Boston, MA, USA, Department of Neurology, Massachuse
[3] Division of Nuclear Medicine and Molecular Imaging, Department of Radiology, Massachusetts General Hospital and Harvard Medical School, Boston, MA, USA; Centre for Alzheimer Research and Treatment, Department of Neurology, Brigham and Women's Hospital and

Background: Alzheimer's disease neuropathologic processes are thought to affect brain function before cognitive manifestations appear. Molecular imaging facilitates the early detection of *Ab* and the study of its effects on brain dysfunction and cognitive decline. Recent development of tau tracers has similarly enabled studies of tau-related pathology. In this study, we evaluated the spatial distribution of a novel tau PET tracer ^{18}F-T807 and identify its relationship with *Ab* deposition and functional network connectivity in normal elderly subjects.

Methods: Twenty-four normal elderly subjects (mean age (SD): 74 (6.6), M/F: 11/13) underwent two PET imaging acquisitions (^{11}C-PIB and ^{18}F-T807) and MRI session. Conventional preprocessing and normalization procedures were performed on the PET images. A functional connectivity map (Buckner et al, 2009; Sepulcre et al, 2010) was obtained in each subject by quantifying the FDR-corrected degree of functional connectivity MRI. We used voxel-by-voxel regressions to evaluate spatial correspondences between maps of ^{18}F-T807, ^{11}C-PIB and functional hubs.

Results: First, we found that ^{18}F-T807 retention in elderly controls predominates in medial temporal regions, matching well with previous descriptions of early tau deposits in Braak stages (Figure **1-A**). Second, ^{18}F-T807 and ^{11}C-PIB images had positive spatial correlations with r coefficients ranging 0.2 to 0.4. Third, while ^{11}C-PIB distributions did not show consistent spatial association with functional hubs, ^{18}F-T807 deposits displayed significant negative correlations from -0.2 to -0.3 (representative examples in Figure **1-B**; and mean in Figure **1-C**). Analyses comparing the regression slopes of ^{11}C-PIB with hubs versus those of ^{18}F-T807 with hubs, show that they differ significantly in explaining functional hub organization of elderly individuals (Figure **1-B**).

Conclusions: Our results suggest that ^{18}F-T807 deposits are inversely related to brain functional hubs in elderly individuals. Further studies are needed to explicitly reveal whether this association relates to brain functional breakdown.

Keywords: *TAU tracer, PIB, PET, Functional Hubs, Elderly Normals*

Presented by: Sepulcre, Jorge

P3

Amyloid PET screening for enrollment into Alzheimer's disease clinical trials: Initial experience in a Phase 1b clinical trial

Sevigny Jeff [1], Suhy Joyce [2], Chiao Ping [1], Klein Gregory [2], Oh Joonmi [2], Purcell Derk [3], Verma Ajay [1], Sampat Mehul [2], Barakos Jerome [4]

[1] *Biogen Idec, Cambridge, MA, USA*
[2] *Synarc Inc, Newark, CA, USA*
[3] *Synarc Inc, Newark, CA, USA, California Pacific Medical Center, San Francisco, CA, USA, University of California San Francisco, San Francisco, CA, USA*
[4] *Synarc Inc, Newark, CA, USA, California Pacific Medical Center, San Francisco, CA, USA*

Introduction: Amyloid PET imaging is a method of Alzheimer's disease (AD) clinical trial enrichment. We report our ongoing experience with amyloid PET imaging as a screening tool in patients with prodromal or mild AD.

Methods: Patients fulfilling criteria for either prodromal or mild AD in a multicenter, Phase 1b clinical trial underwent florbetapir PET scanning at screening. PET, MRI, and co-registered PET/MRI scans were reviewed by two independent readers and binary visual readings tabulated. Ten duplicate cases were presented to the readers to allow for calculation of intra-reader agreement statistics. Results were compared with semi-quantitative standard uptake value (SUV) ratios using a threshold of 1.10 to classify amyloid-negative from amyloid-positive patients.

Results: Of the first 250 PET/MRI scans reviewed, 20 discordant cases were identified when comparing visual readings to quantitative results: 17 with negative visual readings but positive quantitative results (composite SUV ratios 1.100–1.371) and 3 with positive visual readings but negative quantitative results (composite SUV ratios 1.040, 1.052 and 1.089). Inter- and intra-reader agreements from visual readings were 98.4% and 100%, respectively. Of those patients who met all study clinical and laboratory inclusion and exclusion criteria, 36.8% were ultimately excluded due to an amyloid-negative PET scan based on visual readings.

Conclusions: High inter- and intra-reader reliability was achieved. Factors potentially contributing to the high reliability were: a) availability of co-registered PET/MRI scans; b) harmonized spatial resolution and image orientation regardless of scanner model or patient position; c) 20-minute rather than 10-minute acquisition providing better statistics/less noise; and d) dynamic acquisition allowing motion correction. Agreement between visual and quantitative readings was good (92%). These data demonstrate that amyloid PET imaging can be an effective and feasible tool to enrich AD clinical trials in amyloid-positive patients, in particular in patients with earlier stages of the disease.

Keywords: *Alzheimer's disease, amyloid PET imaging, clinical trial, screening, prodromal*

Presented by: Sevigny, Jeff

P20 Antidepressant decreases CSF Aβ production in healthy individuals and in transgenic mice

Yvette Sheline [1], Tim West [2], Kevin Yarasheski [3], Robert Swarm [4], Mateusz Jasielec [5], Jonathan Fisher [6], Ping Yan [6], Chengjie Xiong [7], Christine Frederiksen [8], Robert Chott [3], Randall Bateman [9], John Morris [9], Mark Mintun [10], Jin-Moo Lee [11], John Cirrito [11]

[1] *Departments of Psychiatry, Radiology, and Neurology University of Pennsylvania Perelman School of Medicine, Philadelphia PA*
[2] *C2N Diagnostics LLC, St. Louis MO*
[3] *Department of Medicine, Washington University Medical Center, St. Louis MO*
[4] *Department of Anesthesiology, Washington University Medical Center, St. Louis MO*
[5] *Departments of Biostatistics and Surgery, Washington University Medical Center, St. Louis MO*
[6] *Department of Neurology, Washington University Medical Center, St. Louis MO*
[7] *Department of Biostatistics and The Knight Alzheimer's Disease Research Center, Washington University Medical Center, St. Louis MO*
[8] *Department of Surgery, Washington University Medical Center, St. Louis MO*
[9] *Department of Neurology and The Knight Alzheimer's Disease Research Center, Washington University Medical Center, St. Louis MO*
[10] *Avid Radiopharmaceuticals and Eli Lilly, Inc, Philadelphia PA*
[11] *Department of Neurology, The Knight Alzheimer's Disease Research Center, and Hope Center for Neurological Disorders, Washington University Medical Center, St. Louis MO*

Background: Aggregation of the amyloid-β (Aβ) peptide into plaques appears to be concentration-dependent, and methods for reducing Aβ production may have therapeutic potential. In this study we examined the dose-response effects of the SSRI citalopram, on brain Aβ levels in mice, its effect on individual plaque growth in the same mouse model, and the effects of an approximately equivalent dose of citalopram on human Aβ levels and production.

Methods: In vivo microdialysis assessed brain interstitial fluid (ISF) Aβ over time in the hippocampus of aged, freely moving, plaque-bearing APP/PS1$^{+/-}$ mice. Separately, individual brain plaques of APP/PS1 mice were serially imaged using intravital multiphoton microscopy before and after 28-day treatment with citalopram (10 mg/kg) vs. vehicle. In healthy humans, a randomized double-blind placebo controlled study determined the effect of 60 mg of citalopram. A lumbar catheter was placed at the L3-4 interspace, and hourly sampling of blood and CSF was conducted during and after administration of a stable-isotope labeled amino acid ($^{13}C_6$-leucine). Incorporation of $^{13}C_6$ leucine into Aβ was measured using the stable isotope labeling kinetics (SILK-Aβ®) assay and the concentration of labeled and unlabeled Ab was measured by stable isotope spike absolute quantitation (SISAQ™).

Results: In aged AD mouse models, citalopram produced a dose-dependent decrease in brain ISF Aβ levels. Individual plaques in mice chronically administered citalopram showed 78% reduction in new plaque appearance and 29% decrease in pre-existing plaque growth, but no regression of existing plaques. In humans, the production rate of Aβ was significantly suppressed by 38% in the citalopram group compared to placebo, resulting in 40% decrease in total CSF Aβ levels over 37 hours.

Discussion: The ability to safely decrease Aβ concentrations is potentially important as a preventive strategy for AD. This study demonstrates key target engagement for future AD prevention trials.

Presented by: Sheline, Yvette

P50 Impact of regional flow/perfusion heterogeneity and metabolism on the quantification of amyloid tracers: a preclinical exploration

Ann-Marie Waldron [1], Leonie Wyffels [1], Stefanie Dedeurwaerdere [2], Jill Richardson [3], Mark Schmidt [4], Xavier Langlois [4], Sigrid Stroobants [1], Steven Staelens [1]

[1] *Molecular Imaging Center Antwerp, Antwerp University, BELGIUM*
[2] *Translational Neurosciences, University of Antwerp, Belgium*
[3] *R&D China U.K. Group, GlaxoSmithKline, Stevenage, United Kingdom*
[4] *Neuroscience, Janssen Pharmaceutica NV, Beerse, Belgium*

Introduction: With a view to improving the accuracy of translational amyloid imaging the present study aimed to explore flow/perfusion heterogeneity and tracer metabolism on the quantification of [^{18}F]-AV45 by dynamic µPET studies.

Methods: Healthy (n=12) C57BL6J mice were intravenously injected with 37MBq of [^{18}F]-AV45. At 5, 10, 30 and 60min post injection mice (n=3/time point) were sacrificed and the brain and plasma were analyzed for radiometabolites. Further, for µPET imaging we studied a double transgenic mouse model of amyloidosis (TASTPM, n=5) and its wild-type counterpart (WT, n= 8) at 12 months of age. Mice were injected with 17MBq of [^{18}F]-AV45 via a tail vein catheterization and a dynamic 90min PET acquisition was started simultaneously. Tracer uptake was quantified by normalization for the injected dose.

Results: [^{18}F]-AV45 undergoes rapid metabolism with intact tracer accounting only for 28% of total plasma radioactivity already at 5min and decreasing to 2% at 30min p.i in WT mice. From µPET imaging, there was a notable difference in initial tracer uptake between WT and TASTPM, with the transgenic mice demonstrating lower peak uptake values (insets of Fig.1)

This difference was most prominent in the thalamus (on average relatively 17% lower in TASTPMs) while uptake in the cerebellum was comparable to that of WT. Thereafter a greater retention of [^{18}F]-AV45 in TASTPM mice is apparent at 10min and remains for all subsequent time points (Fig. 2).

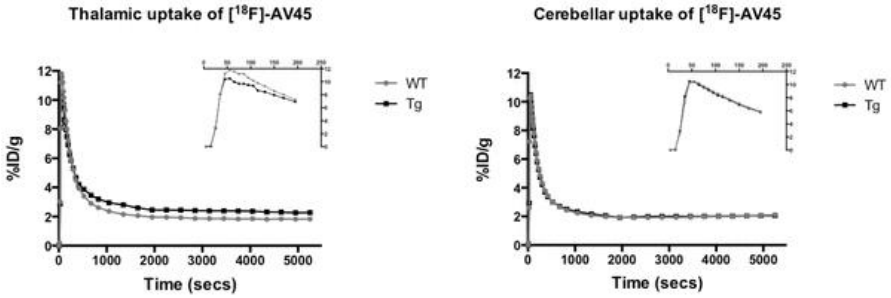

Fig. 1 Dynamic PET TAC's in TASTPM (Tg) and WT mice. All data is expressed as the mean. The first 3 min (peak uptake) is shown in the inset of each graph).

Conclusion: The initial differences in tracer uptake are indicative of regional flow/perfusion issues in TASTPM mice and contend the use of cerebellum as a reference region for normalization. These perfusion issues taken in combination with the rapid metabolism of [^{18}F]-AV45 greatly complicate the accurate estimation of amyloid burden.

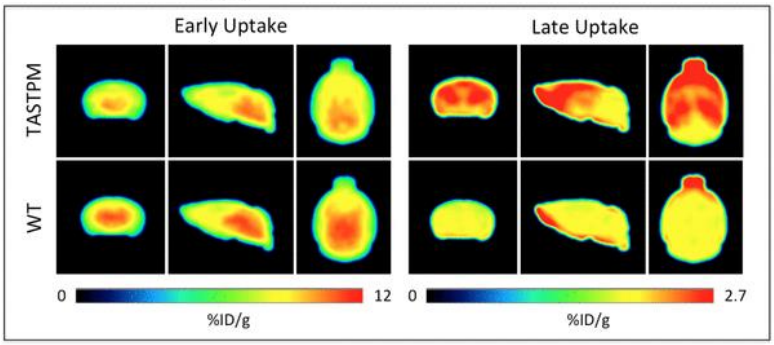

Fig.2 Average images for early (45-170secs) and late (42.5-62.5 min) uptake in WT and TASTPM mice. Images relate to flow/perfusion (early uptake) and specific tracer retention (late uptake) respectively.

ADMINISTRATIVE NOTES:

All animal studies were ethically reviewed and carried out in accordance with European Directive 86/609/EEC Welfare and Treatment of Animals.

This research was performed in conjunction with the European Community's Seventh Framework Program (FP7/2007-2013) for the Innovative Medicine Initiative under the PharmaCog Grant Agreement n°115009.

Keywords: *perfusion, flow, region heterogeneity, SUVR, quantification*

Presented by: Staelens, Steven

P6 In Vivo assessment of two isomers of [^{18}F]-THK5105 and [^{18}F]-THK511

Olivier Barret [1], David Alagille [1], Danna Jennings [1], Nobuyuki Okamura [2], Shozo Furumoto [2], Yukitsuka Kudo [2], Kenneth Marek [1], John Seibyl [1], Gilles Tamagnan [1]

[1] *Molecular Neuroimaging*
[2] *Tohoku University, School of Medicine*

Objective: To assess four quinoline radiopharmeuticals as potential PET biomarkers for tau pathology in Alzheimer's disease (AD) subjects and similarly aged healthy controls (HC): [^{18}F]MNI-718, [^{18}F]MNI-720, [^{18}F]MNI-721 and [^{18}F]MNI-723 ((R)-THK5117, (S)-THK5117, (R)-THK5105 and (S)-THK5105 isomer, respectively),

Methods: 10 AD and 7 HC (Age 72.1 AD and 55.1 HC,, MMSE range in AD subjects 13-26) received (185 ± 3.7 MBq) of one of the four tracers and were, imaged for up to 5 hours. AD subject also underwent amyloid imaging. Venous blood samples collected during imaging session to characterize metabolism of compounds. PET images were co-registered with subject's MRI and the uptake extracted in a variety of grey matter regions. Uptake was normalized to grey matter cerebellar cortex (SUVr) and values between 75-90 min post injection were compared between the two groups.

Results: All compounds displayed very good brain penetrance with a maximum SUV of 4-6 within 10 min of injection. [^{18}F]MNI-718 and [^{18}F]MNI-720 had a similar brain uptake kinetics that were faster than [^{18}F]MNI-721 and [^{18}F]MNI-723. SUVr for [^{18}F]MNI-718, [^{18}F]MNI-720, and [^{18}F]MNI-723 were increased in AD compared to HC in regions expected to demonstrate tau pathology.

Conclusions: These preliminary data suggest that both [^{18}F]MNI-718 and [^{18}F]MNI-720 appear to detect tau pathology in AD subjects. The kinetic profile and tracer performance of [^{18}F]MNI-718 and [^{18}F]MNI-720 appears to be superior to [^{18}F]MNI-723 and [^{18}F]MNI-721 to image the tau protein in human brain. Studies are currently ongoing to further characterize the binding of these tracers in AD and related neurodegenerative disorders.

Keywords: *Tau, imaging, Alzheimer, PET*

Presented by: Tamagnan, Gilles

P26 Evaluation of different target-to-reference region definitions for quantitative categorization of [18F]flutemetamol images into either normal or abnormal amyloid levels

Lennart Thurfjell [1], Roger Lundqvist [1], Johan Lilja [1], Chris Buckley [2], Adrian Smith [2], Paul Sherwin [3]

[1] *GE Healthcare, Uppsala, Sweden*
[2] *GE Healthcare, London, United Kingdom*
[3] *GE Healthcare, Princeton, NJ, United States*

Background: Quantification of PET amyloid imaging typically uses target-to-reference region ratios (SUVR) and the method for defining target and reference regions may impact the results. Our objective was to investigate the performance of different target-to-reference region combinations for quantitative categorization of [18F]flutemetamol (Vizamyl™, GE Healthcare, Princeton, NJ) images as positive or negative for amyloid.

Methods: [18F]Flutemetamol images from 6 prior clinical studies were grouped into an *autopsy cohort* (n = 68; subjects with *post-mortem* brain neuritic plaque density data available) and a *test cohort* (n=172; data from 33 probable AD, 80 MCI, and 59 healthy volunteers (HV)). Blinded visual image categorizations were available for all scans. A fully automated PET-only adaptive template quantification method was used to compute SUVR in a composite volume of interest. An SUVR threshold for classifying scans as positive or negative was derived through ROC analysis of the data from the autopsy cohort. The derived threshold was subsequently used to categorize the 172 scans in the test cohort as negative or positive, and results were compared to categorization using blinded visual assessment. This analysis was repeated for all target-to-reference region combinations. Reference regions were pons, whole cerebellum and cerebellar grey and we used three types of composite region (statistical, narrow, large).

The three composite regions outlined on the MNI average T1 template

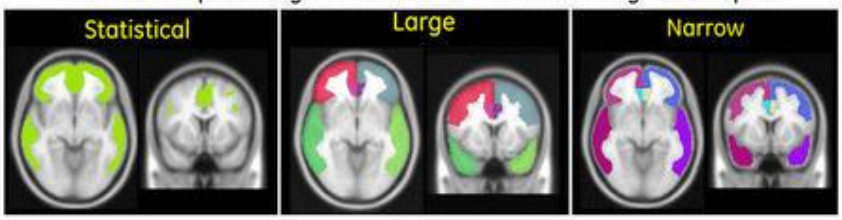

Results: The area under the ROC curve (AUC) for the autopsy cohort ranged from 0.91-0.93 (pons), 0.89-0.90 (whole cerebellum) to 0.83-0.84 (cerebellar gray). In the test cohort, the concordance between quantitative and blinded visual read categorization was 98.3-100.0% (pons), 97.7-98.8% (whole cerebellum) and 95.9-97.1% (cerebellar gray). The range for each reference region indicates variability due to target region definition. The best agreement was obtained using pons and with the statistical or narrow definition of the composite region.

Conclusions: Quantitative categorization of [18F]flutemetamol PET scans showed strong concordance with blinded visual read results across all target-to-reference region combinations.

SUVR threshold and AUC based on the autopsy cohort and the concordance with visual read results in the test cohort

Reference region	Target regions	SUVR Threshold	AUC Autopsy cohort (n=68)	Concordance with visual read Test cohort (n=172)
Pons	Statistical	0.62	0.93	100%
	Narrow	**0.59**	**0.93**	**99.4%**
	Large	0.56	0.92	98.3%
Cerebellar gray	Statistical	1.53	0.84	97.1%
	Narrow	1.53	0.84	97.1%
	Large	1.48	0.83	95.9%
Whole Cerebellum	Statistical	1.35	0.90	97.7%
	Narrow	1.30	0.90	98.8%
	Large	1.25	0.89	98.3%

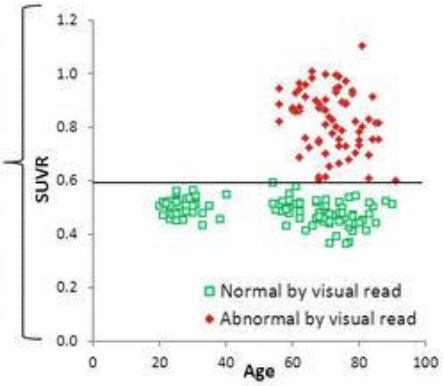

Keywords: *flutemeatmol, quantification, classification*

Presented by: Thurfjell, Lennart

P38 *En attendant* Centiloid

Victor L Villemagne [1], Paul Yates [1], Kevin Ong [1], Belinda Brown [2], Svetlana Pejoska [1], Robert Williams [1], Robyn Veljanoski [1], Stephanie Rainey-Smith [2], Kevin Taddei [2], Ralph Martins [2], Colin L Masters [3], Christopher C Rowe [1]

[1] *Department of Nuclear Medicine & Centre for PET, Austin Health, Melbourne, VIC, Australia*
[2] *Edith Cowan Univerity, Perth, WA, Australia*
[3] *The Florey Institute of Neuroscience and Mental Health, The University of Melbourne, VIC, Australia*

Background: Researchers often validate their assessments against the amount of Aβ in the brain. Given that the range of available Aβ tracers have different kinetics and recommended quantification procedures as well as different autopsy-validated SUVR thresholds to determine high and low Aβ burden, there is a need to standardize all these results and display them under a single universal scale. There is an international effort to establish this single scale that, under the name of Centiloid, (Mintun, 2012) will perform head-to-head comparison with the different tracers and PiB in both young and elderly as well as Alzheimer's disease patients, in order to cover the whole spectrum of Aβ deposition. In the meantime, large cohort studies like AIBL require validation of results now, so we adopted a linear regression approach to transform the results of each tracer generated with their own validated quantification method into PiB-like units.

Methods: Aβ imaging in 534 participants was performed with three different radiotracers: flutemetamol (n=245), florbetapir (n=172) and florbetaben (n=117). The results generated with the tracer-specific methods were classified as High or Low based on their respective neuropathologically-validated thresholds. Linear regression transformations based on reported head-to-head comparisons of each tracer with PiB were applied to each tracer result. Each tracer native classification was compared with the classification derived from the transformed data into PiB-like SUVR using 1.50 as a cut-off.

Results: Misclassification after transformation to PiB-like SUVR compared to native classification was extremely low, with only 3/245 (1.2%) of flutemetamol, and 0% of florbetapir and florbetaben cases assigned into the wrong category. When misclassification occurred it was restricted to an extremely narrow margin around the 1.50 SUVR threshold.

Conclusions: While a definitive conversion into centesimal units is worked out, application of linear regression transformations provide an interim, albeit robust, way of converting results from different Aβ imaging tracers into familiar PiB SUVR units.

Keywords: *Aβ imaging, Aβ radiotracers, centiloid*

Presented by: Villemagne, Victor L

P33 Investigating the involvement of the striatum in Down's syndrome and Alzheimer's disease with 11C-Pittsburgh Compound B-positron emission tomography (PiB-PET)

Liam Reese Wilson [1], Tiina Annus [1], Shahid Zaman [1], Young Hong [2], Tim Fryer [2], Robert Smith [2], Franklin Aigbirhio[2], Anthony Holland [1]

[1] Cambridge Intellectual and Developmental Disabilities Research Group (CIDDRG), Department of Psychiatry, University of Cambridge, UK.
[2] Wolfson Brain Imaging Centre, Department of Clinical Neurosciences, University of Cambridge, UK.

Introduction: Down's syndrome (DS) brings an elevated risk for early onset Alzheimer's disease (AD). In a subset of people with DS the early symptoms of AD appear to be changes in behaviour and personality (Holland et al., 2000), yet post mortem studies indicate AD pathology in DS is indistinguishable from sporadic AD. However, a recent PiB-PET study of non-demented adults with DS found binding in the striatum for several subjects (Handen *et al*., 2012), an area usually thought to be involved later in the course of AD.

Aims: PiB-PET and MRI data from the present study were analysed to investigate PiB retention in the striatum of DS adults with dementia, in the early stages of dementia, and without dementia.

Methodology: Forty-two participants with DS underwent a MRI scan and a ninety-minute dynamic PiB-PET scan. BP_{ND} maps were created using the simplified reference tissue model (Gunn *et al*., 1997), with the superior grey matter of the cerebellum as the reference tissue. A T-1 template was created using the DARTEL toolbox in SPM8, on which regions of interest (ROIs) were drawn manually. Regional BP_{ND} values were then obtained for 5 cortical and 2 subcortical areas.

Results: Binding was most frequently seen in the striatum, which had the highest average BP_{ND} value of any region. Participants who were positive for PiB binding in more than one ROI were always positive in the striatum. A further 3 non-demented participants retained PiB solely in the striatum.

Conclusion: Findings suggest that the striatum may be involved in the early stages of AD in DS; this is in contrast to published data on sporadic AD but is comparable to data from studies of familial autosomal dominant mutations causing AD (e.g. Klunk *et al*., 2007). The implications for people with DS and AD require further investigation.

Keywords: *Alzheimer's, Down's syndrome, PiB, Striatum.*

Presented by: Wilson, Liam Reese

P8 Utility of regional [18F]-Florbetapir PET imaging SUVRs in discriminating Alzheimer's disease and its prodromal stages

Qi Zhou [1], Mohammed Goryawala [1], David Loewenstein [2], Warren Barker [3], Ranjan Duara [3], Malek Adjouadi [1]

[1] *Center for Advanced Technology and Education, Florida International University*
[2] *Psychological Services and Neuropsychology Laboratory, Mount Sinai Medical Center*
[3] *Wien Center For Alzheimer's Disease & Memory Disorders, Mount Sinai Medical Center*

Purpose: Amyloid-β PET imaging is reported to be effective in diagnosing Alzheimer's disease (AD) and mild cognitive impairment (MCI). The goal of this study is to explore the efficacy of AV45 PET scans for delineating different stages of AD by performing exhaustive two-class classifications of AD, cognitive normal (CN), EMCI and LMCI subjects.

Methods: 476 dynamic AV45 baseline PET scans from ADNI2 (AD (n=65), EMCI (n=133), LMCI (n=124) and CN (n=154)) were included in this study. Mean SUVRs for six regions (cerebellum, brainstem, frontal, cingulate, parietal, and temporal) and weighted whole brain SUVR were used as the 7 classification features. A statistical feature selection method was used for classification between any two groups using a Support Vector Machine (SVM) classifier. The results were based on 50 independent and randomized 2-fold cross validation.

Results: Among all the SUVRs, mean frontal SUVR showed the most discriminative power for the classification of AD, LMCI and EMCI from CN; mean temporal SUVR for both EMCI versus AD and LMCI versus EMCI; and mean cingulate SUVR for AD versus LMCI. An error analysis was used to select the top-ranked features that yielded the highest accuracy [see Table 1]. A maximum accuracy of 84.4% (sensitivity: 89.0%) for AD versus CN, 72.5% (sensitivity: 61.2%) for LMCI versus CN, 62.5% (sensitivity: 40.8%) for EMCI versus CN, 60.1% for LMCI versus EMCI, 60.4% for AD versus LMCI and 73.3% for AD versus EMCI was obtained. Generally, mean SUVRs of brainstem and cerebellum were found to be insignificant features for most classification.

Conclusion: Regional amyloid burden can be utilized as a potential biomarker for classification and staging of the disease, however, its utility is best observed for discriminating AD from CN individuals. Also, mean frontal and temporal SUVRs were deemed most significant towards classification applications.

Table 1: Summary of significant features and classification performance

Classification Type	Rank of SUVRs*							Accuracy (%)
	1	2	3	4	5	6	7	
CN vs AD	**Frontal**	**WBW****	**Cingulate**	**Parietal**	**Temporal**	**Cerebellum**	**Brainstem**	84.4
CN vs LMCI	**Frontal**	**WBW****	**Parietal**	**Temporal**	**Cingulate**	**Brainstem**	**Cerebellum**	72.5
CN vs EMCI	**Frontal**	**WBW****	**Parietal**	**Cingulate**	**Temporal**	**Brainstem**	Cerebellum	62.4
AD vs LMCI	**Cingulate**	**Parietal**	**WBW****	**Temporal**	**Frontal**	**Cerebellum**	Brainstem	60.4
AD vs EMCI	**Temporal**	**WBW****	**Cingulate**	**Parietal**	**Frontal**	**Cerebellum**	**Brainstem**	73.2
LMCI vs EMCI	**Temporal**	**Frontal**	**WBW****	**Parietal**	**Cingulate**	Cerebellum	Brainstem	60.1

*SUVR: standardized uptake value ratio
**WBW: whole brain weighted SUVR
For each classification type, the significant SUVRs based on statistical testing are bolded, and those SUVRs that yield the highest accuracy based on support vector machine (SVM) classifier are highlighted.

Keywords: *[18F]-Florbetapir PET Imaging, Alzheimer's disease, mild cognitive impairment, classification*

Presented by: Zhou, Qi

P5 Diagnostic value of Amyloid imaging in early onset dementia

Marissa Zwan [1], Femke Bouwman [2], Wiesje van der Flier [3], Adriaan Lammertsma [4], Bart van Berckel [4], Philip Scheltens [2]

[1] Alzheimer Center & Department of Neurology, Neuroscience Campus Amsterdam, VU University Medical Center, Amsterdam, the Netherlands Department of Radiology & Nuclear Medicine, Neuroscience Campus Amsterdam, VU University Medical Center, Amsterdam, the Ne
[2] Alzheimer Center & Department of Neurology, Neuroscience Campus Amsterdam, VU University Medical Center, Amsterdam, the Netherlands
[3] Alzheimer Center & Department of Neurology, Neuroscience Campus Amsterdam, VU University Medical Center, Amsterdam, the Netherlands Department of Epidemiology & Biostatistics, Neuroscience Campus Amsterdam, VU University Medical Center, Amsterdam, the Ne
[4] Department of Radiology & Nuclear Medicine, Neuroscience Campus Amsterdam, VU University Medical Center, Amsterdam, the Netherlands

Introduction: In early onset dementia approximately one out of three patients has an atypical clinical presentation, which substantially complicates correct etiological diagnosis. [18F]Flutemetamol PET, an investigational imaging agent, is being studied for detection of amyloid deposition, a pathological hallmark of Alzheimer's Disease (AD).

Methods: We included 80 patients with early onset dementia (age <70 years) and physician diagnostic confidence less than 90% after a full routine diagnostic work-up for dementia. All patients underwent a [18F]Flutemetamol PET scan which were visually assessed as amyloid positive or negative. Before and after disclosing PET results, confidence in clinical diagnosis was determined. Also, impact on patient healthcare management was assessed after disclosing of the PET imaging results.

Results: [18F]Flutemetamol PET scans were positive in 48 out of 63 (76%) patients diagnosed (pre-PET imaging) with AD, 1 out of 9 (11%) patients diagnosed with frontotemporal dementia (FTD), and 3 out of 8 (38%) patients diagnosed with other dementias. Overall, confidence in etiological diagnosis increased from 76±12% to 90±16% after disclosing PET results ($p<0.001$). Access to [18F]Flutemetamol PET results led to a change in diagnosis in 16 (20%) patients. In 11 out of 13 patients, a negative [18F]Flutemetamol PET caused a change of the initial AD diagnosis to another dementia. In 3 out of 4 other dementia patients, the initial diagnosis was changed to AD after receiving a positive PET scan. In 27 (34%) patients, PET results led to a change in patient healthcare management. For 13 patients additional ancillary investigations were planned after access to the PET results.

Conclusion: [18F]Flutemetamol PET resulted in changes in the diagnostic process work-up of early onset dementia patients and the diagnostic confidence of the managing physicians. Especially in patients diagnosed with AD pre-PET imaging, a negative PET scan resulted in more changes in clinical diagnosis and patient management.

Keywords: *Amyoid Imaging; [18F]Flutemetamol PET; Diagnostic Value; Early onset dementia*

Presented by: Zwan, Marissa

NOTES

The 8h Human Amyloid Imaging Conference is supported through educational grants from:

Funding for this conference was made possible, in part by 1 R13 AG042201-01 from The National Institute on Aging and the National Institute of Biomedical Imaging and Bioengineering. The views expressed in written conference materials or publications and by speakers and moderators do not necessarily reflect the official policies of the Department of Health and Human Services; nor does mention by trade names, commercial practices, or organizations imply endorsement by the U.S. Government.

National Institute on Aging

NIBIB

PLATINUM

Lilly

For further information
concerning Lilly grant funding
visit www.lillygrantoffice.com

This activity is supported by an educational grant from Lilly USA, LLC.

GOLD

GE Healthcare

SILVER

Roche

Navidea BIOPHARMACEUTICALS

biogen idec
Transforming Discovery Into Care®

Piramal | Life Sciences
knowledge action care

Associate

ALZFORUM
NETWORKING FOR A CURE

SYNARC
Start here, finish first.